

ABSTRACT

LIU, ZIFEI. Measurement and Modeling Ammonia Emissions from Broiler Litter.
(Under the direction of Lingjuan Wang.)

Ammonia is a very important atmospheric pollutant. Agricultural activities, livestock production in particular, have been reported to be the largest contributor of ammonia emissions into the atmosphere. Accurate estimation of ammonia emission rate from individual operations or sources is important and yet a challenging task for both regulatory agencies and animal producers. The overall research objective of this study was to develop an emission model which can be used to estimate ammonia emission from broiler litter. In the reported model, the ammonia flux is essentially a function of the litter's total ammoniacal nitrogen (TAN) content, moisture content, pH, and temperature, as well as the Freundlich partition coefficient (K_f), mass transfer coefficient (K_G), ventilation rate (Q), and emission surface area (A). A dynamic flow-through chamber system and a wind tunnel were designed to measure ammonia fluxes from broiler litter. The dynamic flow-through chamber experiments evaluated the reported model with various litter samples under a constant temperature and wind profile. The wind tunnel experiments evaluated the reported model under various temperatures and wind profiles. Regression sub-models were developed to estimate K_f as a function of litter pH and temperature and to estimate K_G as a function of air velocity and temperature. Sensitivity analysis of the model showed that ammonia flux is very sensitive to litter pH and to a lesser extent temperature. A validation metric based on the mean and covariance in the measurement and in the model parameters were used to validate the model in the presence of measurement and model parameter uncertainties.

Measurement and Modeling Ammonia Emissions from Broiler Litter

by
Zifei Liu

A dissertation submitted to the Graduate Faculty of
North Carolina State University
in partial fulfillment of the
requirements for the Degree of
Doctor of Philosophy

Biological and Agricultural Engineering

Raleigh, North Carolina

2009

APPROVED BY:

Lingjuan Wang
Chair of Advisory Committee

David Beasley
Co-Chair of Advisory Committee

Sanjay Shah

Peter Bloomfield

BIOGRAPHY

Zifei Liu received his BS degree from Nanjing University in China. After graduation, he worked in the Environmental Monitoring Center of Anhui Province and obtained extensive experiences in environmental technology and management. Before he came to US, he spent one year in Japan as a research trainee in the Kochi Prefectural Environmental Research Center. In 2005, Zifei obtained a MS degree in environmental engineering from University of Cincinnati. Then he joined the Department of Biological and Agricultural Engineering at NCSU to pursue his PhD's degree. His research here focuses on agricultural air quality.

ACKNOWLEDGEMENTS

I would like to express the deepest appreciation to my committee chair, Dr. Lingjuan Wang, who continually and convincingly conveyed a spirit of adventure in regard to research and scholarship, and an excitement in regard to teaching. She directed me to a wide range of academic resources. Without her guidance and persistent encouragement this dissertation would not have been possible.

I would like to thank my committee members, Dr. David Beasley, Dr. Sanjay Shah and Dr. Peter Bloomfield for their valuable advices and support throughout my research.

In addition, a thank you to my peer research group: Dr. Qianfeng (Jeff) Li, Roberto Munilla and Zihan Cao. I am grateful for your assistance in the study and I enjoyed the time with all of you.

I would also like to thank Rachel Huie in the BAE Environmental Analysis Laboratory and David Buffaloe in the BAE Research Shop for their continuous support.

TABLE OF CONTENTS

LIST OF TABLES	x
LIST OF FIGURES	xi
LIST OF SYMBOLS, ABBREVIATIONS OR NOMENCLATURE	xv
1. INTRODUCTION	1
1.1 Ammonia as an air pollutant	1
1.2 Ammonia emissions from broiler houses	2
1.3 Estimation of ammonia emission: A challenging task.....	3
1.4 Emission models	4
1.5 Research objectives.....	6
2. LITERATURE REVIEW	7
2.1 Broiler house management	7
2.2 Reported ammonia emission from broiler houses	8
2.3 Theoretical bases of ammonia emission	10
2.3.1 General model.....	10
2.3.2 Generation of ammonia.....	11
2.3.3 Partitioning between adsorbed phase and dissolved phase ammonia.....	12
2.3.4 Chemistry of ammonia in aqueous solution.....	13
2.3.5 Partitioning between dissolved phase and gaseous phase ammonia.....	14
2.3.6 Mass transfer of ammonia gas from emission surface to the free air stream	15
2.3.7 The mass transfer coefficient.....	18

2.4 Factors influencing ammonia emissions from broiler litter	21
2.4.1 Air and litter temperature	21
2.4.2 Ventilation rate	22
2.4.3 Litter pH value	23
2.4.4 Litter moisture content	24
2.4.5 Litter nitrogen content (diet, litter age and bird age)	25
2.4.6 Litter type	25
2.5 Review of ammonia emission models in animal houses	25
2.5.1 Mechanistic models	26
2.5.2 Process based models	29
2.5.3 Statistical models	29
2.5.4 Mass balance and N-flow models	30
2.5.5 Inverse dispersion models	31
2.5.6 Summary	32
3. EXPERIMENTAL METHODS	33
3.1 Experimental setup	33
3.1.1 Dynamic flow-through chamber	33
3.1.2 The Wind tunnel	38
3.2 Measurement of ammonia concentration	45
3.2.1 Chemiluminescence ammonia analyzer (Thermo Environmental Instruments)	45
3.2.2 Acid scrubber	47
3.3 Analysis of litter properties	48
3.4 Measurement of litter moisture content	49

3.5 Measurement of relative humidity and temperature of air.....	51
4. COMPARISON OF THREE TECHNIQUES FOR DETERMINING AMMONIA EMISSION FLUXES	52
4.1 Research Objective	52
4.2 Methodology	53
4.2.1 Experimental Setup.....	54
4.2.2 Litter Samples and Moisture Content Treatments	54
4.2.3 Ammonia Concentration Measurements.....	55
4.2.4 Determination of Ammonia Emission Flux	56
4.3 Results and Discussion	59
4.3.1 Comparison of Ammonia Concentration Measurements.....	59
4.3.2 Comparison of Ammonia Emission Fluxes	63
4.4 Conclusion	67
5. EFFECT OF MOISTURE CONTENT ON AMMONIA EMISSIONS	68
5.1 Research Objective	68
5.2 Methodology	69
5.2.1 Experimental Setup.....	69
5.2.2 Litter Samples and Moisture Treatments.....	69
5.2.3 Measurement of Ammonia Concentrations in the Chamber.....	70
5.2.4 Measurement of Nitrogen Loss of Litter Samples	70
5.3 Results and discussions.....	71
5.3.1 Effect of Added Water over a Short Period of Time	71
5.3.2 Effect of Litter Moisture Contents over Time	72
5.3.3 TAN Contents in Litter vs. Ammonia Emissions	73

5.3.4 Effect of Litter Moisture Contents on TAN Contents	75
5.3.5 Nitrogen Losses from Litter Samples	76
5.4 Conclusion	78
6. MODELING AMMONIA EMISSIONS FROM BROILER LITTER AT LABORATORY SCALE	79
6.1 Research Objective	80
6.2 Model development	80
6.2.1 The general mass transfer flux equation	80
6.2.2 Sub-model of the equilibrium gas phase ammonia concentration ($C_{g,0}$)	83
6.3 Experimental methods	85
6.3.1 Dynamic flow-through chamber	85
6.3.2 The Wind tunnel	86
6.3.3 Litter samples	87
6.3.4 Model evaluation parameters	87
6.3.5 Sensitivity analysis	88
6.4 Results and discussions	89
6.4.1 $C_{g,0}$ of different litter samples at constant temperature	89
6.4.2 $C_{g,0}$ at various temperatures	94
6.4.3 Regression model of K_f	98
6.4.4 Evaluation of the model	98
6.4.5 Simulation of $C_{g,0}$ in time series	99
6.4.6 The mass transfer coefficient (K_G)	100
6.4.7 Model predicted ammonia flux	101
6.4.8 Sensitivity analysis	102

6.5 Conclusion	103
7. MASS TRANSFER COEFFICIENT OF AMMONIA EMISSIONS	104
7.1 Research Objective	104
7.2 Experimental method.....	105
7.2.1 The wind tunnel	105
7.2.2 Litter samples.....	105
7.2.3 Measurements of ammonia emission and the mass transfer coefficient K _G	105
7.3 Results and discussion	106
7.3.1 Ammonia concentration at outlet and emission flux	106
7.3.2 Effect of air temperature and air velocity on mass transfer coefficient K _G	108
7.3.3 Regression model of K _G	113
7.3.4 Validation of the K _G regression model with independent experimental data set.....	116
7.3.5 Dimensionless analysis	117
7.4 Conclusion	121
8. VALIDATION AND UNCERTAINTY ANALYSIS OF THE MODEL.....	123
8.1 Introduction.....	123
8.2 Research Objective	124
8.3 Model Structure	124
8.4 Validation Metrics	125
8.4.1 Uncertainties in model validation	125
8.4.2 The r ² metric	126
8.5 Validation of the Emission Model	128

8.5.1 Validation of core model considering uncertainties of K_f and K_G	128
8.5.2 Validation of the k_f sub-model considering uncertainties of pH and temperature	130
8.5.3 Validation of the K_G sub-model considering uncertainties of air velocity and temperature	131
8.6 Conclusion	138
9. FUTURE DIRECTION	139
REFERENCES	140
APPENDIX.....	158
Appendix A. Summary of litter analysis data.....	159
Appendix B. Effects of Litter pH, moisture content and total carbon content on TAN/TKN ratio.....	164
Appendix C. Experimental data of $C_{g,0}$ AND K_f in the dynamic flow through chamber study	166
Appendix D. Experimental data of $C_{g,0}$ and K_f for litter A in the wind tunnel study.....	167
Appendix E. Experimental data of $C_{g,0}$ and K_f for litter B in the wind tunnel study.....	169
Appendix F. Experimental data for K_G regression model development (Litter A) in the wind tunnel study.....	173
Appendix G. Experimental data for K_G regression model validation (Litter B) in the wind tunnel study.....	177
Appendix H. Calculation of dimensionless numbers.....	180

LIST OF TABLES

Table 2-1. Reported ammonia concentrations and emission rates in broiler houses	9
Table 3-1. Calibration data of the AV-2 rotating vane anemometer	42
Table 4-1. Comparison of the chemiluminescence analyzer and the acid scrubber measurements for litter samples under various litter moisture content treatments (litter age = one year).	60
Table 5-1. TAN content and ammonia emissions.....	74
Table 6-1. Influence of the relative magnitude of Q/A and K_G value on K_e	82
Table 6-2. $C_{g,0}$ for various litter samples ($T=22$ °C).....	90
Table 6-3. Properties of the two litter samples	94
Table 6-4. Baseline values and percentage change of ammonia flux for 10% increase of variables.....	102
Table 6-5. Relative sensitivity S_r for ammonia emission flux from litter with respect to litter pH and temperature at different pH and temperature ranges	103
Table 7-1. Constant C_k and exponents a, b in Equation 7-1	113
Table 7-2. Constant C_k and exponents a, c in Equation 7-6	120
Table 8-1. Validation results of the K_f sub-model	131
Table 8-2. Validation results of the first sub-model of K_G	133
Table 8-3. Validation results of the second sub-model of K_G	137

LIST OF FIGURES

Figure 2-1. Illustration of processes related to ammonia emissions from broiler litter ...	11
Figure 2-2. Illustration of the two-film theory	16
Figure 3-1. Diagram of the dynamic flow-through chamber system.....	34
Figure 3-2. Photographs of the dynamic flow-through chamber system.....	35
Figure 3-3. The horizontal air velocity profile at selected impeller speeds (Flow rate=10L min ⁻¹).....	37
Figure 3-4. The horizontal air velocity profile at different flow rates (RPM=110).....	38
Figure 3-5. Diagram of the wind tunnel system	40
Figure 3-6. Photographs of the wind tunnel system	41
Figure 3-7. Calibration curve of AV-2 rotating vane anemometer (Data points are average values of 6 measuring points; when U>5 m s ⁻¹ , calibration data were measured by pitot tube. When U<5 m s ⁻¹ , calibration data were measured by hotwire anemometer.)	43
Figure 3-8. Air velocity profiles at the start point (upwind) and end point (downwind) of the emission section in the wind tunnel for the nominal velocity values of 0.15, 0.50, 1.00, 1.50, and 2.00 m s ⁻¹	45
Figure 3-9. Calibration curve of the ammonia analyzer	47
Figure 3-10. Photograph of the litter sample	49
Figure 3-11. Manufacturer's calibration curve of the ECH2O moisture sensor.....	50
Figure 3-12. Comparison of the ECH2O moisture sensor measurement and the mass based moisture content of litter samples.....	50
Figure 3-13. Comparison of the Novus humidity and temperature transmitter and psychrometer measurements of relative humidity	51
Figure 4-1. TN and TKN measurements of litter samples.....	55

Figure 4-2. Ammonia concentrations in the flux chamber in ten preliminary tests (measured by the chemiluminescence ammonia analyzer).....	56
Figure 4-3. Relationship between average measurements by the chemiluminescence analyzer and the acid scrubber.....	61
Figure 4-4. Ratios of the average chemiluminescence analyzer measurements over the acid scrubber measurements.....	62
Figure 4-5. Comparisons of ammonia emission fluxes derived using different techniques (Sample ID 1-1 to 1-9 are used to represent the nine samples in set 1, and sample ID 4-1 to 4-9 are used represent the nine samples in set 4)	64
Figure 4-6. Relative errors between ammonia fluxes estimated by the nitrogen mass balance approach and by the chemiluminescence analyzer measurements.	66
Figure 5-1. Average ammonia concentrations vs. litter moisture content	71
Figure 5-2. Average ammonia concentrations from litter E over time (Each data point is an average of three replicates)	73
Figure 5-3. Ammonia concentrations vs. TAN contents in the litter samples.....	75
Figure 5-4. TAN contents in litter vs. litter moisture contents (litter A).....	76
Figure 5-5. Nitrogen losses of litter samples vs. litter moisture contents (litter A).....	77
Figure 6-1. Flux and concentration vs. flow rate	89
Figure 6-2. $C_{g, \infty}$ vs. emission flux J.....	90
Figure 6-3. The K_d ratio α vs. litter moisture content	91
Figure 6-4. Estimated distribution of TAN content of the tested ten litter samples	92
Figure 6-5. The model predicted values and the observed values of $C_{g, 0}$ of the tested nine litter samples (T=22°C).....	93
Figure 6-6. K_f vs. pH.....	93
Figure 6-7. The model predicted values and the observed values of $C_{g, 0}$ for the litter A at various temperatures (using $K_f=1.87 \text{ L kg}^{-1}$ in model)	95

Figure 6-8. The model predicted values and the observed values of $C_{g,0}$ for the litter B at various temperatures (using $K_f=2.15 \text{ L kg}^{-1}$ in model)	95
Figure 6-9. K_f vs. temperature for the litter A	96
Figure 6-10. K_f vs. temperature for the litter B.....	96
Figure 6-11. The model predicted values and the observed values of fraction of free ammonia nitrogen over TAN for litter A and B	97
Figure 6-12. The model predicted values and the observed values of $C_{g,0}$	99
Figure 6-13. Comparison of the model predicted $C_{g,0}$ and observed $C_{g,0}$ in time series	100
Figure 6-14. The model predicted ammonia fluxes under various temperatures and pH values (baseline values, all on dry basis: TAN = $3553 \mu\text{g g}^{-1}$, moisture content = 32.94 w/w%, $K_G = 8.11 \text{ m h}^{-1}$, Q/A = 100 m h^{-1})	101
Figure 7-1. Measurements of ammonia concentration at outlet of the wind tunnel at various air velocities (Litter A).....	107
Figure 7-2. Wind tunnel flow rate vs. nominal air velocity inside the wind tunnel	107
Figure 7-3. Ammonia emission fluxes at various air velocities (Litter A)	108
Figure 7-4. K_G value at various air temperatures (Litter A)	109
Figure 7-5. Effect of air temperature on the mass transfer coefficient K_G at various air velocities	110
Figure 7-6. K_G value at $T=20^\circ\text{C}$ and the slope of regression line of K_G over air temperature at various air velocities.....	111
Figure 7-7. Effect of air velocity on mass transfer coefficient K_G at three air temperatures	112
Figure 7-8. Observed K_G vs. model predicted K_G (litter A)	114
Figure 7-9. Residual vs. temperature (litter A).....	115
Figure 7-10. Residual vs. air velocity (litter A)	115
Figure 7-11. Residual vs. observed K_G (litter A).....	116

Figure 7-12. Observed K_G vs. model predicted K_G (litter B)	117
Figure 7-13. Observed K_G vs. K_G calculated by Equation 7-9 and 7-10	121
Figure 8-1. The overall model structure	125
Figure 8-2. Comparison of measured and model predicted ammonia emission fluxes for the tested ten litter samples ($K_f=2.08 \text{ L kg}^{-1}$, $K_G=8.11 \text{ m h}^{-1}$)	129
Figure 8-3. Comparison of measured and model predicted K_G for litter A at selected combinations of air velocity and temperature	134
Figure 8-4. Comparison of measured and model predicted K_G for litter A at $T=25^\circ\text{C}$.	135
Figure 8-5. Comparison of measured and model predicted K_G for litter B at selected combinations of air velocity and temperature	136

LIST OF SYMBOLS, ABBREVIATIONS OR NOMENCLATURE

a is regression coefficients, dimensionless;

A is the area of emission surface or the exposed manure, m^2 ;

b is regression coefficients, dimensionless;

c is regression coefficients, dimensionless;

C_0 is ammonia concentration in the inlet gas stream, $mg\ m^{-3}$;

$C_{Ag,0}$ is ammonia concentration at the immediate gas film surface, or phase ammonia concentration at the emission surface, $mg\ m^{-3}$;

$C_{Ag,i}$ is ammonia concentration at the interface in gas phase, $mg\ m^{-3}$;

$C_{Al,i}$ is ammonia concentration at the interface in liquid phase, $mg\ m^{-3}$;

$C_{Al,0}$ is ammonia concentration at the immediate liquid film surface, $mg\ m^{-3}$.

$C_{g,0}$ is gas phase ammonia concentration in equilibrium with dissolved ammonia in litter, $mg\ m^{-3}$;

$C_{g,\infty}$ is gas phase ammonia concentration in the free air stream, $mg\ m^{-3}$;

C_{house} is gas phase ammonia concentration in house air, $mg\ m^{-3}$;

C_{inlet} is gas phase ammonia concentration at inlet of the wind tunnel, $mg\ m^{-3}$;

C_k is regression coefficients, dimensionless;

C_{out} is gas phase ammonia concentration in outside air, $mg\ m^{-3}$;

C_{outlet} is gas phase ammonia concentration at outlet of the wind tunnel, $mg\ m^{-3}$;

C_{Pi} is model predicted value of $C_{g,0}$, $mg\ m^{-3}$;

C_{Oi} is observed value of $C_{g,0}$, $mg\ m^{-3}$.

C_P is mean predicted value of $C_{g,0}$, $mg\ m^{-3}$;

C_o is mean observed value of $C_{g,0}$, $mg\ m^{-3}$;

D is the diffusivity in air, $\text{m}^2 \text{s}^{-1}$;

F_c is corrected fraction of free ammonia nitrogen over TAN, dimensionless;

H^* is the effective Henry's constant, dimensionless;

J is emission flux, $\text{mg m}^{-2} \text{h}^{-1}$;

J_1 is ammonia fluxes estimated by the nitrogen mass balance approach, $\text{mgN h}^{-1} \text{m}^{-2}$;

J_2 is ammonia fluxes estimated by the chemiluminescence analyzer measurements, $\text{mgN h}^{-1} \text{m}^{-2}$;

ΔJ is change of ammonia emission flux, $\text{mg h}^{-1} \text{m}^{-2}$;

K_{d0} is the dissociation constant of ammonia in water, dimensionless;

K_d is the dissociation constant in litter or manure, dimensionless;

K_e is overall emission coefficient, m h^{-1} ;

K_f is the Freundlich partition coefficient, L kg^{-1} ;

k_g is mass transfer coefficient in the gas film, m h^{-1} or $\text{g cm}^{-2} \text{atm}^{-1} \text{h}^{-1}$;

K_G is overall mass transfer coefficient in gas phase, m h^{-1} ;

K_h is Henry's constant, dimensionless;

k_l is mass transfer coefficient in the liquid film, m h^{-1} or cm h^{-1} ;

K_L is overall mass transfer coefficient in liquid phase, m h^{-1} ;

L is the characteristic length that influences the air flow, m ;

MC is the moisture content in litter, $\text{w/w}\%$;

MW_{air} is molecular weights of ammonia air, g mol^{-1} ;

MW_{NH_3} is molecular weights of ammonia, g mol^{-1} ;

N_{loss} is loss of nitrogen in the litter sample during testing time, g ;

N_i is initial total nitrogen content in the litter sample at the beginning of the test, g ;

N_f is final total nitrogen content in the litter sample at the end of the test, g ;

$[\text{NH}_4^+ - \text{N}]_l$ is the concentration of dissolved phase $\text{NH}_4^+ - \text{N}$, $\mu\text{g L}^{-1}$;

NME is Normalized Mean Error, %;

P is air pressure, atm;

Q is the ventilation rate, or flow rate of the carrier gas through the chamber, $\text{m}^3 \text{s}^{-1}$ or $\text{m}^3 \text{h}^{-1}$;

r is the mass transfer resistance, day m^{-1} ;

R is ideal gas law constant, $0.082 \text{ L atm K}^{-1} \text{ mol}^{-1}$;

RE = relative error, %;

Re is Reynolds number, dimensionless;

Sc is Schmidt number, dimensionless;

Sh is Sherwood number, dimensionless;

S_r is relative sensitivity, dimensionless;

t is testing time for each sample, h;

T is temperature in K or $^{\circ}\text{C}$;

[TAN] is the TAN content in litter or manure, $\mu\text{g g}^{-1}$, or kg m^{-3} ;

U is air velocity, m s^{-1} ;

$U(z)$ is air velocity at any height z, m s^{-1} ;

U^* is friction velocity, m s^{-1} ;

V is volume of the chamber space above litter, m^3 ;

x is baseline value of the variable of interest;

Δx is change of the variable of interest over the range being considered;

z_0 is surface roughness, m;

$\rho_{\text{H}_2\text{O}}$ is density of water, kg L^{-1} ;

κ is von Karman's constant, 0.4-0.42, dimensionless;

ν is the kinematic viscosity of air, $\text{m}^2 \text{s}^{-1}$, which equals air viscosity divided by air density;

θ is the vector of model parameters;

$(\sum v)_{\text{NH}_3}$ is the sum of atomic diffusion volumes of ammonia;

$(\sum v)_{\text{air}}$ is the sum of atomic diffusion volumes of air.

1. INTRODUCTION

1.1 AMMONIA AS AN AIR POLLUTANT

Ammonia is a very important atmospheric pollutant due to its impact on ecosystems. Major impacts associated with atmospheric ammonia and its deposition include eutrophication, soil acidification, and aerosol formation. Deposition of excessive amounts of ammonia may detrimentally affect nitrogen limited ecosystems (Schulze et al., 1989). It can lead to over enrichment of nutrients which may cause eutrophication of aquatic ecosystems. When ammonia is deposited onto the soil, it is converted by bacteria into nitrate. The nitrification process forms hydrogen ions leading to acidification of the soil. Moreover, as the most abundant alkaline specie in the atmosphere, atmospheric ammonia reacts with sulfur dioxide and nitrogen oxides to form ammonium aerosols such as ammonium nitrate, so ammonia can be a precursor for fine particle particulate matter, which is a human health concern (Barthelmie and Pryor, 1998), and is regulated by the US Environmental Protection Agency's National Ambient Air Quality Standards PM_{2.5} (particulate with an aerodynamic equivalent diameter less than or equal to 2.5 μm). Ammonia has a residence time of 1 to 10 days in the atmosphere, and ammonium aerosols can be transported hundreds of kilometers (NRC, 2003).

The health effects of ammonia are well known. Ammonia can be rapidly absorbed in the upper airway of human respiratory system. Also, ammonia is an odorant with irritant properties. It has a pungent, acrid odor at concentrations greater than 0.7 ppm. Concentrations of 50-150 ppm can lead to severe cough and mucous production (Leduce et

al., 1992). In addition to pulmonary disease, exposure to ammonia leads to irritation of the eyes, sinus, and skin (Latenser et al., 2000). Research and regulatory agencies have shown increasing interest in ammonia as an air pollutant.

1.2 AMMONIA EMISSIONS FROM BROILER HOUSES

Agricultural activities, livestock production in particular, have been reported to be the largest contributor of ammonia emissions into the atmosphere (Arogo et al., 2002). Over the last ten years, concentrated animal feeding operations (AFOs) in the United States have expanded greatly. These operations produce large amounts of waste on relatively small areas, and ammonia emission from those AFOs is a growing concern due to potential effects on animal health, human health, and environmental pollution. The importance of ammonia emissions from AFOs has been well recognized (Van der Hoek, 1991; Zhao et al., 1994; Sutton et al., 1995; Aneja et al., 2000; Arogo et al., 2001; Hutchings et al., 2001; Lee and Park, 2002; Battye et al., 2003; Hyde et al., 2003; Xin et al., 2003; Wheeler et al., 2003; Liang et al., 2003; Gates et al., 2004). With increasingly stringent federal, state and local air pollution regulations and the emerging pressure to regulate agricultural enterprises, emissions of ammonia and other pollutants from AFOs have become an increasing concern to regulators, producers, and environmental groups in the United States.

Broiler production in North Carolina is increasing throughout the state. Production can be found in the mountain, Piedmont and Coastal Plain regions of the state. In broiler production, ammonia is a big concern in confined broiler production, not only because it causes environmental problems, but also because ammonia in broiler house has a direct impact on bird health and productivity (Brewer and Costello, 1999).

Broiler chickens are normally raised on bedding material made up of wood shavings, saw dust, or peanut hulls above an earthen floor. The bedding serves as a manure absorbent, and the mixture of manure and bedding material is called broiler litter. Broiler litter typically contains 4% to 6% nitrogen, much of which is in the ammonia form (Carr et al., 1990). The broiler litter represents a significant source of ammonia emissions in broiler houses. Using 2003 USDA data on broiler production numbers, broiler housing is estimated to contribute 240 to 324 kT ammonia for new and built-up litter nationally (Gates. et al., 2008).

Concern about ammonia in broiler operations has been mainly with ammonia levels inside broiler houses, but now, emissions of ammonia are receiving increasing scrutiny. As poultry production is concentrated geographically and much of the ammonia emitted from broiler litter escapes into the environment with ventilated air, the impact of ammonia emissions on the environment could be considerable. Ammonia emission from broiler houses has become the primary concern for regulatory reporting under the Emergency Planning and Community Right-to-Know Act (EPCRA). Reasonable estimates of ammonia emission rates from U.S. broiler facilities are needed to guide discussions about the industry's impact on local and regional air quality.

1.3 ESTIMATION OF AMMONIA EMISSION: A CHALLENGING TASK

Ammonia emission inventories in the United States have largely relied on emission factors developed in Europe in the early 1990's (Battye et al., 1994; Asman, 1992), and scientific estimates of ammonia emissions from U.S. facilities are limited. In 2003, the National Research Council (NRC) of the National Academies of Science released a report entitled "Air Emissions from Animal Feeding Operations: Current Knowledge, Future

Needs.” The report pointed out that ammonia emission from AFOs was a major concern at the global, national, and regional scales, and recommended strengthening the scientific basis for estimating ammonia emissions from AFOs.

Climatic, diurnal and seasonal emission patterns, house design, and management practices, all affect ammonia emission from AFOs. Therefore, measurements obtained from a particular animal production facility cannot be generalized to other operations, because of differences in environmental, management, and production conditions (Arogo et al., 2003; Arogo et al., 2006; Harper, 2005; Ni and Heber, 2001). Accurate estimation of ammonia emission rate from individual operations or sources is important and yet a challenging task for both regulatory agencies and animal producers. Measurement of ammonia emission from livestock buildings is technically complex, expensive, and labor intensive using current measurement methodologies (NRC, 2003).

In order to improve the accuracy and simplicity of estimating ammonia emissions, and to reduce the need for measurements under all possible conditions, development of emission models is desirable.

1.4 EMISSION MODELS

Emission models can be used for predictive simulations, experimental testing, and sensitivity analysis. The National Research Council (NRC)'s Ad Hoc Committee on Air Emissions from AFOs identified the limitation of available methodologies to estimate national emissions from animal agriculture and recommended that the U.S. EPA develop a process-based modeling approach for estimating emissions from AFOs (NRC, 2003).

Emission models allow users to calculate site-specific emissions, using local operating parameters, and obtain realistic emission estimation according to variable climatic and management conditions. Emission models can also be used to quantify and evaluate the effectiveness of various emission control strategies.

Previous ammonia emissions inventories have not adequately addressed seasonal and geographical variations in emissions factors. Emission models can be used to simulate the seasonal and geographic variations in ammonia emission factors, which are required for chemical transport modeling for accurately predicting the formation of ammonium nitrate and ammonium sulfate aerosols.

Numerous emission models have been applied in evaluating swine lagoons (Liang et al. 2002; De Visscher et al. 2001), swine slurries (Ni et al, 2000; Oelesen and Sommer 1993), dairy cow barns (Monteny et al. 1998; Webb and Misselbrook, 2004), chicken slurries (Hashimoto and Ludington 1971), land application of manures (Roelle and Aneja, 2005), and whole farm production systems (Pinder et al. 2004).

The influence of management factors and litter conditions on ammonia emissions from broiler litter have also been documented (Nicholson et al., 2004; Redwine et al., 2002; Reece et al., 1985; Elliot and Collins, 1982; Elwinger and Svensson, 1996; Carr et al. 1990; Brewer and Costello, 1999). Much work remains to be done to adequately incorporate these factors into emission models. Further evaluation and improvement in emission models for AFOs are desirable (Arogo et al., 2006).

1.5 RESEARCH OBJECTIVES

The overall research objective of this study was to develop an emission model which can be used to estimate ammonia emission from broiler litter. The specific objectives were:

To obtain a better understanding of the processes involved in ammonia emission from broiler litter and identify the main factors that influence emission flux such as litter moisture content;

To evaluate different ammonia concentration measurement techniques and address the limitations of these techniques.

To develop a mathematical emission model that simulates ammonia release from broiler litter using established physical and chemical relationships;

To measure the mass transfer coefficient of ammonia in the emission model and generate correlations between the mass transfer coefficient and environmental conditions;

To calibrate and validate the emission model with measured results.

The direct results of the study include a mathematical emission model that combines the effects of various influencing factors and can be used to predict ammonia emission from broiler litter under given conditions. The model aims to provide a realistic picture of the basic processes involved and provide increased flexibility in ammonia emission estimation. The results could provide a basis for developing process-based emission models that accurately predict ammonia emission from broiler houses, and subsequently contribute to design and development of effective ammonia control strategies.

2. LITERATURE REVIEW

In this chapter, a literature review is provided on the theoretical bases of ammonia emission. Factors that influence ammonia emission are evaluated and existing emission models are discussed.

2.1 BROILER HOUSE MANAGEMENT

The growth cycle of birds in broiler houses is typically 46 to 54 days (Lacey, 2003), from 0-day-old to the time of slaughter (In North Carolina the growth cycle has actually increased to as much as 60 to 63 days). Conditions within the broiler houses are managed to optimize bird health and productivity. Temperature in broiler houses is usually regulated with an initial temperature of 32 to 35 °C which is lowered by 3 °C every seven days to 22 ± 2 °C after 3 weeks of age (Nicholson et al., 2004; Elwinger and Svensson, 1996). The houses are usually ventilated according to temperature. The air ventilation rate can vary in a wide range, such as from 0.2 to 1.2 m^3s^{-1} (the minimum ventilation rate was calculated to be $1.9 \times 10^{-4} \text{m}^3\text{s}^{-1}\text{kg}^{-0.75}[\text{lw}]$) in the study by Nicholson et al. (2004), and 0.02-2.76 m^3s^{-1} (80 to 9936 m^3h^{-1} for 5086 chickens) in the study of Guiziou and Beline (2005).

Broiler chickens are often grown in production houses containing 20,000 or more birds at densities of 13.5 - 21.2 bird m^{-2} (Guiziou and Beline, 2005; Nicholson et al., 2004; Redwine et al., 2002; Brewer and Costello, 1999). Commonly used bedding material types include wood shavings, saw dust, peanut hulls, etc. Litter depth was reported to be about 5 cm (Nicholson et al., 2004) but in current commercial practice it is often 2 to 4 times higher.

Elwinger and Svensson (1996) reported that the amount of litter used in practice was from 0.25 to 1.0 kg m⁻² floor area. Used litter may be sent for land application.

2.2 REPORTED AMMONIA EMISSION FROM BROILER HOUSES

Measurement of ammonia emissions from broiler houses is not easy. A number of different methods of measuring ammonia emissions have been developed. Usually, ammonia concentration in the broiler houses is measured, and then ammonia emission rate is calculated by multiplying concentration by the ventilation rate. Acid traps (Lockyer, 1983) and diffusion tubes (Hargreaves and Atkins, 1987) have been used for measuring ammonia concentrations in poultry houses. Many studies have been reported throughout the world on ammonia emissions from broiler houses, and wide variations have been found among different studies. Emission rates are usually expressed in terms of mass of NH₃ or ammonia nitrogen (NH₃-N) per unit time and per animal (or liveweight units) or per unit area (surface sources). Measurements from broiler houses indicated that ammonia emission rates vary 55-fold, from 283 to 15718 mg [NH₃-N] h⁻¹ AU⁻¹ (Redwine et al., 2002). The reported ammonia concentrations and emission rates in literature are summarized in Table 2-1. Most of the data are from observations in Europe. In order to compare these measurements, all emission rate data were converted to a common unit in mg [NH₃-N] h⁻¹AU⁻¹. As indicated in this table, ammonia emission rates varied in a wide range in different studies or under different conditions in the same study. While such variations in ammonia emissions could mainly be attributed to the differences in management practices and seasonal or regional conditions, the uncertainties associated with the different methods used in measuring and computing ammonia emissions may also be one of the reasons.

Table 2-1 Reported ammonia concentrations and emission rates in broiler houses

References	Farm location	Ventilation rates of the house	Concentrations	Emission rates in original units	Emission rates in mg[NH ₃ -N] h ⁻¹ AU ⁻¹ (b)
Nicholson et al. (2004)	Nottinghamshire, UK	0.2-1.2 m ³ s ⁻¹		1.0-2.0 g [NH ₃ -N] h ⁻¹ 500kg ⁻¹ [lw] ^(a)	1000-2000
Missl brook, et al (2000)	UK			1.56-6.84 g [NH ₃ -N] h ⁻¹ 500kg ⁻¹ [lw]	1560-6840
Elwinger & Svensson(1996)	Sweden		10 ppm – 19 ppm at 28 d of age 26 ppm – 43 ppm at 35 d of age	5.4 g [NH ₃ -N] h ⁻¹ 500kg ⁻¹ [lw]	5400
Da Borso & Chiumenti(1999)	Italy			0.028- 0.154 g [NH ₃] day ⁻¹ bird ⁻¹	389-2139
Guiziou & Beline(2005)	North Brittany, France	0.02-2.76 m ³ s ⁻¹	0.8-32 ppm	5.74 g [NH ₃ -N] per bird produced 36.6-53.7 gN h ⁻¹	1594
Brewer & Costello (1999)	Arkansas, US		18 ppm	149-208 mg [NH ₃ -N] h ⁻¹ m ⁻²	2759-3852
Lacey et al.(2003)	Texas, US	27.8-90.6 m ³ s ⁻¹		12.8 g [NH ₃] h ⁻¹ 500kg ⁻¹ [lw]	10541
Redwine et al. (2002)	Texas, US	0.58-89 m ³ s ⁻¹	2-45 ppm	38-2105 g [NH ₃] h ⁻¹	283-15718

a: [lw] is liveweight;

b: Unit conversion is based on: 1 animal unit (AU) = 500kg [lw]; animal unit factor is 0.003 AU/bird; production cycle is 50 days; bird stocking density is 18 bird m⁻².

Emission rates are dependent on physical and chemical properties of litter (e.g., moisture content) and operational considerations (e.g., ventilation rate). Factors that affect these conditions include weather conditions and management practices, such as housing design, ventilation and heating/cooling system, drinker system, feed factors, litter management, etc.

2.3 THEORETICAL BASES OF AMMONIA EMISSION

2.3.1 General model

The mechanisms related to ammonia emissions from manure involve many processes and have been summarized by Ni (1999). Theoretically, the processes involved in ammonia emissions from litter-based manure include conversion of uric acid to urea, hydrolysis of urea, enzymatic and microbial generation of ammonia, diffusion of ammonia in litter, partitioning between the adsorbed and dissolved phase ammonia, the chemistry of ammonia in aqueous solution, partitioning between dissolved phase and gaseous phase ammonia, and the convective mass transfer of ammonia gas from the litter surface into the free air stream. These processes are summarized and illustrated in Figure 2-1. As shown in the figure, ammonia in the litter is generated from the biomass by means of enzymatic and microbial activities. Ammonium ions (NH_4^+) partitioning between solid phase and dissolved phase can be described using the Freundlich partition coefficient (K_f). Dissolved ammonia in the liquid layer on the surface of litter can exist in the form of NH_4^+ and free ammonia (NH_3). This can be expressed with the dissociation constant (K_d). Henry's constant (K_h) describes the equilibrium of free ammonia in the aqueous phase and in the gaseous phase. With convective mass transfer, the gaseous ammonia at the litter surface is emitted to the free air stream.

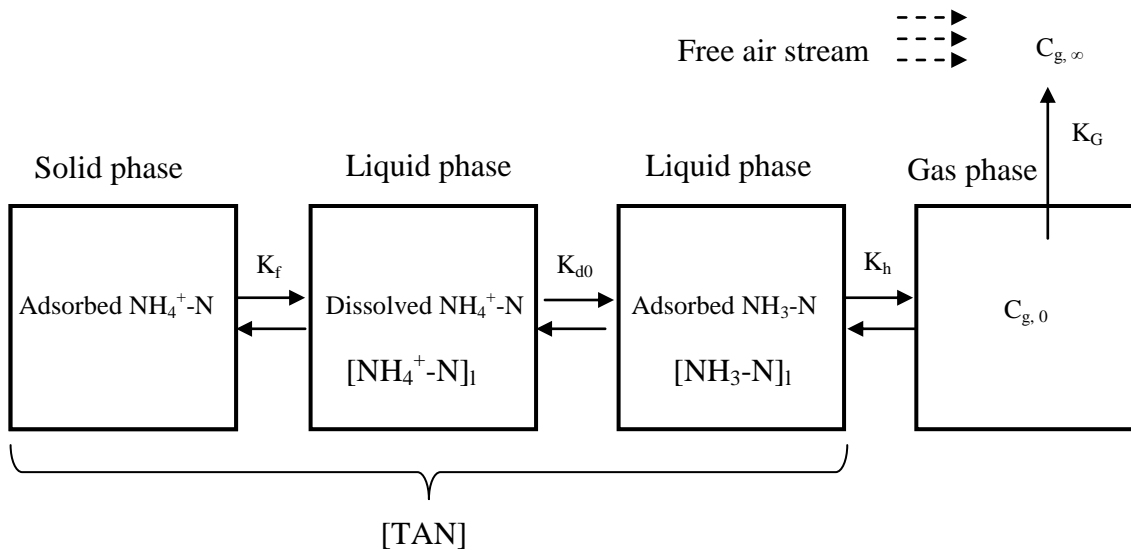
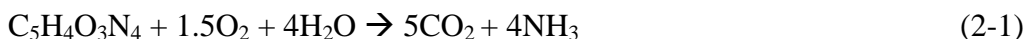


Figure 2-1. Illustration of processes related to ammonia emissions from broiler litter

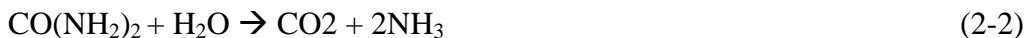
2.3.2 Generation of ammonia

When referring to the sum of NH₃ and NH₄⁺, the term “Total Ammonia” (TA) is adopted. Sometimes “Ammoniacal Nitrogen (AN)” or “Total Ammoniacal Nitrogen (TAN)” are used. The TA includes the mass of the hydrogen ion in the ammonia (NH₃) molecule and in the ammonium (NH₄⁺) ion, whereas the AN or TAN are based only on the mass of the nitrogen. The biochemical degradation processes of uric acid, urea and undigested proteins to produce TAN are complex but can be simplified as shown in Equations 2-1 to 2-3 (Koerkamp et al., 1998).

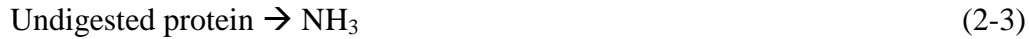
Aerobic decomposition of uric acid:



Urea hydrolysis:



Mineralization:



The degradation of uric acid and undigested protein is influenced by temperature, pH, and moisture content (Elliot and Collins, 1982; Whitehead and Raistrick, 1993; Bussink and Oenema, 1998). Urea hydrolysis is influenced by urease activity, pH, and temperature (Elzing and Monteny, 1997b).

Zhang (1992) developed 12 equations from laboratory studies to predict the generation rate of $\text{NH}_3\text{-N}$ and TA in the accumulating manure. They were functions of time, temperature and manure depth. Monteny et al. (1996) and Ruxton (1995) took into account the rate of urea conversion to ammonia to model production of ammonia. The maximum conversion rate was $2.7 \times 10^{-3} \text{ kg m}^{-3} \text{ s}^{-1}$ (Monteny et al. 1996).

2.3.3 Partitioning between adsorbed phase and dissolved phase ammonia

Ammonium ions in litter will partition into the adsorbed and dissolved phases. In the adsorbed phase, NH_4^+ binds onto the litter surface. The NH_4^+ in the adsorbed and that dissolved phases are in equilibrium. Freundlich isotherm has been used to describe NH_4^+ partitioning between adsorbed phase and dissolved phase (Bolt, 1976). It may be expressed as:

$$\text{Adsorbed } \text{NH}_4^+\text{-N} = 1000 \times K_f \times [\text{NH}_4^+\text{-N}]_l^{1/n} \quad (2-4)$$

In which,

Adsorbed $\text{NH}_4^+\text{-N}$ is the adsorbed $\text{NH}_4^+\text{-N}$ concentration on litter or medium, $\mu\text{g g}^{-1}$;

K_f is the Freundlich partition coefficient, L kg^{-1} ;

$[\text{NH}_4^+\text{-N}]_l$ is the concentration of dissolved phase $\text{NH}_4^+\text{-N}$, $\mu\text{g L}^{-1}$;

1/n is the Freundlich exponent, dimensionless.

For solutions with low concentrations, the Freundlich isotherm can be simplified to a linear isotherm by setting 1/n in Equation 2-4 equal to one.

2.3.4 Chemistry of ammonia in aqueous solution

The NH_3 and NH_4^+ in the solution are in aqueous equilibrium, which can be expressed as an acidic dissociation.



It is obvious that, as pH increases, the equilibrium is shifted towards more ammonia being released. The ratio of free ammonia nitrogen to TAN in solution increases with pH. The ammonia dissociation in litter can be calculated using the dissociation constant (K_d).

$$K_d = [\text{NH}_3] [\text{H}^+] / [\text{NH}_4^+] \quad (2-6)$$

The dissociation constant (K_d) is a function of temperature (in K). The dissociation constant in water solution (K_{d0}) can be expressed with the following semi-empirical equation (Kamin et al., 1979). At 25°C (298 K), $K_{d0} = 10^{-9.3}$.

$$\text{Log } K_{d0} = -0.0918 - 2729.92/T \quad (2-7)$$

In which,

K_{d0} is the dissociation constant of ammonia in water, dimensionless;

T is temperature in K.

Equation 2-6 assumes the activity of NH_3 , NH_4^+ and H^+ to be equal to the concentration of these species. These assumptions are valid in dilute aqueous solutions (Stumm and Morgan, 1996). Various dissociation constants have been reported in livestock manure, and

differences in K_d between ammonium-water solutions and manure have been documented (Hashimoto and Ludington, 1971; Arogo et al., 2003; Zhang, 1992). These differences are attributed to two factors: 1) the presence of organic matter and 2) the presence of other ions in solution (Montes, 2008). In the study of Srinath and Loehr (1974), Cumby et al. (1995), Olesen and Sommer (1993), and van der Molen et al. (1990), the dissociation constants in livestock manure were reported to be approximately the same as that for ammonia in water. However, Hashimoto and Ludington (1971) reported that, for ammonia in concentrated chicken manure, the dissociation constant was about one-sixth of that for ammonia in water. Zhang (1992) reported that, for ammonia in diluted finishing pig manure of 1% total solids content, the dissociation constant was approximately one-fifth of that for ammonia in water. The dissociation constant in manure (K_d) was often expressed by multiplying K_{d0} with a ratio α that incorporates the effect of solids and ions.

$$K_d = \alpha K_{d0} \quad (2-8)$$

The reported ratio α varied from 0.16 to 1 (Hashimoto and Ludington, 1971; Zhang, 1992; van Der Molen et al., 1990; Liang et al., 2002; Arogo et al., 2003).

2.3.5 Partitioning between dissolved phase and gaseous phase ammonia

At low concentrations (e.g. less than 1000 mg/L) in the solution, the partition between gas phase and dissolved phase ammonia can be assumed to obey Henry's law (Anderson, et al., 1987). The equilibrium concentration of gas phase ammonia can be estimated from the concentration of dissolved phase $\text{NH}_3\text{-N}$ and Henry's constant (K_h).

$$K_h = [\text{NH}_3\text{-N}]_l / (14/17 \times C_{g, 0}) \quad (2-9)$$

In which,

K_h is Henry's constant, dimensionless.

$[\text{NH}_3\text{-N}]_l$ is the concentration of dissolved phase $\text{NH}_3\text{-N}$, $\mu\text{g L}^{-1}$;

$C_{g,0}$ is gas phase ammonia concentration in equilibrium with dissolved ammonia in litter, mg m^{-3} ;

Ni (1999) found that Henry's constants in the models of ammonia release from manure had diverse forms and adopted different definitions and units. He suggested that the non-dimensional form of Henry's constant was more convenient when incorporated in ammonia release models. Hales and Drewes (1979) developed the following empirical equation to calculate K_h in non-dimensional form as a function of temperature.

$$\text{Log } K_h = -1.69 + 1477.7/T \quad (2-10)$$

In Equation 2-10, T is temperature in K. The equation indicates that an increase of temperature will result in a lower Henry's constant, and therefore result in an increase of the gas phase ammonia concentration.

2.3.6 Mass transfer of ammonia gas from emission surface to the free air stream

The process of ammonia emissions from litter is essentially the transport of dissolved phase ammonia to gaseous phase ammonia in the free air stream. The two-film theory (Welty et al., 1984) and boundary layer theory (Ni, 1999) have been used to describe the interface transport system.

(1) Two-film theory

The two-film theory (Welty et al., 1984) has been used to model ammonia released from flooded soil systems (Jayaweera and Mikkelsen, 1990) and pig manure (Zhang, 1992, Anderson et al., 1987). Figure 2-2 illustrates the two-film theory. In the two-film theory, under steady state conditions, ammonia flux through the gas film is the same as that through the liquid film as expressed in Equation 2-11 (Welty et al., 1984).

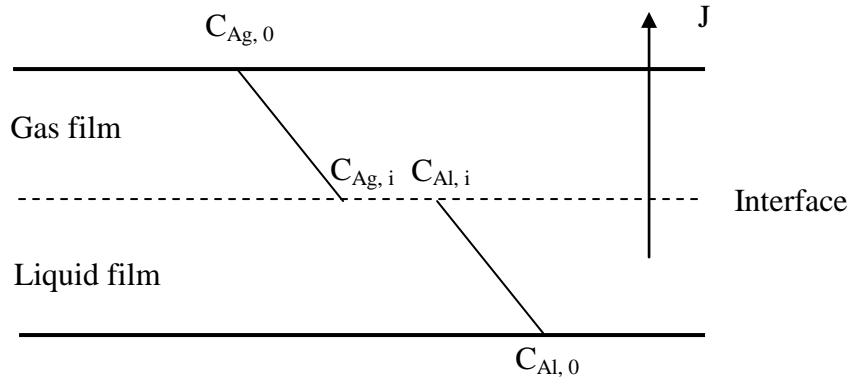


Figure 2-2. Illustration of the two-film theory

$$J = k_g (C_{Ag, i} - C_{Ag, 0}) = k_l (C_{Al, 0} - C_{Al, i}) \quad (2-11)$$

In which,

J is emission flux, $\text{mg m}^{-2} \text{h}^{-1}$;

k_g is mass transfer coefficient in the gas film, m h^{-1} ;

k_l is mass transfer coefficient in the liquid film, m h^{-1} ;

$C_{Ag, 0}$ is ammonia concentration at the immediate gas film surface, mg m^{-3} ;

$C_{Ag, i}$ is ammonia concentration at the interface in gas phase, mg m^{-3} ;

$C_{Al, i}$ is ammonia concentration at the interface in liquid phase, mg m^{-3} ;

$C_{Al, 0}$ is ammonia concentration at the immediate liquid film surface, mg m^{-3} .

$C_{Ag, i}$ and $C_{Al, i}$ are practically not measurable. Jayaweera and Mikkelsen (1990) defined the Henry's constant (K_h) in a non-dimensional form, as

$$K_h = C_{Ag, i} / C_{Al, i} \quad (2-12)$$

Therefore, the ammonia flux can be calculated on the overall driving force between $C_{Ag,0}$ and $C_{Al,0}$.

$$J = K_G (K_{h,0} \times C_{Al,0} - C_{Ag,0}) = K_L (C_{Al,0} - C_{Ag,0} / K_{h,0}) \quad (2-13)$$

$$1 / K_G = 1 / k_g + K_{h,0} / k_l \quad (2-14)$$

$$1 / K_L = 1 / k_l + 1 / (K_{h,0} \times k_g) \quad (2-15)$$

In which,

K_G is overall mass transfer coefficient in the gas film, $m\ h^{-1}$;

K_L is overall mass transfer coefficient in the liquid film, $m\ h^{-1}$;

Ni (1999) reviewed ammonia emission models using the two-film theory and found that the ammonia transfer in gas phase was the major focus in these models. The mass transfer inside manure and across the interface has received less attention. Zhang (1992) and Arogo et al. (1996) accepted the assumption that, for highly soluble gases such as ammonia, the transfer through the gas film controls the interface transport system. In their equation, $C_{Ag,i}$ was approximated by the gas phase concentration at the emission surface $C_{Ag,0}$. In their models, the thickness of the gas and liquid films was not defined, and the ammonia flux was calculated based on the concentration difference between gas phase concentration at the emission surface and in the free air stream (Ni, 1999).

$$J = k_g (C_{Ag,0} - C_{g,\infty}) \quad (2-16)$$

In which,

$C_{Ag,0}$ is gas phase ammonia concentration at the emission surface, $mg\ m^{-3}$;

$C_{g,\infty}$ is gas phase ammonia concentration in the free air stream, $mg\ m^{-3}$.

In Equation 2-16, the application of the two-film theory in the models of ammonia

released from manure has been simplified. It actually did not include the mass transfer across the films.

(2) Boundary layer theory

In the boundary layer theory, when a free air stream flows over a surface and the gas phase ammonia concentration at the surface $C_{g,0}$ differs from that in the free air stream $C_{g,\infty}$, a concentration boundary layer will develop (Ni, 1999). Conditions within the concentration boundary layer determine the mass transfer flux. The boundary layer theory has a simpler structure than the two-film theory, and it has been used in the models of ammonia released from applied fertilizer (van der Molen et al., 1990) and stored pig slurry (Olesen and Sommer, 1993). In those models, the gas phase ammonia concentration difference was taken between the slurry surface and a specified height above the surface, and the flux equation took a form similar to Equation 2-16.

2.3.7 The mass transfer coefficient

The mass transfer coefficient is an important parameter in modeling ammonia emission. In the literature, the values of the mass transfer coefficient obtained in different experiments of ammonia emission from manure vary widely ranging from 1.3×10^{-6} to 11.7×10^{-3} m/s (Ni, 1999). The variation is partly due to the physical characteristics of the mass transport process, such as air flow velocity and flow pattern, and partly due to the various forms of mass transfer coefficient (k_g , k_l , K_G , and K_L). The overall mass transfer coefficient (K_G and K_L) may include cumulative effects of various assumed values for the Henry's and dissociation constants used in different models (Montes, 2008).

There were also many reported empirical relationships for ammonia emissions from manure based on the mass transfer coefficient obtained in the laboratory or field experiments (Zhao and Chen, 2003; Arogo et al. 1999; Elzing and Monteny (1997a, b; Monteny et al., 1998; Monteny and Lamaker, 1997; Aarnink, 1997; Monteny et al., 1996;

Ruxton, 1995; Zhang, 1992; Anderson et al., 1987; Muck and Steenhuis, 1982; Koelliker and Miner, 1973). Almost all of the reported mass transfer coefficients are very closely related to the air velocity on the manure surfaces, which suggests that convective transfer plays a dominant role in the mass transfer process (Ni, 1999). Most of the reported empirical relationships estimated mass transfer coefficient as function of air velocity and temperature. In those correlations, the influence of either or a combination of the two factors on the mass transfer coefficient of ammonia was considered. Rachhpal-Singh and Nye (1986) reported that surface roughness was also an important factor, but did not give an equation.

Through empirical measurements, Haslam et al. (1924) determined mass transfer coefficients k_g and k_l for ammonia as:

$$k_g = 5.31 \times 10^3 (3.28U)^{0.8} T^{-1.4} \quad (2-17)$$

$$k_l = 5.1 \times 10^{-7} T^4 \quad (2-18)$$

In which,

k_g is mass transfer coefficient in the gas phase, $\text{g cm}^{-2} \text{atm}^{-1} \text{h}^{-1}$;

k_l is mass transfer coefficient in the liquid phase, cm h^{-1} ;

U is air velocity, m s^{-1} ;

T is temperature, K.

It can be seen that the k_g defined by Haslam et al. (1924) is negatively related to the temperature, while k_l is positively related to the temperature. The negative power of the temperature in Equation 2-17 is explained by the increasing viscosity of the air at higher temperature, which is inversely related to k_g (Haslam et al., 1924). Mass transfer coefficients developed by Haslam et al. (1924) were widely cited and used as a basis for

emission models in literature (Koelliker and Miner, 1973; Muck and Steenhuis, 1982; Ruxton, 1995; Monteny et al., 1996; Monteny and Lamaker, 1997; Aarnink, 1997; Anderson et al., 1987). Chaoui et al. (2008) did a transformation to convert the unit of k_g to $m s^{-1}$. The result of this transformation is:

$$k_g = 0.1842 U^{0.8} T^{-0.4} \quad (2-19)$$

Arogo et al. (1999) calculated the overall mass transfer coefficient (K_L) of ammonia in liquid swine manure, and reported that K_L increased as liquid temperature increased and decreased as air temperature increased. The possible reasons for the positive effect of liquid temperature on K_L include: increased diffusivity of the solute, high equilibrium dissociation constant and a lower solubility of ammonia in water at higher liquid temperature (Arogo et al., 1999).

Zhang (1992) developed the following overall mass transfer coefficient for the liquid phase in laboratory experiments using swine manure.

$$K_L = 1.4625 \times 10^{-6} - 3.6685 \times 10^{-6} U + 2.3611 \times 10^{-7} U T + 6.4618 \times 10^{-6} U^2 \quad (2-20)$$

In which, K_L is in $m s^{-1}$, T in $^{\circ}C$, and U in $m s^{-1}$.

Zhao and Chen (2003) measured the gas phase mass transfer coefficient in dairy manure and reported that the mass transfer coefficient decreased logarithmically with an increase in temperature under both aerated and anaerobic conditions. Elzing and Monteny (1997a, b) and Monteny et al. (1998) also reported similar negative relationships between temperature and the mass transfer coefficient.

Based on the equations in Incropera et al. (1990), mass transfer coefficients for laminar and turbulent air conditions were developed as shown below.

For laminar air conditions (Cortus et al., 2006),

$$k_g = 0.821T^{0.7}U^{0.5}L^{-0.5}D^{0.67} \quad (2-21)$$

For turbulent conditions (Teye and Hautala, 2008)

$$k_g = 3T^{0.13}U^{0.8}L^{-0.2}D^{0.67} \quad (2-22)$$

In which, L is the characteristic length, m; D is the diffusivity in air, $m^2 s^{-1}$; T is air temperature in K; U is air velocity in $m s^{-1}$.

It was found that while the empirical mass transfer coefficients were reported to be influenced by temperature in different ways due to their different forms, there is general agreement that mass transfer coefficients are proportional to air velocity to the 0.8 power or so. Air velocity has the effect of reducing the boundary layer thickness over the liquid surface. As the velocity increases, the turbulence intensity also increases resulting in a thinner boundary layer formed at the interface. The thinner the boundary layer, the lower the resistance to the volatilization process, thereby leading to a larger mass transfer coefficient and mass transfer rate (Arogo et al., 1999).

2.4 FACTORS INFLUENCING AMMONIA EMISSIONS FROM BROILER LITTER

Ammonia emission from litter can be influenced by both litter properties and environmental conditions. In general, factors that may influence ammonia emissions from broiler litter include: air and litter temperature, ventilation rate, litter pH value, litter nitrogen content, and litter moisture content.

2.4.1 Air and litter temperature

Temperature is a very important variable in the process of ammonia emission from litter. Air temperature influences the convective mass transfer coefficient. Litter temperature influences Henry's constant, the dissociation constant, and also the diffusion and generation of ammonia in litter. Therefore, ammonia flux can be greatly affected by

temperature variation. In broiler houses air temperature is usually managed to optimize bird health and productivity. It is often set at an initial temperature of 32 to 35°C during brooding and lowered by 3°C every seven days to $22 \pm 2^\circ\text{C}$ after 3 weeks of age (Nicholson et al., 2004; Elwinger and Svensson, 1996). The whole growth cycle of birds in broiler houses is typically up to 7 weeks (Lacey et al., 2003), from 0-day-old to the time of slaughter. In warm weather, it is a common practice to increase the ventilation rate to maintain the target air temperature. The ventilation requirement will change with ambient air temperature, and variation in ventilation rate causes variation in ammonia fluxes. For summer housed flocks, mean ammonia fluxes were almost double those from winter housed flocks because of higher ventilation rates in warm weather (Nicholson et al., 2004).

2.4.2 Ventilation rate

Ventilation is the primary method used to control the air quality inside the broiler houses. It removes heat, moisture and gas pollutants from broiler houses. The ventilation rate in broiler houses can vary in a wide range. Ventilation rates were measured between 0.58 and $89 \text{ m}^3\text{s}^{-1}$ per house in the study by Redwine et al (2002). It was reported that the higher ventilation rates resulted in lower ammonia concentrations in broiler house (Redwine et al., 2002), but higher ammonia emission rates (Nicholson et al., 2004). As ventilation rates increase, there will be more dilution in the broiler house. Therefore, the ammonia concentration in the free air stream in broiler house will decrease. In the general mass transfer flux equation (Equation 2-16), it is obvious that emission flux will increase as $C_{g, \infty}$ decreases and the difference between $C_{g, 0}$ and $C_{g, \infty}$ increases.

The higher ammonia fluxes at higher ventilation rates is also due to a higher mass transfer coefficient, as the mass transfer coefficient is a function of air velocity at the litter surface. There are very few studies which have reported the air velocity at the litter surface. Although the ventilation rates can vary widely in practice, Brewer and Costello (1999) reported that the mean air speed at 25 cm height was 0.24 m/s with a standard deviation of 0.14 m/s in a conventional cross-ventilated house (sidewall ventilation). No report has been

found on the litter surface horizontal air velocity in tunnel-ventilated houses, though the average air velocity estimated from ventilation rate and dimension of the house (Lacey et al., 2003) was more than 0.8 m/s.

2.4.3 Litter pH value

The pH value of litter is one of the most important factors that determines the aqueous phase ammonia concentration, and therefore influences ammonia release. Research has demonstrated that in broiler houses ammonia release from litter is negligible at litter pH below 7 (Reece et al., 1985). Ammonia release began when pH was near 7 and increased dramatically as pH further increased above 7. Chemical treatments have been studied in laboratory tests as a way to suppress ammonia volatilization, by chemically lowering the litter-solution pH so that the majority of ammoniacal N remains ionized and nonvolatile. Witter and Kirchmann (1989) tested calcium chloride and magnesium chloride applications to liquid chicken manure and found reductions in total ammonia losses of 30 and 50%, respectively. Moore et al. (1996) tested several treatments for broiler litter and found that aluminum sulfate, phosphoric acid, and ferrous sulfate each worked well in reducing ammonia losses. However, control of litter pH over the life of the flock has proven to be a difficult task (Lacey et al., 2004; Carr et al., 1990).

During the process of gas release, the pH of litter will also be influenced by the release of gases. Release of CO₂ will increase the pH. Because of its large concentration in manure, the release of CO₂ acts as an accelerating factor for the release of ammonia (Ni, 1998). In liquid animal manure, pH is also influenced by buffer systems. Husted et al. (1991) found that HCO₃⁻ and NH₄⁺ were the dominating buffer components in the release of ammonia.



2.4.4 Litter moisture content

Urea hydrolysis is a major source of ammonia. Litter moisture content will affect the conversion rate of uric acid to ammonium-N (Sims and Wolf, 1994). It has been reported qualitatively that wet litter can lead to high ammonia levels in broiler houses (Elliot & Collins, 1982) and may cause bird health problems such as hock burn (Tucker & Walker, 1992). However, overly dry litter may result in more dust particulates, which can serve as a transport mechanism for ammonia. On the other hand, very wet conditions may slow/shut down microbial and enzymatic activities due to scarcity of oxygen.

Litter moisture content may vary in a wide range. Elwinger and Svensson (1996) reported that the dry matter content was 91.6%-92.2% for fresh bedding materials, and was about 64% at 35 d of age. In practice, litter moisture is also influenced by ventilation and drinking system management. The design of broiler drinking systems has been shown to influence the usage of water and broiler litter moisture content (Tucker & Walker, 1992). Spillage causes excessive litter moisture.

It has been reported that higher litter dry matter content and lower ammonia emissions were measured from broilers using nipple drinkers than those using traditional bell drinkers (Nicholson et al., 2004; Elwinger and Svensson, 1996). Similar results were also obtained by Da Borso and Chiumenti (1999) who found that buildings equipped to prevent water dripping onto the litter from nipple drinkers emitted less ammonia than those with standard design nipple drinkers. Carr et al. (1990) commented that it was desirable to maintain litter moisture below 30% for ammonia control. However, Carr et al. (1990) also reported a decrease in ammonia concentrations at high moisture (44% wet basis) and temperature (29 °C). The decrease in ammonia concentrations at high moisture levels has also been reported by Valentine (1964) and Schefferle (1965). The comprehensive effect of litter moisture content is complex and still not fully understood.

2.4.5 Litter nitrogen content (diet, litter age and bird age)

It would be reasonable to assume that ammonia emissions are positively related with litter nitrogen or TAN content. An increase in feed protein level significantly increased litter nitrogen content, and therefore increased ammonia emission rate (Elwinger and Svensson, 1996). Re-used litter (use of old litter as bedding for subsequent flocks) has more nitrogen content. It has been reported that ammonia flux from reused litter was six times that from new bedding material at the start of a grow-out (Brewer and Costello, 1999). Several researchers reported that ammonia emissions increased with age of bird (Elwinger and Svensson, 1996; Redwine et al., 2002). It may also be due to increase of litter nitrogen content with increase in bird age.

Elwinger and Svensson (1996) reported that nitrogen content in broiler litter was about 45 g/kg dry matter; for fresh wood shavings, it was 1.0 g/kg dry matter; for fresh wheat straw, 4.6 g/kg dry matter. It can be seen that the nitrogen content in litter is mainly from manure.

2.4.6 Litter type

Generally there was no difference in ammonia emissions related to litter type or amount used (Elwinger and Svensson, 1996). It has been reported that ammonia emissions from broilers on straw were higher than for those on wood shavings, but the lower emission rates from birds on wood shavings were considered to be due to the greater amount of dry bedding solids added (Nicholson et al., 2004).

2.5 REVIEW OF AMMONIA EMISSION MODELS IN ANIMAL HOUSES

Emission models that have been published for ammonia emission from AFOs include mechanistic models (Ni, 1999; Arogo et al., 2006), statistical models (Carr et al., 1990; Wheeler et al., 2006), nitrogen-mass flow models (Reidy and Menzi, 2006; Dammgen et

al., 2002), and inverse dispersion models (Siefert et al., 2004). Mechanistic models provide physical and chemical understanding as well as quantitative description of ammonia release. Mechanistic models are basis of so called process-based models, which were recommended by the NRC (NRC, 2003). Process based models consider each of the processes occurring on a typical livestock farm, and calculate the resulting ammonia emissions from each (Zhang et al., 2006; Pinder et al., 2004). Nitrogen-mass flow models start with a specific amount of nitrogen excreted by animals and simulate the TAN flow over the different stages of emissions (grazing, housing, manure storage and application). Statistical models simply describe the statistical correlations between emissions and selected influencing factors. Inverse dispersion plume models can be used to estimate ammonia emissions after being fitted to the observed downwind ammonia concentration profile. This section provides a brief review of these models and their applications in animal houses.

2.5.1 Mechanistic models

Mechanistic models account for the major physical and chemical processes determining emission. Mechanistic models that represent the processes involved, as influenced by production and environmental conditions, provide robust tools for evaluating management impacts on emissions (Ni, 1999; Arogo et al., 2006). The core in the mechanistic approaches is usually a model of convective mass transfer of ammonia in the liquid-air interface (Ni, 1999).

The animal housing emission model described in Hutchings et al (2006) and Pinder et al (2004) used the following formula to calculate the instantaneous ammonia emission in an animal house.

$$\text{Emissions} = A [\text{TAN}] H^* \times r^{-1} \quad (2-25)$$

In which,

A is the area of exposed manure, m^2 ;

[TAN] is the concentration of total ammoniacal nitrogen (TAN) in manure, kg/m^3 ;

H^* is the effective Henry's constant, dimensionless, which determines the partitioning between gas phase ammonia and TAN.

r is the mass transfer resistance, $day\ m^{-1}$.

Calculation of H^* requires knowledge of the temperature and pH of the manure. The mass transfer resistance (r) is the sum of the aerodynamic, quasi-laminar, and surface resistances. A complete description of the calculations for these resistances can be found in Olesen and Sommer (1994). The mass transfer resistance (r) is related to air velocity, which can be calculated using a ventilation sub-model for the animal house.

The following is another equation that has been used to calculate ammonia emissions in animal houses (Zhang et al., 2006).

$$\text{Emission rate} = Q (C_{\text{house}} - C_{\text{out}}) \quad (2-26)$$

In which,

Q is the ventilation rate, $m^3\ s^{-1}$;

C_{house} is gas phase ammonia concentration in house air, $mg\ m^{-3}$;

C_{out} is gas phase ammonia concentration in outside air, $mg\ m^{-3}$;

Mass balances were used to derive differential equations to calculate the concentration of ammonia in the house air. Energy balances were used to predict indoor air temperature and ventilation rate, which were incorporated into the ammonia emission rate calculations. Various sub-models have been used in the mechanistic approaches. They included the mass transfer coefficient, Henry's constant, dissociation constant, ammonia generation in manure

and ammonia diffusion in manure (Ni, 1999). Zhang (2006) used a mechanical ventilation sub-model calculate ventilation rate.

(1) Ventilation sub-models

The large temporal variation in ammonia emissions from agriculture is caused partly by the weather and partly by growth stage of the animals. It is a common practice in the broiler industry to manipulate minimum ventilation rates continuously to strike a balance between the need for energy conservation and indoor air conditions (Gates et al., 1996).

Thermal energy models have been used to simulate the inside temperature and ventilation rate of animal housing with forced ventilation (Hutchings et al. 2006; Zhang et al. 2005; Koerkamp et al. 1998). The models assume that the aim of management is to maintain the indoor temperature at a target value suitable for the animal species. The ventilation rate necessary to achieve this objective is calculated from the outside temperature and the sensible heat production of the animals (CIGR, 2002). An empirical constant is then used to obtain the resistance to ammonia transport. Casey et al. (2003) reported that daily mean ventilation rate increased with bird age.

(2) N-excretion sub-models

The source of TAN is animal excretion. An animal excretion sub-model was proposed to calculate the manure and nitrogen excretion of animals in response to type and growth stage of animals, feed rations, animal productivity and animal management practices (Zhang et al., 2006).

The American Society of Agricultural and Biological Engineers (ASABE) developed standard methods for estimating manure and nutrient production from different types of animals based on animal nutrition models (ASABE, 2005). A model for estimating poultry manure nutrient excretion has been published by Applegate et al. (2003). The ASABE Standard (ASABE, 2005) for animal manure production and characteristics were used as

the basis for developing the manure and N excretion model.

2.5.2 Process based models

Activities are underway, nationwide, to study emissions from AFOs as a whole from various system components including animal housing, and manure storage (Mukhtar et al., 2004). Process based models consider each of the processes occurring on a typical livestock farm, and calculate the resulting ammonia emissions from each. They account for site-specific design and management practices as variables and reflect interactions between emission sources.

Certain processes of the animal enterprise are likely to be more important for some emissions than for others. Development of a process-based model would enable system analysis and simulation for determining critical control points for emissions (Kohn et al., 1997). It would also highlight fruitful research areas and identify knowledge gaps that need to be filled in order to improve understanding of whole farm processes.

The NRC recommended that EPA and USDA should use process based mathematical models with mass balance constraints for nitrogen-containing compounds, methane, and hydrogen sulfide to identify, estimate, and guide management changes that decrease emissions for regulatory and management programs (NRC, 2003).

2.5.3 Statistical models

Statistical models simply describe the statistical correlations between target parameters and selected influencing factors. They can be directly used for emission estimation, and may also be useful in assessing the accuracy of mechanistic approaches.

By using the SAS GLM Procedure, Carr et al (1990) developed a semi-logarithmic model, which shows that ammonia concentration increased with litter pH, temperature, and litter moisture content. A non-linear model was also developed which was capable of

predicting pH as a function of house atmospheric temperature, relative humidity, and litter moisture content (Carr et al., 1990).

Excellent fit has been observed for the regression of emission rates with bird age in broiler houses. These regressions can be used to estimate emission rates during similar weather conditions for any bird age between 1 – 60 days (Gates et al. 2004; Wheeler et al. 2004).

Statistical models usually are simple in structure and are easy to use. However, they do not contribute much to the understanding of the physical and chemical processes of ammonia release.

2.5.4 Mass balance and N-flow models

The mass balance modeling approach was regarded as one of the best methods to estimate ammonia emissions by the National Research Council (2003). In the mass balance model, the total nitrogen inputs and outputs in the various components of an animal waste management system are quantified, and the difference between inputs and outputs is assumed to be volatilized nitrogen. This method does not distinguish among losses of N as N_2 , NO_x , or NH_3 . Also, it cannot predict daily cycles in emissions or maximum concentrations. However, it can provide an accurate estimate of the upper limits on ammonia emissions over long production cycles (several days to months) (Keener and Zhao, 2006). The mass-balance approach is simple and costs less, and it appears to be a promising method for providing accurate long-term ammonia emission estimates from poultry broiler production units.

Mass-conservative N-flow models, such as DYNAMO (Dynamic Ammonia Emission Model), have been used in the framework of the national NH_3 emission inventory calculations and manure policy analyses in different countries of Europe (Reidy et al., 2006). These models start with a specific amount of nitrogen (N) excreted by a defined

livestock category and simulate the TAN flow over the different stages of emissions (grazing, housing, manure storage, and application). At each stage of manure management, a proportion of TAN will be subtracted from the TAN pool, mainly as emitted NH₃, and the rest passed on to the next stage. Ammonia emissions are generally calculated with EF (emission factors), where EF is the percentage of the respective TAN pool emitted.

The EFs used in N-flow models are largely empirical, and they are specific to certain types of management or climatic regions. The variations in the calculated emissions are primarily the result of the distinct national emission factors and N excretion rates. The current EFs do not reflect annual variability.

The N-mass flow model enables rapid and easy estimation of the consequences of upstream emission at downstream emissions. It has been adopted to calculate the interaction between abatement techniques at various stages of manure management (Dammgen et al., 2002).

2.5.5 Inverse dispersion models

An inverse dispersion model was developed to measure ammonia emissions from broiler houses (Siefert et al., 2004). Passive samplers were deployed in an array downwind from the broiler house. A Lagrangian-based, inverse Gaussian dispersion plume model was fitted to the observed ammonia concentration profile to determine the total ammonia emissions from the house. Normalizing this value to the number of birds allowed one to calculate an emission factor corresponding to the sampling period. The primary advantage of this approach was that it allowed for the determination of ammonia emissions at various growth stages under “real world” growing conditions (Siefert et al. 2004).

Various dispersion models such as ISCST3, AERMODPRIME, WindTrax®, and AUSTAL have been used determining ammonia emissions rates. ISCST3 and AERMOD are Gaussian plume models, while WindTrax® and AUSTAL are backward and forward

Lagrangian Stochastic models, respectively. It has been reported that calculated emission rates and/or emission factors are model specific, and no simple conversion factor can be used to adjust factors between models. Therefore, emission factors developed using one model should not be used in other models to determine downwind pollutant concentrations (Faulkner et al. 2006).

2.5.6 Summary

Emission models can increase the simplicity of emission estimation over direct measurement. Various emission models have been developed to fit different objectives. For example, when considering the acute health effects of emissions for nearby residents, short-term emissions would be needed, and a dynamic mechanistic model to predict emissions on a daily basis or more frequent basis may be recommended. When considering long-term emissions, an aggregated model such as a mass balance model may be adequate.

Chemical transport modeling requires daily or even hourly variations in ammonia emission estimation for accurately predicting formation of ammonium nitrate and ammonium sulfate. Therefore, it would be important to improve temporal resolution as well as geographical resolution of ammonia emission models to meet the requirement.

Models are being further developed, and many challenges exist. Much work remains to be done because of the number of variables in practice. Further evaluation of these variables is needed for enhanced understanding of the wide variation in ammonia emission rates.

3. EXPERIMENTAL METHODS

3.1 EXPERIMENTAL SETUP

Conducting experiments in actual broiler houses and controlling environmental conditions is difficult and expensive, and it may also generate high uncertainties. For this study, a dynamic flow-through chamber system and a wind tunnel were designed to measure ammonia emissions from broiler litter. The dynamic flow-through chamber was mainly used to investigate ammonia emissions from various litter samples. The wind tunnel was used to investigate ammonia emissions under various wind profiles.

3.1.1 Dynamic flow-through chamber

Air chamber methods of flux measurement can be categorized as “static” or “dynamic”. Static methods often consist of a sealed glass jar or open bottomed cylinder placed over the sample area. Such systems contain ammonia absorbers to quantify ammonia production. Moore et al. (1996) used a static chamber to estimate ammonia flux from broiler litter. In their technique, aerial ammonia concentration in the chamber was measured at regular intervals using Sensidyne ammonia detection tubes. They attempted to promote gas mixing inside the chamber using a manual stirring fan prior to each gas sampling event; however, no air movement was provided during other times (Brewer and Costello, 1999; Moore, et al., 1996). Static methods allow for only periodic ventilation (if any) which significantly reduces convective air movement and ammonia volatilization (Marshall and DeBell, 1980). In the other hand, dynamic methods employ a ventilated chamber where fresh and ammonia free air is directed into the chamber and passed over the samples to promote convective conditions similar to that outside the chamber (Brewer and Costello, 1999).

A diagram and the photographs of the chamber system developed for this study are shown in Figures 3-1 and 3-2 respectively. The chamber body has a cylindrical shape with

bottom diameter (inside measurements) of 0.400 m and height of 0.394 m. Broiler litter (2000g) was placed on the bottom of the chamber and a vacuum pump was used to draw air through the chamber at a design flow rate via flow meters (Gilmont Shielded Industrial Flow meter, accuracy $\pm 5\%$). Before entering the chamber, the ambient air passed through an acid scrubber or an activated carbon filter so that background ammonia was removed. A motor driven stainless steel impeller mixed the air inside the chamber and provided convective conditions. The entire chamber body was made of stainless steel to minimize ammonia adsorption. Ammonia concentration at the chamber outlet was measured by a Thermo Environmental Instruments (TEI) chemiluminescence ammonia analyzer (Model 17C) as well as an acid scrubber. A HOBO data logger was used to record the measurements of the ammonia analyzer at one-minute intervals.

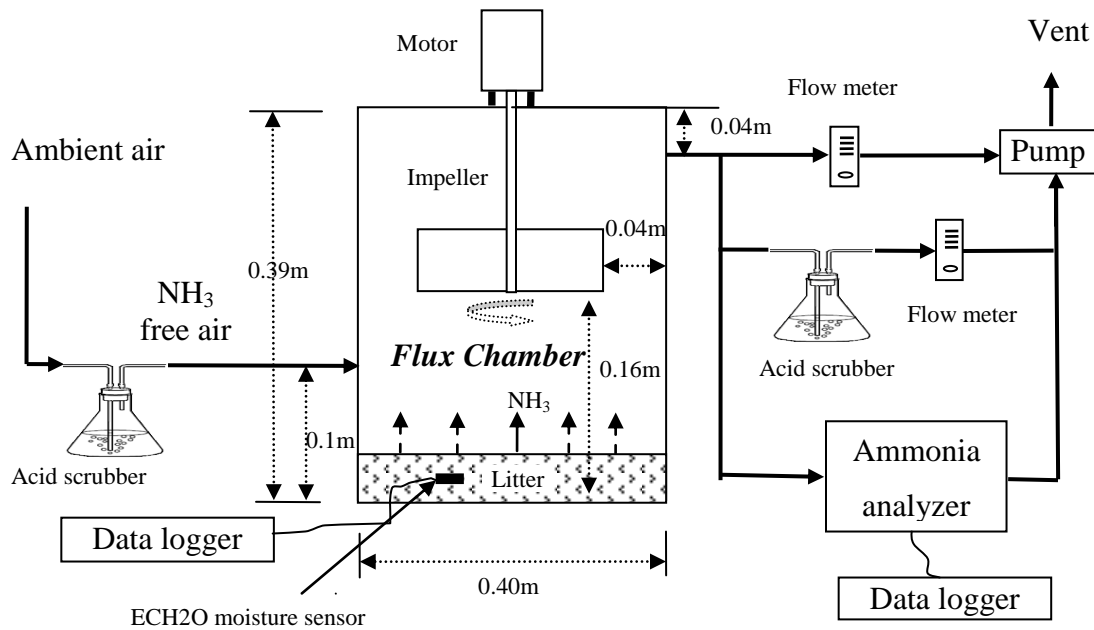


Figure 3-1. Diagram of the dynamic flow-through chamber system

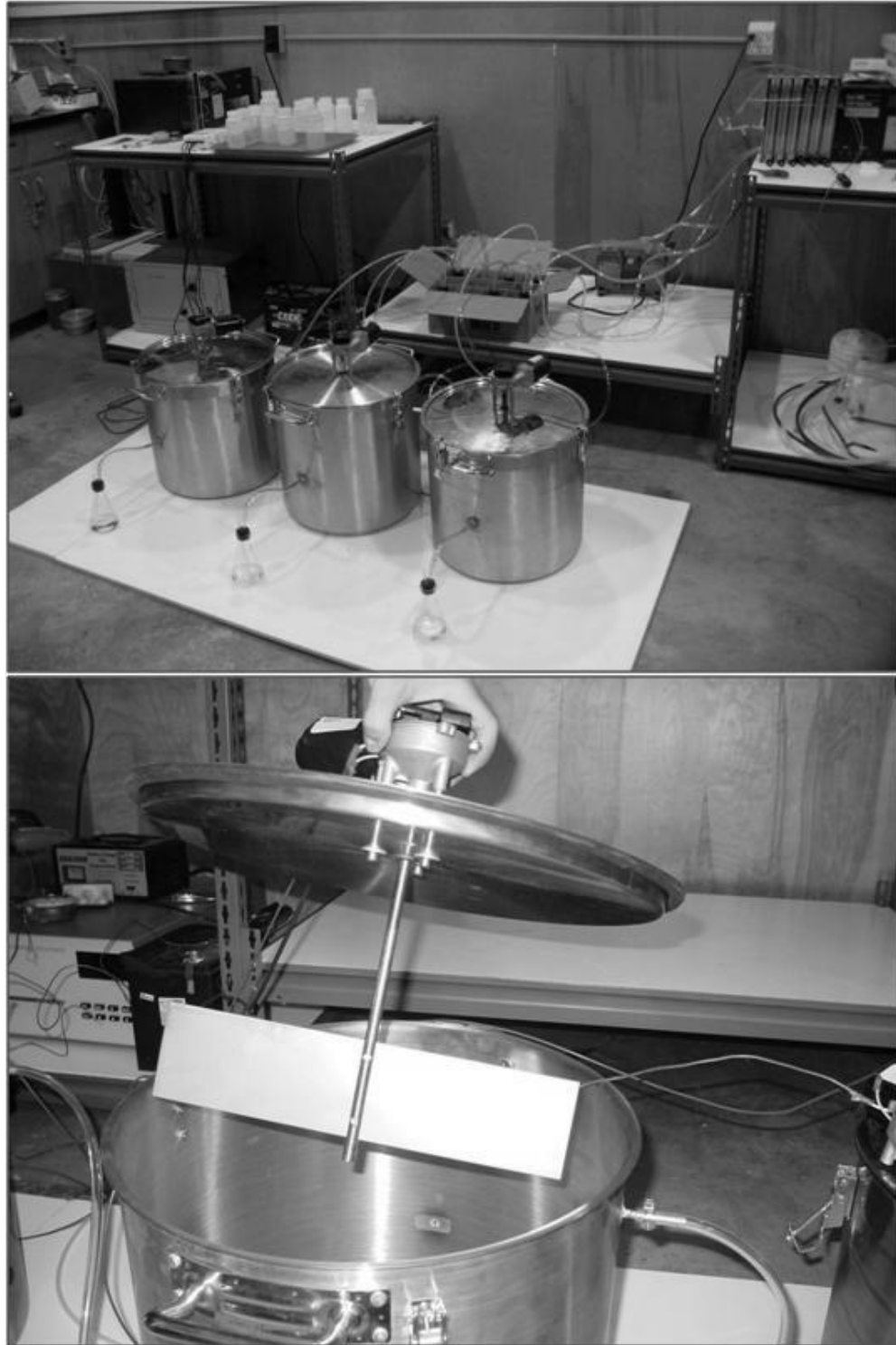


Figure 3-2. Photographs of the dynamic flow-through chamber system

The dynamic chamber system, with the continuous stirring provided by the impeller, meets the necessary criteria for performance as a continuously stirred tank reactor (CSTR) (Aneja, 1976). Measurements of ammonia concentration at different locations in the chamber also showed no significant difference. Therefore, measurements at the chamber outlet were assumed to represent the ammonia concentration in the chamber.

The ammonia fluxes from the litter surface inside the chamber were calculated using the following mass balance equation (Aneja et al., 2000):

$$dC/dt = QC_0/V + JA/V - QC/V \quad (3-1)$$

In which,

C is ammonia mass concentration in the chamber, mg m^{-3} ;

Q is flow rate of the carrier gas through the chamber, $\text{m}^3 \text{h}^{-1}$;

C_0 is ammonia concentration in the inlet gas stream, mg m^{-3} ;

V is volume of the chamber space above litter, m^3 ;

J is ammonia emission flux, $\text{mg m}^{-2} \text{h}^{-1}$;

A is chamber bottom surface area, m^2 .

Since background ammonia was removed from the carrier gas, $C_0=0$. At steady state, $dC/dt=0$. So the ammonia emission flux J can be obtained from the following equation:

$$J = (Q/A) C \quad (3-2)$$

Where C is the ammonia concentration in the chamber at steady state.

The ventilation rates of the chamber (air flow rates through the chamber) were set from 8.3 to 74 L min^{-1} , which caused the residence time of air in the chamber to be from 40 to

375 seconds. Although the ventilation rates can vary widely in practice, Brewer and Costello (1999) reported that the mean air speed at a 0.25 m height was 0.24 m s^{-1} with a standard deviation of 0.14 m s^{-1} in a conventional cross-ventilated house. Although no report has been found on the litter surface horizontal air velocity in tunnel-ventilated houses, the average air velocity estimated from ventilation rate and dimensions of those houses (Lacey et al., 2003) was more than 0.8 m s^{-1} .

A hotwire anemometer (Dwyer Model 641-18-LED; range: $0\text{-}10 \text{ m s}^{-1}$; accuracy: 3% full scale) was placed at about 0.025 m height above the litter surface at the center of the chamber to measure the horizontal air velocity profile in the chamber. It was found that the air velocity at the litter surface was mainly dependent on the speed (RPM) of the stirring impeller when the flow rate of chamber was less than or equal to 74 L min^{-1} . At 110 rpm , the air velocity was 0.1 m s^{-1} at the center of the chamber and 0.99 m s^{-1} near the wall of the chamber. The average air velocity in the chamber was 0.7 m s^{-1} with a standard deviation of 0.3 m s^{-1} . The air velocity profiles in the chamber are presented in Figures 3-3 and 3-4.

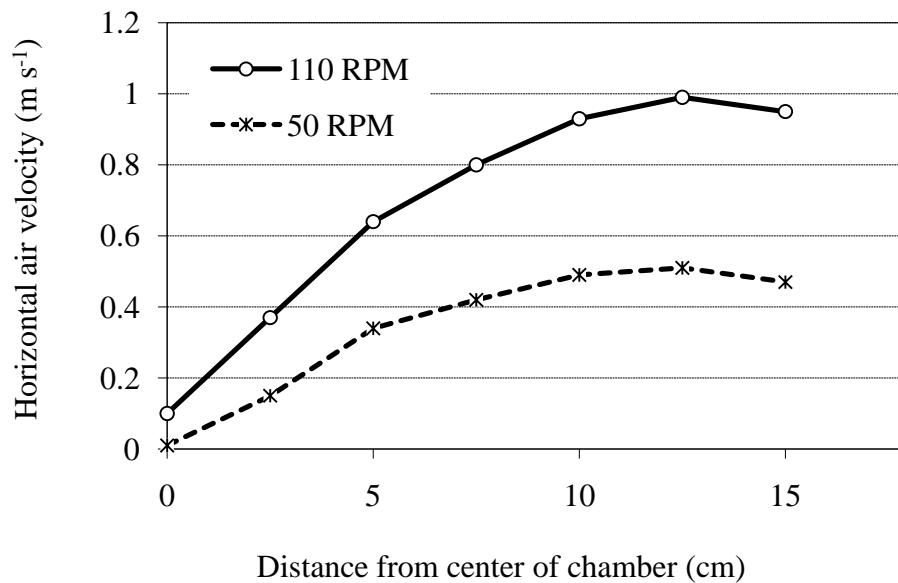


Figure 3-3. The horizontal air velocity profile at selected impeller speeds (Flow rate= 10 L min^{-1})

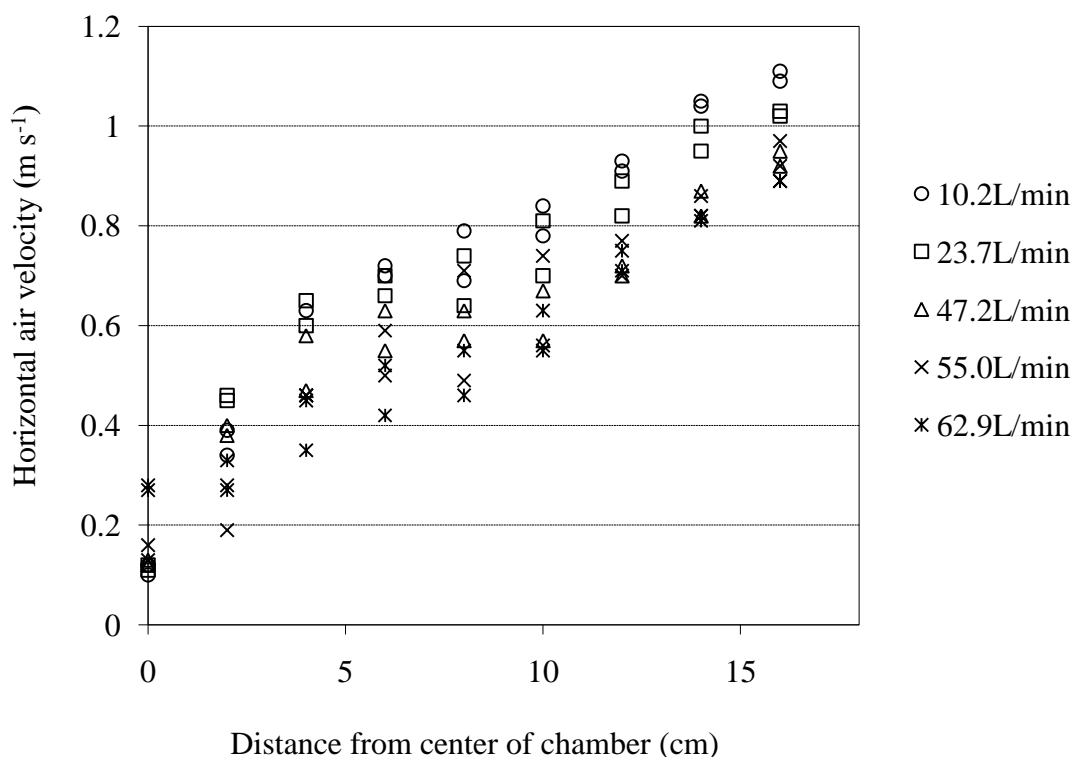


Figure 3-4. The horizontal air velocity profile at different flow rates (RPM=110)

3.1.2 The Wind tunnel

A wind tunnel was also designed for this ammonia emission study. The diagram and the photographs of the wind tunnel are shown in Figure 3-5 and Figure 3-6. The main body of the wind tunnel is 2.286 m in length, 0.2032 m in width and 0.2032 m in height. The bottom was made of stainless steel, and the top and sidewall were made of 3.2mm thick Lexan polycarbonate sheet. Airflow was provided by a centrifugal blower (JABSCO, Model 35400) with a maximum airflow rate of $0.1167 \text{ m}^3 \text{ s}^{-1}$ (250 cfm). The blower was located at the downwind end of the tunnel and was connected to the tunnel through a 0.1016 m diameter cylindrical duct.

A rotating-vane anemometer (AV-2, uncertainty 0.5% of display, Airflow

Developments Ltd., High Wycombe, U.K.) was placed in the duct to measure the airflow rate in the wind tunnel. Before being placed into the duct, the anemometer was calibrated using both a pitot tube and a hotwire anemometer (Dwyer Model 641-18-LED; range: 0-10 m s^{-1} ; accuracy: 3% full scale) with the log-Tchebycheff traversing method (6 measuring points were used). The calibration curve achieved an R squared of 0.9967. The calibration data is presented in Table 3-1. Figure 3-7 shows the calibration curve of the AV-2 rotating vane anemometer.

Broiler litter samples were placed on the 0.762 m long emission section of the wind tunnel to a depth of 0.025 m. There was a 1.27 m long flow stabilizing section upwind of the litter sample and a 0.254 m long transition and flow stabilizing section downwind of the litter sample, which were both filled with 0.025m-deep wood chips. Velocity profiles inside the wind tunnel were measured using the hotwire anemometer. Ammonia concentrations at the outlet and the inlet of the wind tunnel were measured using the TEI chemiluminescence ammonia analyzer (Model 17C).

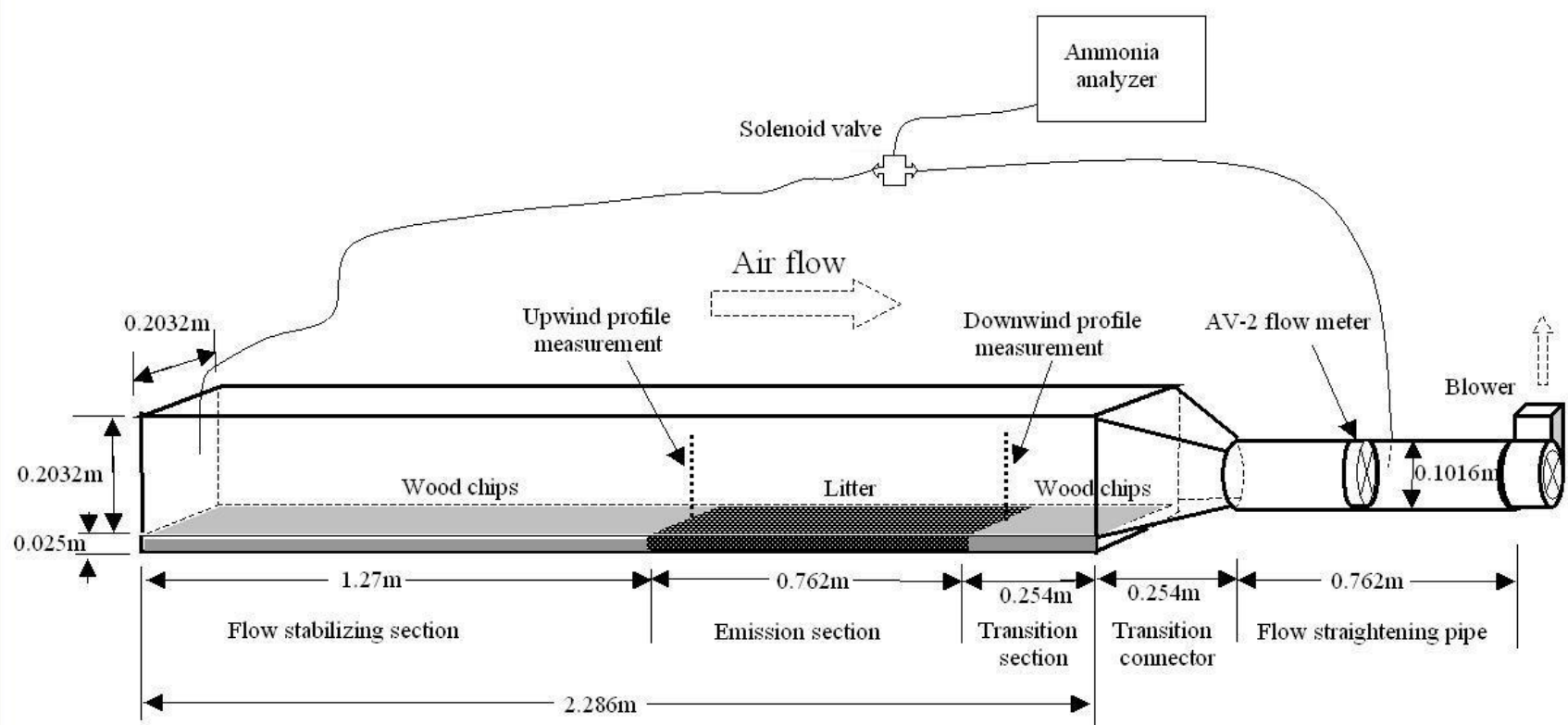


Figure 3-5. Diagram of the wind tunnel system

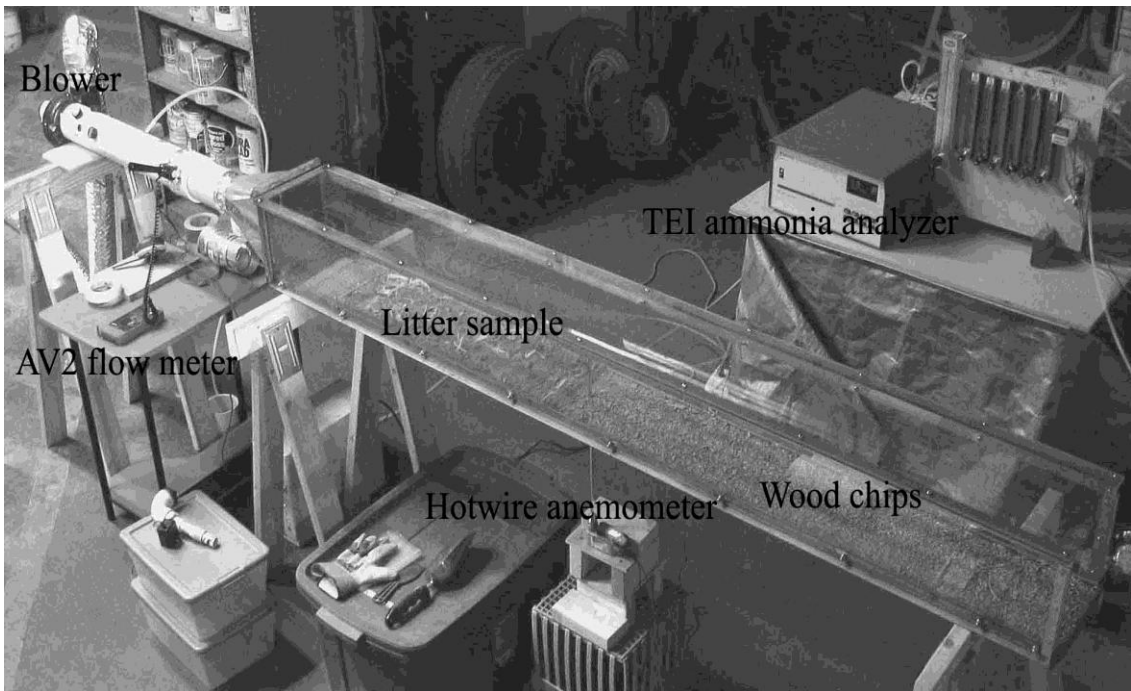
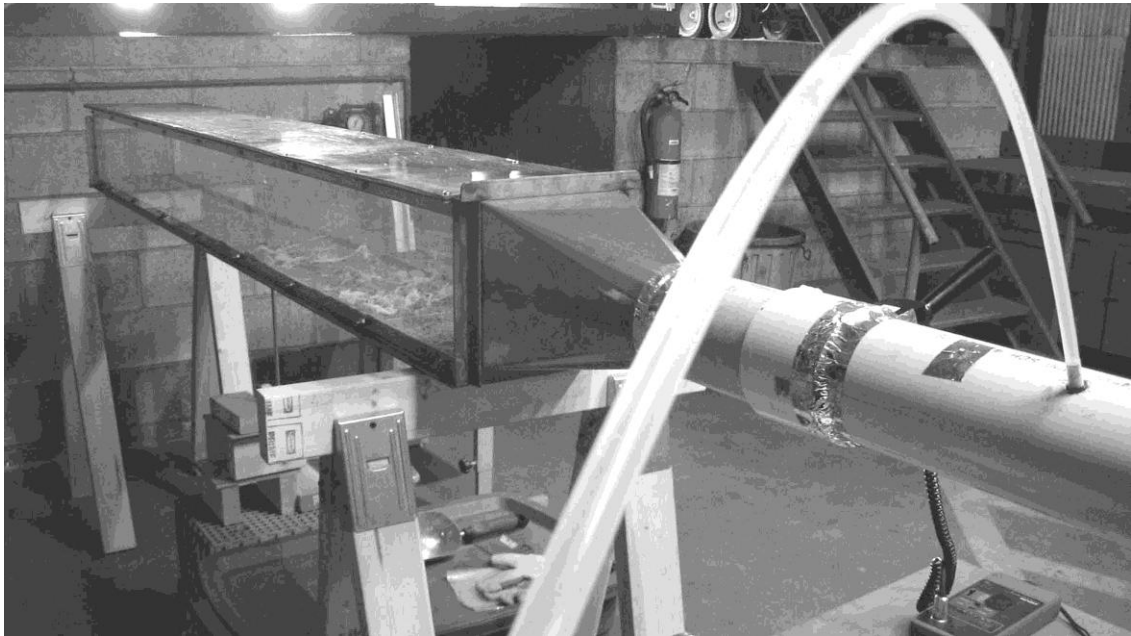


Figure 3-6. Photographs of the wind tunnel system

Table 3-1. Calibration data of the AV-2 rotating vane anemometer

AV-2 rotating vane anemometer air velocity reading (m s ⁻¹)	Calibration air velocity measured by pitot tube or hotwire anemometer (m s ⁻¹)						
	Distance relative to inner wall of the duct (dia is diameter of the duct)						Average
	0.032dia	0.135dia	0.321dia	0.679dia	0.856dia	0.968dia	
14.65	12.85	13.72	11.68	11.94	13.97	10.31	12.41
14.67	12.07	14.48	11.53	11.89	13.51	11.07	12.42
14.28	13.82	13.67	11.07	10.67	13.82	14.12	12.86
12.37	11.53	11.18	9.14	9.14	11.38	12.07	10.74
10.20	8.94	9.19	7.11	7.42	9.19	7.92	8.30
8.39	6.45	6.81	9.04	8.94	6.10	5.79	7.19
5.71	5.13	5.18	4.84	4.94	5.33	5.58	5.17
4.42	4.31	4.20	3.92	3.84	4.20	4.22	4.11
3.76	3.57	3.50	3.26	3.35	3.66	3.66	3.50
3.10	3.05	2.89	2.77	2.65	3.09	3.09	2.92
2.61	2.45	2.36	2.22	2.19	2.58	2.57	2.39
1.98	1.87	1.85	1.64	1.57	1.88	2.01	1.80
1.23	1.11	1.10	1.04	1.03	1.16	1.19	1.10
0.73	0.70	0.67	0.63	0.61	0.67	0.65	0.65
0.59	0.55	0.53	0.50	0.51	0.62	0.61	0.55

Note: When $U > 5 \text{ m s}^{-1}$, calibration data were measured by pitot tube. When $U < 5 \text{ m s}^{-1}$, calibration data were measured by hotwire anemometer.

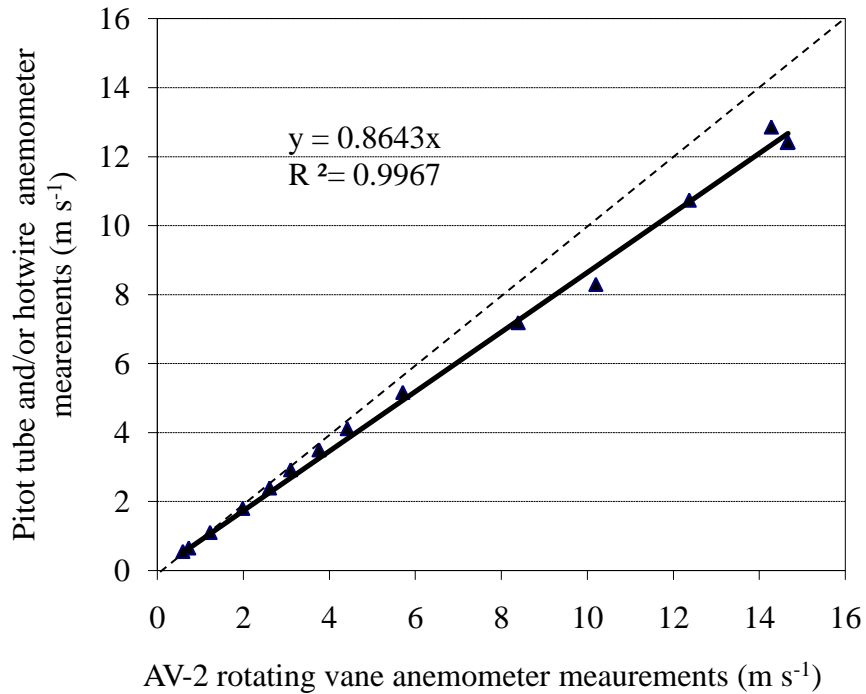


Figure 3-7. Calibration curve of AV-2 rotating vane anemometer (Data points are average values of 6 measuring points; when $U > 5 \text{ m s}^{-1}$, calibration data were measured by pitot tube. When $U < 5 \text{ m s}^{-1}$, calibration data were measured by hotwire anemometer.)

Ryden and Lockyer (1985) showed that the flow was turbulent within their wind tunnel. The transfer of gas between a surface and the flow depends mainly on the dynamic structure of the flow in the boundary layer (Townsend, 1976). Within the boundary layer, the turbulence intensity reaches maximum near the surface and then decreases with height (Raupach, et al., 1991). According to Loubet et al. (1999b), the boundary layer stabilized in the end part of their wind tunnel, approximately after a distance from the inlet $x=1.0$ to 1.5m and the boundary layer was about 0.12m . According to Shah et al. (2007), the velocity profile fully developed and stabilized over a 1.0 m distance starting at $x=0.6\text{m}$ and the boundary layer was 0.06 to 0.08m above the bottom.

The ammonia fluxes from the litter samples on the emission section inside the wind tunnel can be calculated using the following equation:

$$J = (Q/A) (C_{\text{outlet}} - C_{\text{inlet}}) \quad (3-3)$$

In which,

C_{outlet} is gas phase ammonia concentration at outlet of the wind tunnel, mg m^{-3} ;

C_{inlet} is gas phase ammonia concentration at inlet of the wind tunnel, mg m^{-3} .

The air velocity profiles at the start point (upwind) and end point (downwind) of the emission section in the wind tunnel are presented in Figure 3-8. Air profiles were measured for the nominal velocity values of 0.15, 0.50, 1.00, 1.50, and 2.00 m s^{-1} . It can be seen that there was not a big difference between the height of boundary layer (the height at which air velocity was no longer affected by the underlying surface) at the start point and the end point of the emission section. The height of boundary layer increased with the nominal velocity, and it was about 0.13 m above litter surface when the nominal velocity was 2.00 m s^{-1} .

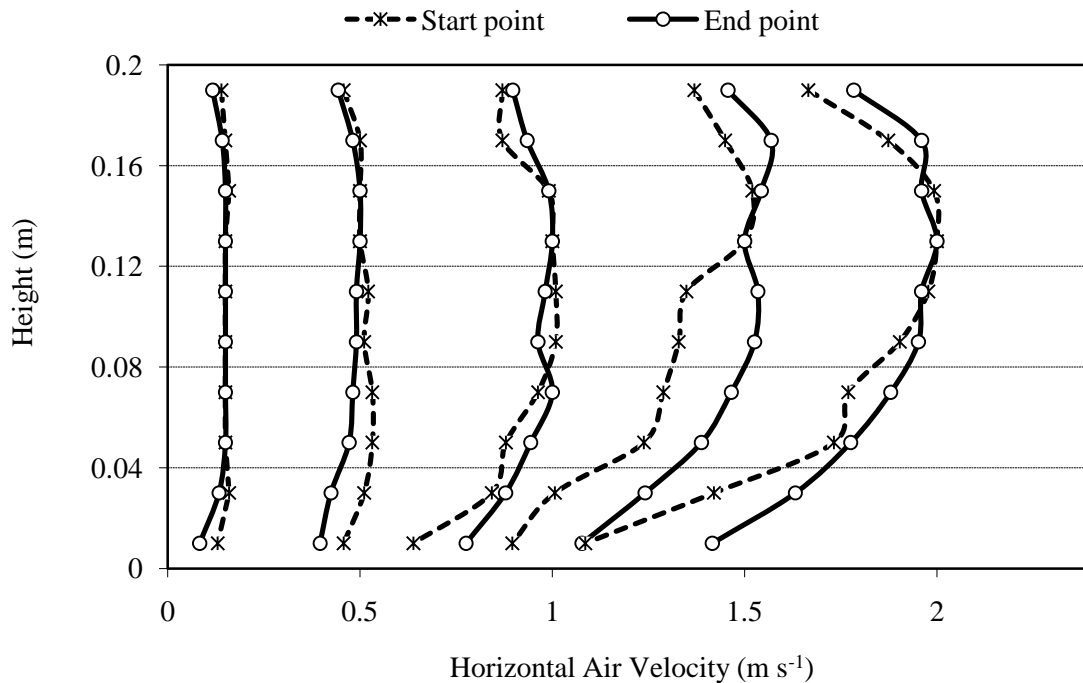


Figure 3-8. Air velocity profiles at the start point (upwind) and end point (downwind) of the emission section in the wind tunnel for the nominal velocity values of 0.15, 0.50, 1.00, 1.50, and 2.00 m s⁻¹.

3.2 MEASUREMENT OF AMMONIA CONCENTRATION

3.2.1 Chemiluminescence ammonia analyzer (Thermo Environmental Instruments)

The Thermo Environmental Instruments (TEI) chemiluminescence ammonia analyzer (Model 17C) was used to measure the nitric oxide (NO), nitric dioxide (NO₂), and NH₃ concentrations. The ammonia analyzer uses the reaction of NO with ozone (O₃) to measure gas phase ammonia concentrations. The ammonia analyzer consists of two separate modules, a converter module and an analyzer module. The gas sample is drawn into the ammonia analyzer by an external pump with a sample flow rate of 0.4 L/min. Ammonia in the gas sample is first converted to NO by the solid state catalytic converter, and then the sample

reaches the reaction chamber, and mixes with O₃, which is generated internally. The reaction of NO with O₃ produces a characteristic luminescence with an intensity that is proportional to the concentration of NO. The light emission is detected by a photomultiplier tube (PMT), which in turn generates a proportional electronic signal. The electronic signal is processed by the microcomputer into a NO concentration reading.

To measure the NO, NO₂, and NH₃ concentrations, NO₂ and NH₃ are transformed to NO in a stainless steel converter heated to approximately 775 °C before reaching the reaction chamber. Upon reaching the reaction chamber, the converted molecules, along with the original NO molecules react with O₃. The resulting signal represents the total NO, NO₂, and NH₃ reading (N_t). Separately, NO₂ is transformed into NO in a molybdenum converter heated to approximately 340 °C. The resulting signal represents the sum of NO and NO₂ reading (NO_x). The NH₃ concentration is determined by subtracting the signal obtained in the N_t mode from the signal obtained in the NO_x mode. The NO₂ concentration is determined by subtracting the signal obtained in the NO mode from the signal obtained in the NO_x mode. Concentrations of NO, NO₂, and NH₃ concentrations are displayed on the front panel of the Model 17C. There is also analog output, and a data logger can be used to record the measurements. The Model 17C analyzer has a measurement range of 0 to 100 ppm for ammonia. The ammonia analyzer was multipoint calibrated over the range of 0-100 ppm using standard ammonia gas (400ppm, ±2%, National Specialty Gases) and a gas mixing system (EnviroNics S-4000, Tolland, Conn. with airflow rate accuracy of 1% full scale). Figure 3-9 shows the calibration curve of the ammonia analyzer.

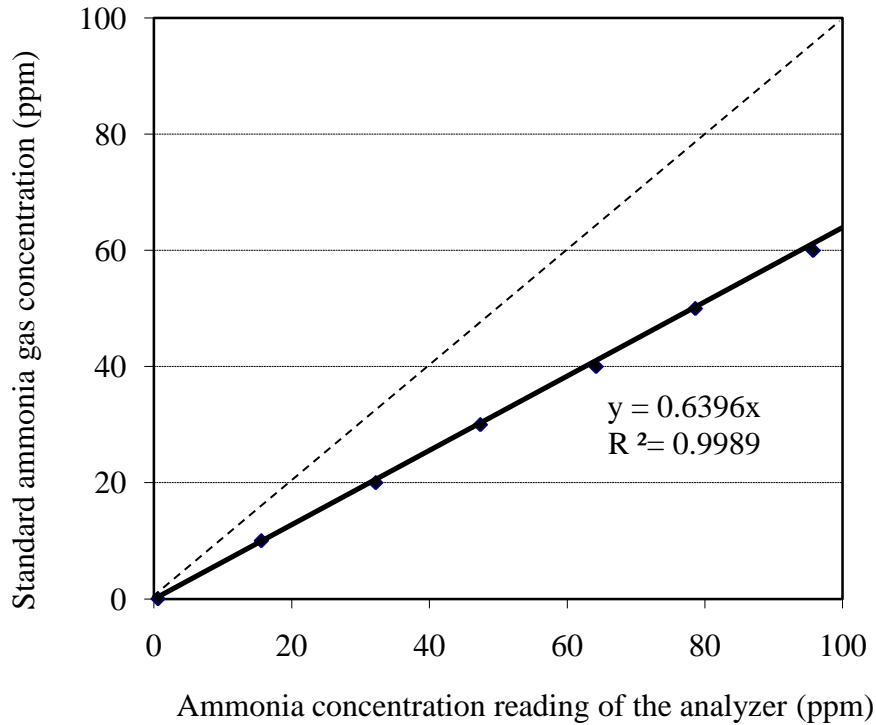


Figure 3-9. Calibration curve of the ammonia analyzer

3.2.2 Acid scrubber

In the first stage of the study, ammonia concentration in the chamber was simultaneously measured by an acid scrubber and the chemiluminescence ammonia analyzer. The acid scrubber technique can provide a time-weighted average concentration measurement using standard wet chemistry analysis, which has high trapping efficiencies (Shah et al., 2006; Misselbrook et al., 2005), low detection limits (DL), and low equipment costs. One hundred and fifty mL 2% boric acid was used in the acid scrubber. The collection efficiency of the scrubber was determined to be as high as 99.78% when the sampling flow rate was kept at 2 L/min. The acid scrubber system collected gaseous ammonia into a boric acid solution. The solution was analyzed in the Environmental Analysis Laboratory of the Department of Biological and Agricultural Engineering (BAE) at NC State University. Thus, the mass of nitrogen was determined for given sampling time. In the meantime, the volume of air passed

through scrubber was recorded, average ammonia mass concentration for this given period of sampling time was calculated based upon the mass of nitrogen (converted to the mass of ammonia), and the volume of air passing through the scrubber during the sampling period. Comparison of the measurements using the acid scrubber and the chemiluminescence ammonia analyzer is discussed in Chapter 4.

3.3 ANALYSIS OF LITTER PROPERTIES

Litter samples were taken from multiple locations of commercial broiler farms in North Carolina during the clean-out period. The litter material consisted of wood shavings. Each litter sample was well mixed together before testing. Figure 3-10 shows a photograph of the broiler litter sample. The analyses of litter samples were conducted in the BAE Environmental Analysis Laboratory at North Carolina State University.

The analyses included total Kjeldahl nitrogen (TKN), total ammoniacal nitrogen content (TAN), moisture content, pH, total nitrogen content and total carbon content. Litter subsamples were preserved at 4 °C before analysis. For the analyses, the litter subsamples were prepared "as is" without further drying or grinding. Total nitrogen content and total carbon content were determined through thermal conductivity detection with a Leco C/N 2000 analyzer [Official Method 990.03 (AOAC, 1998)]. For determination of TKN, the litter subsamples were first digested with a catalyst (K_2SO_4 , $CuSO_4 \cdot 5H_2O$, and pumice) and H_2SO_4 (Schuman et al., 1973). For determination of TAN, the litter subsamples were extracted in 1.25 N K_2SO_4 . The ammonia-salicylate method was used for TKN and TAN analysis using EPA Method 351.2 (EPA, 1979) or Standard Method 4500-NH₃ G, (APHA, 1998), with slight modifications including dialysis. Litter moisture content was obtained by comparing litter weight before and after oven drying (at 105°C).



Figure 3-10. Photograph of the litter sample

3.4 MEASUREMENT OF LITTER MOISTURE CONTENT

An ECH2O moisture sensor (EC5) was used in the chamber and wind tunnel to continuously monitor litter moisture contents during the tests. The ECH2O moisture sensor measures moisture content based on dielectric constant measurement. The manufacturing company (Decagon Device, Inc) provides a converting calibration equation to convert signal outputs to volumetric moisture ratio. Litter samples were sent to the manufacturer to perform “soil” specific calibration. Figure 3-11 shows the manufacturer’s calibration curve of the sensor using litter samples. Since we were more interested in mass based moisture content, measurements with the ECH2O moisture sensor were further compared at eight moisture levels using the standard moisture content measurement method by comparing litter weight before and after oven drying (103°C-105°C). The moisture content obtained using the standard method was in the range from 22.61 to 48.91 w/w% (wet-basis). As shown in Figure 3-12, the reading of ECH2O moisture sensor showed a high correlation ($r^2=0.9789$) with the standard method measurement.

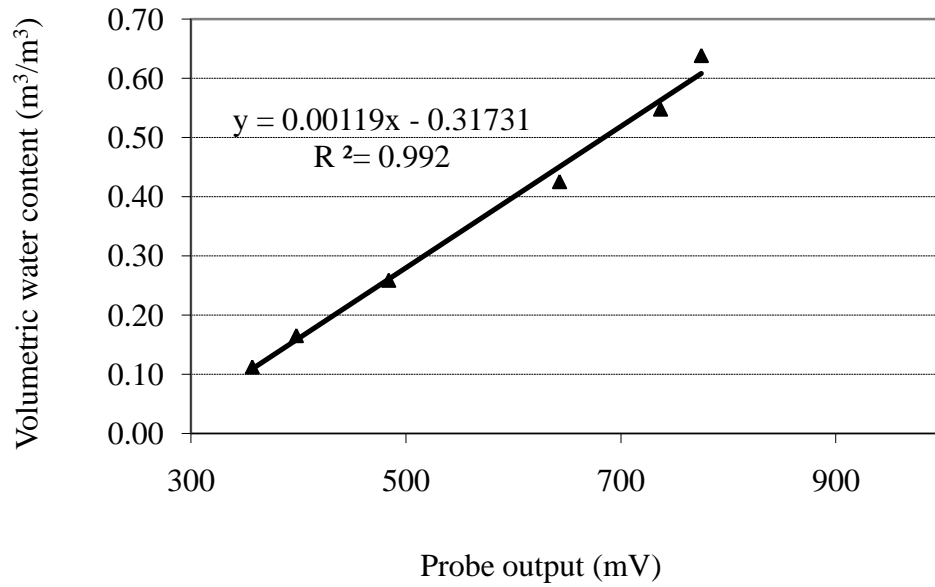


Figure 3-11. Manufacturer's calibration curve of the ECH2O moisture sensor

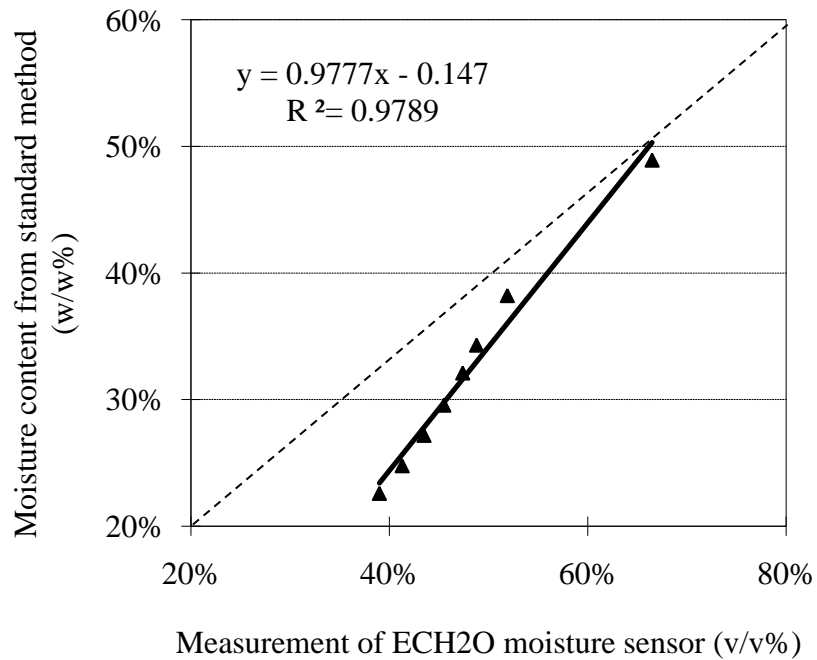


Figure 3-12. Comparison of the ECH2O moisture sensor measurement and the mass based moisture content of litter samples

3.5 MEASUREMENT OF RELATIVE HUMIDITY AND TEMPERATURE OF AIR

A NOVUS humidity and temperature transmitter (Model RHT/WM; Accuracy: $\pm 5\%$ RH in the range of 20 to 80% RH, $< \pm 1^\circ\text{C}$ in the range of 10 to 40 $^\circ\text{C}$) was placed at inlet of the wind tunnel and was connected to a HOBO data logger to record the relative humidity and temperature measurements at one-minute intervals. The relative humidity measurements of the NOVUS humidity and temperature transmitter were compared with measurements using a psychrometer, and the results are shown in Figure 3-13.

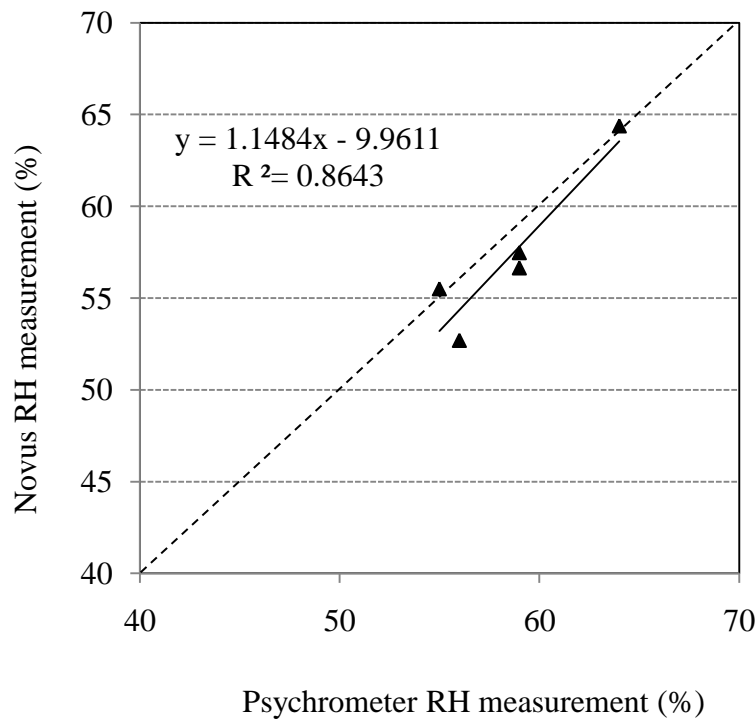


Figure 3-13. Comparison of the Novus humidity and temperature transmitter and psychrometer measurements of relative humidity

4. COMPARISON OF THREE TECHNIQUES FOR DETERMINING AMMONIA EMISSION FLUXES

This chapter reports the results of the studies on comparison of three techniques in ammonia emission flux determination. Ammonia concentrations in a dynamic flow-through chamber with broiler litter were measured simultaneously by a chemiluminescence ammonia analyzer and an acid scrubber. At the beginning and end of each test, the litter samples were analyzed for conducting a nitrogen mass balance. Ammonia emissions were estimated from the two concentration measurements and the mass balance approach. It was observed that the chemiluminescence analyzer measurements tended to overestimate ammonia concentration compared with the acid scrubber measurements, especially when litter moisture was high. Statistical results indicated that the effect of litter moisture content on the magnitude of the overestimation, and a p-value of 0.0104 was obtained. Considerable uncertainties were observed for the mass balance approach, especially when the percentages of the total nitrogen losses in litter samples were small (less than 2%). In order to apply the mass balance approach to estimate ammonia emissions and to achieve acceptable accuracy, a substantially longer testing period (more than 80 h) is needed for the observed ammonia emission level (104 to 1137 mg N h⁻¹ m⁻²). Also, more effort is needed to reduce the uncertainties associated with sampling and analyzing litter nitrogen content.

4.1 RESEARCH OBJECTIVE

In the literature, wide variations have been found for ammonia emissions from AFOs among different studies. Measurements from broiler houses indicated that ammonia emission rates vary 55-fold, from 283 to 15718 mg [NH₃-N] h⁻¹ AU⁻¹ (Redwine et al., 2002). While such variations in ammonia emissions could mainly be attributed to the differences in management practices and seasonal conditions, the uncertainties associated with the different

methods used in measuring and computing ammonia emissions may also be one of the reasons. Accurate estimation of ammonia emission rates from individual operations is important and yet a challenging task. Hence, there is a need for studying different measurement techniques used in ammonia emission determination.

Currently, there are no standard methods and protocols for measuring and estimating ammonia emissions from AFO facilities. Some commonly used techniques for determining ammonia emissions include: (1) standard wet chemistry analysis with an acid scrubber system, which usually provides measurement of average concentrations over a relatively long period of time (the common averaging time can be from several hours to several days); (2) spectrometric analysis such as the chemiluminescence ammonia analyzer, which is able to measure ammonia in real time; and (3) the nitrogen mass balance approach, which has been recommended together with the process based model approach to determine gas emissions from AFO houses by the National Academy of Sciences (NRC, 2003). In the first two techniques, ammonia emission fluxes can be calculated from measured concentrations and corresponding house ventilation rates. In the nitrogen mass balance approach, the average ammonia emission fluxes can be estimated from total nitrogen losses of an emission source for a period. The objective of this part of research was to investigate the differences in ammonia emission determination among these three techniques under various source conditions, and thus to address the limitations of these methods.

4.2 METHODOLOGY

The dynamic flow-through chamber system was used to measure and determine ammonia emission from broiler litter with three different techniques under designed conditions. These three techniques are (1) an acid scrubber system, (2) a chemiluminescence ammonia analyzer (model 17C, Thermo Environmental Instruments, Franklin, Mass.), and (3) the nitrogen mass balance approach. Litter samples of various ages and various moisture levels were used to investigate the agreement of the three techniques under various source conditions.

4.2.1 Experimental Setup

The dynamic flow-through chamber system was designed at North Carolina State University to measure ammonia emissions from broiler litter. Design and construction details of the chamber system are presented in Chapter 3.

4.2.2 Litter Samples and Moisture Content Treatments

Litter samples were taken from two commercial broiler farms in North Carolina. Both broiler farms had similar management practices: the grow-out period was 56 to 60 days (per flock) with two weeks of clean-out time. The litter material used by both farms was wood shavings. The ages of the built-up litter samples tested in this study were one, two, and four years. To ensure their representativeness, the litter samples of each age were mixtures of samples taken from multiple locations in the broiler house during the clean-out period. The samples were stored in airtight buckets in an air-conditioned laboratory with the temperature around 22 °C for three to four months before the tests.

At the beginning of each test, 2100 g of litter sample was placed into the testing chamber and was well mixed by hand. Then, a 100 g subsample was taken from the chamber for analysis. The analyses of litter samples were conducted in the BAE Environmental Analysis Laboratory at North Carolina State University. The analyses methods for the litter samples are provided in Chapter 3. The ammonia emissions from the remaining 2000 g litter sample in the chamber were measured simultaneously by the acid scrubber system and the chemiluminescence ammonia analyzer. The testing time was in the range of 60 min to 82 h. After each test, another 100 g subsample was taken from the chamber for the same analysis.

Figure 4-1 shows that the TN and TKN measurements of litter samples were closely correlated. In the mass balance approach, the total nitrogen loss of the litter sample during the testing period was estimated by comparing TN analysis results of the subsamples taken before and after the test. In order to estimate the uncertainty of the TN results, six replicate

analyses of the same litter sample were performed, and a standard deviation of $1816 \mu\text{g g}^{-1}$ was obtained, which was 4.2% of the average value of TN ($42667 \mu\text{g g}^{-1}$).

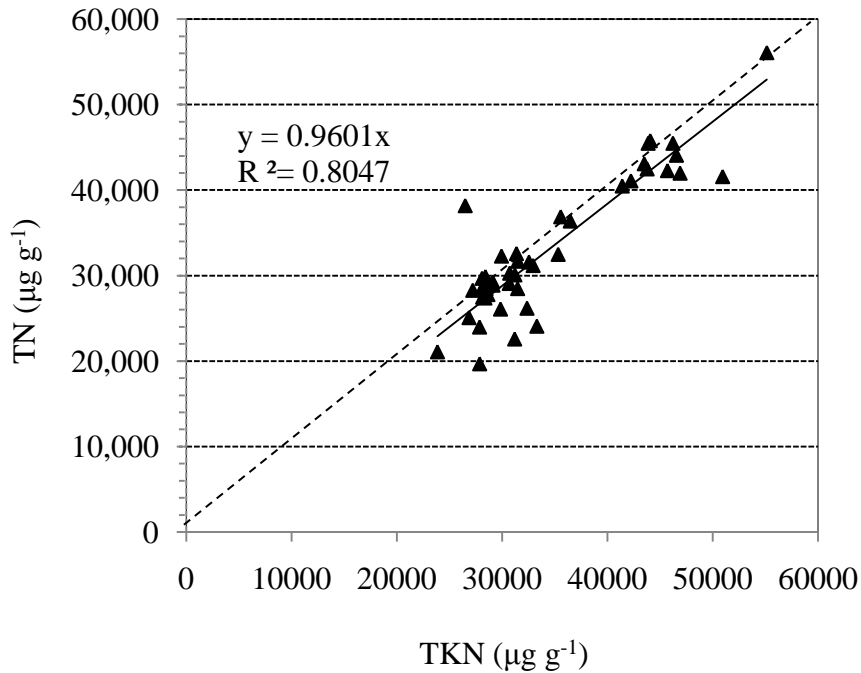


Figure 4-1 TN and TKN measurements of litter samples.

Various amounts of water were uniformly sprinkled and incorporated into the 2100 g litter samples so that the ammonia measuring techniques could be evaluated under various levels of litter moisture content. Details of the litter sample moisture treatments are described in Chapter 5, which reported the effects of litter moisture on ammonia emission.

4.2.3 Ammonia Concentration Measurements

After the litter sample was put into the chamber, the chamber was closed and the pump started to draw air through chamber immediately. The initial ammonia concentration in the chamber was close to zero, and the concentration began to increase quickly after the chamber was closed. According to the preliminary tests using the chemiluminescence ammonia

analyzer, the ammonia concentration in the chamber increased to the maximum value in less than 10 minutes and then began to decrease gradually, which is supposedly due to nitrogen depletion at the litter surface over time.

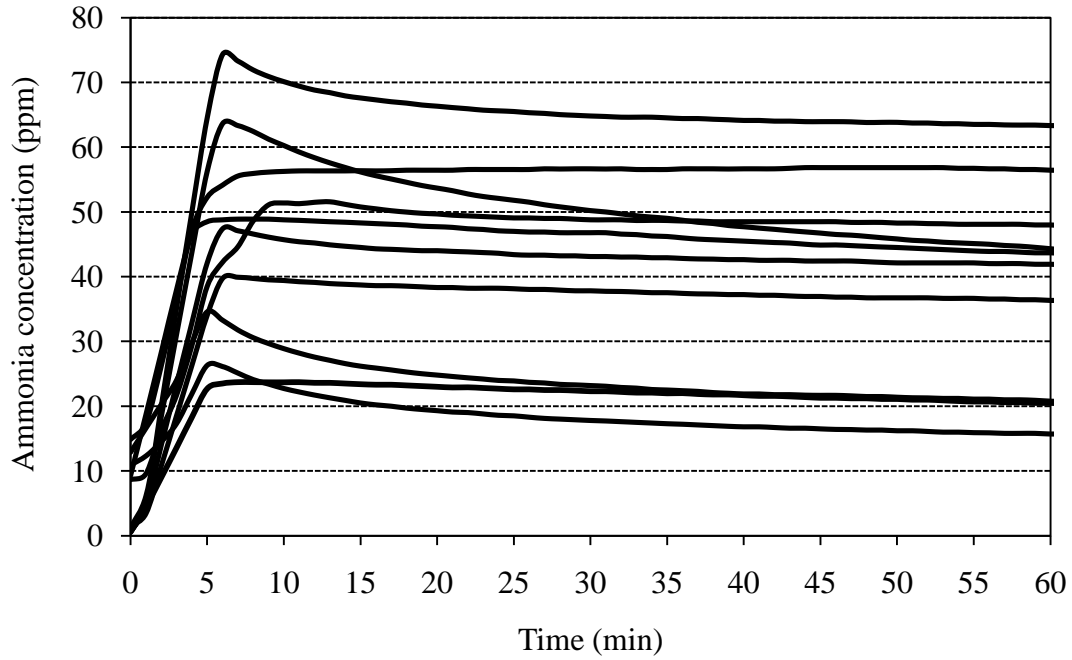


Figure 4-2. Ammonia concentrations in the flux chamber in ten preliminary tests (measured by the chemiluminescence ammonia analyzer).

Ammonia concentration in the dynamic flow-through chamber was simultaneously measured by an acid scrubber system and a chemiluminescence ammonia analyzer at 15 minutes after the chamber was closed. Room temperature was kept at 22 °C during the tests.

4.2.4 Determination of Ammonia Emission Flux

The chemiluminescence ammonia analyzer provided ammonia concentrations in ppm. Equation 4-1 was used to convert ammonia concentration (in ppm) to its mass concentration (in g m^{-3}). Once the average mass concentration of ammonia in the chamber through each test run was determined by either the ammonia analyzer or the acid scrubber, the average

ammonia emission flux was calculated using Equation 4-2.

$$C_{\text{mass}} = \frac{P}{RT} \times C_{\text{ppm}} \times MW_{\text{NH}_3} \times 10^{-3} \quad (4-1)$$

$$J_{\text{NH}_3} = \frac{3600 \times C_{\text{mass}} \times Q}{A} \quad (4-2)$$

In which,

C_{mass} is ammonia concentration, g m^{-3} ;

P is air pressure, atm; (1 atm was used in this research)

R is ideal gas law constant, $0.082 \text{ L atm K}^{-1} \text{ mol}^{-1}$;

T is absolute temperature, K;

C_{ppm} is ammonia concentration, ppm;

MW_{NH_3} is ammonia molecular weight, g mol^{-1} ;

J_{NH_3} is ammonia emission flux, $\text{g m}^2 \text{ h}^{-1}$;

Q is airflow rate through the flux chamber system, $\text{m}^3 \text{ s}^{-1}$;

A is surface area of the litter sample (same as the chamber footprint area; $A = 0.126 \text{ m}^2$).

A nitrogen mass balance approach was also used to estimate the nitrogen lost and to evaluate the emission fluxes. Equation 4-3 is the basic mathematical model for this mass balance approach is

$$N_{\text{loss}} = N_i - N_f \quad (4-3)$$

In which,

N_{loss} is loss of nitrogen in the litter sample during testing time, g;

N_i is initial total nitrogen content in the litter sample at the beginning of the test, g;

N_f is final total nitrogen content in the litter sample at the end of the test, g.

The NH_3 emission flux determined by the mass balance approach is

$$J_{\text{NH}_3} = \frac{N_{\text{loss}} \times (17/14)}{A \times t} \quad (4-4)$$

Where t is the testing time for each test run (h), and (17/14) is the molecular weight ratio of NH_3 to N. Fluxes from Equations 4-2 and 4-4 were used to compare fluxes derived by the three methods (the chemiluminescence ammonia analyzer, the acid scrubber, and the nitrogen mass balance).

Equations 4-5 and 4-6 were also used to calculate the losses of nitrogen in litter samples to compare results from the basic mass balance approach (Equation 4-3) with the results from the chemiluminescence ammonia analyzer and the acid scrubber:

$$N_{\text{loss}} = J_{\text{N}} \times A \times t \quad (4-5)$$

$$J_{\text{N}} = J_{\text{NH}_3} \times \frac{14}{17} \quad (4-6)$$

In which,

J_{NH_3} is NH_3 emission flux determined by the chemiluminescence ammonia analyzer or the acid scrubber methods, $\text{g m}^2 \text{h}^{-1}$;

J_{N} is nitrogen loss rate, $\text{g m}^2 \text{h}^{-1}$;

t is testing time for each sample, h.

4.3 RESULTS AND DISCUSSION

4.3.1 Comparison of Ammonia Concentration Measurements

Three sets of tests were conducted with litter samples at three different ages (one, two, and four years). In each set of tests, ammonia concentrations from litter samples with various moisture contents were measured using the chemiluminescence ammonia analyzer and the acid scrubber simultaneously. The first set of tests included nine litter samples (litter age = one year) with moisture contents in the range from 16.61% to 32.95%, and the testing time was about 5 h per test.

The average chemiluminescence analyzer measurements were compared with the acid scrubber measurements in the same testing period. It was found that the average chemiluminescence analyzer measurements generally provided higher values. The ratios of the average chemiluminescence analyzer measurements over the acid scrubber measurements were in the range from 1.02 to 1.65. Comparison of the average ammonia concentrations measured by the chemiluminescence analyzer and by the acid scrubber for the first set of tests (litter age = one year) are shown in Table 4-1.

Table 4-1. Comparison of the chemiluminescence analyzer and the acid scrubber measurements for litter samples under various litter moisture content treatments (litter age = one year).

Litter Moisture Content (m/m %) ^[a]	[1] Acid Scrubber Ammonia Conc. ^[b] (ppm)	[2] Chemiluminescence Ammonia Conc. ^[c] (ppm)	Ratio of [2] to [1]
16.61	16.8	17.1	1.02
17.79	20.7	24.1	1.16
20.13	18.5	26.5	1.43
21.60	50.5	63.3	1.25
28.02	33.2	53.1	1.60
28.06	13.7	20.4	1.49
28.38	10.4	15.5	1.48
32.00	29.2	48.1	1.65
32.95	38.2	58.6	1.53

^[a] litter moisture contents were expressed on wet basis.

^[b] Ammonia concentration measured by the acid scrubber (ppm).

^[c] Average ammonia concentration measured by the chemiluminescence analyzer during the test period (ppm).

For the second set of tests, eight litter samples (litter age = two years) with moisture contents in the range from 28.7% to 60.7% were tested. For the third set of tests, six litter samples (litter age = four years) with moisture contents in the range from 23.2% to 40.5% were tested. For both the second and third sets of tests, the testing time was set at 60 min. Since some of these aged litter samples had ammonia concentrations higher than 100 ppm, which is the full-scale reading of the chemiluminescence analyzer, the sample air was diluted

with an improvised dilution system before entering the analyzer. The dilution ratio was calibrated using standard ammonia gas (400 ppm, $\pm 2\%$, National Specialty Gases). For the second set of tests (litter age = two years), a dilution ratio of 6.86 was applied. For the third set of tests (litter age = four years), a dilution ratio of 12.86 was applied. Three replicate measurements were taken for each litter sample and the average values were recorded.

Figure 4-3 shows a comparison of the chemiluminescence analyzer and the acid scrubber measurements for all three sets of tests. A linear regression line was developed between the chemiluminescence analyzer measurements and the acid scrubber measurements. It was observed that the ammonia concentrations measured by the chemiluminescence analyzer were constantly higher than those measured by the acid scrubber.

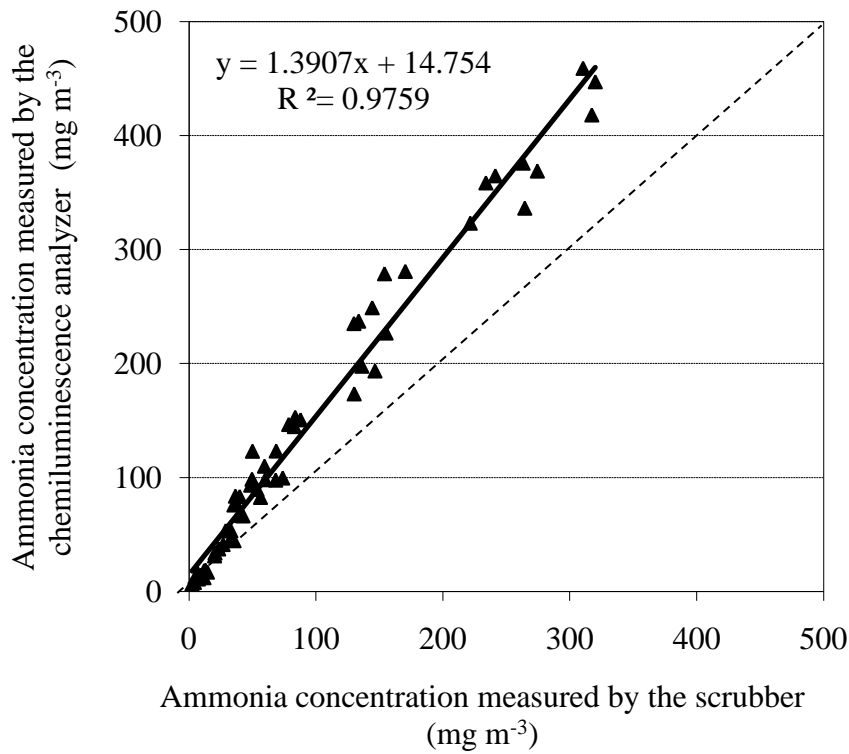


Figure 4-3. Relationship between average measurements by the chemiluminescence analyzer and the acid scrubber.

Ratios of the average chemiluminescence analyzer measurements over the acid scrubber measurements for all the litter samples are plotted against litter moisture contents in Figure 4-4. It can be seen that the ratios of the average chemiluminescence analyzer measurements over the acid scrubber measurements were higher when litter moisture contents were higher. An analysis of variance (ANOVA) using SAS procedures was conducted to evaluate this effect of litter moisture content on the differences in average ammonia concentration measurements between these two methods. The three sets of tests (at three litter ages) were treated as three blocks. A p-value of 0.0104 was obtained for the effect of litter moisture content on the ratios of the average chemiluminescence analyzer measurements over the acid scrubber measurements. The result indicated that litter moisture content may contribute to the overestimation of ammonia concentrations by the chemiluminescence analyzer. Further investigation is needed to find the reason behind this effect.

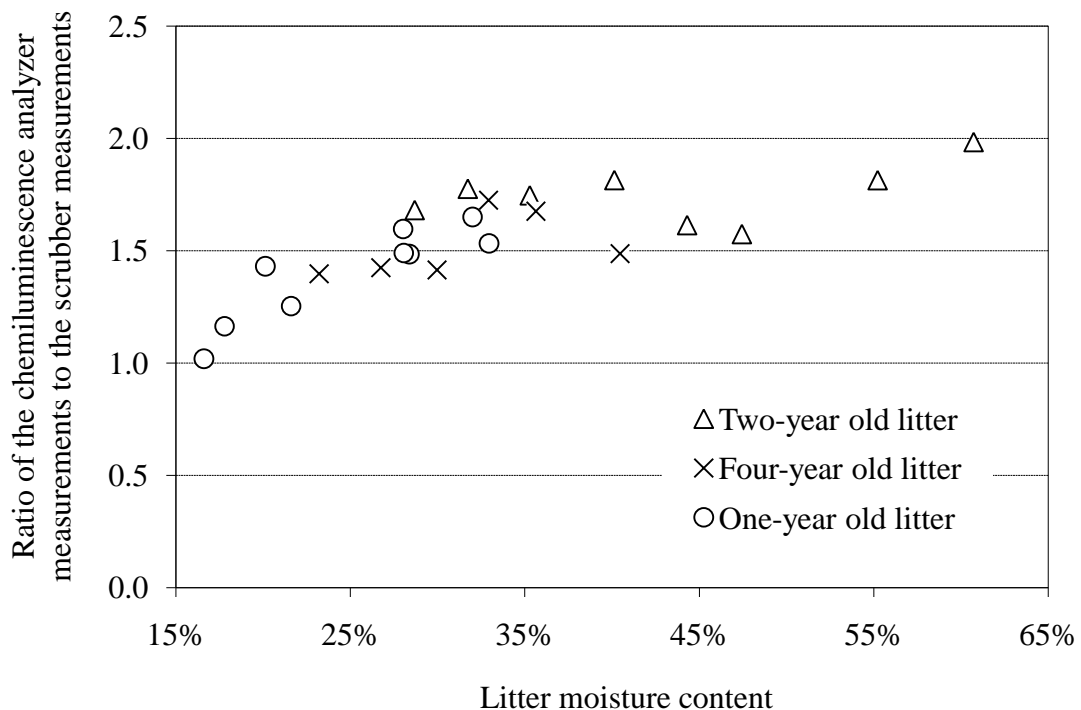


Figure 4-4. Ratios of the average chemiluminescence analyzer measurements over the acid scrubber measurements.

4.3.2 Comparison of Ammonia Emission Fluxes

The mass balance approach was recommended to estimate ammonia emissions from AFO houses by the National Research Council (NRC, 2003). In the mass balance model, the total nitrogen inputs and outputs of a broiler house are quantified, and the difference between the inputs and outputs is assumed to be volatilized nitrogen. This method does not distinguish among losses of N as NH_3 , N_2 or NO_x . However, it can provide an estimation of the upper limits of ammonia emissions fluxes.

In the first set of tests (nine litter samples with an age of one year), Equations 4-1 through 4-6 were used to determine ammonia emission fluxes using the three techniques. The total nitrogen losses from the litter samples during each test were calculated using Equations 4-5 and 4-6. The testing time was about 5 h, and the chamber airflow rate was set at 39.8 L min^{-1} . In the fourth set of tests, nine new litter samples (litter age of less than one year) were tested under a higher chamber airflow rate (74.0 L min^{-1}) and longer testing time (up to 82 h). No acid scrubber was used in the fourth set of tests. Figure 4-5 summarizes the comparison of ammonia emission fluxes derived using different techniques (three techniques in set 1, and two techniques in set 4).

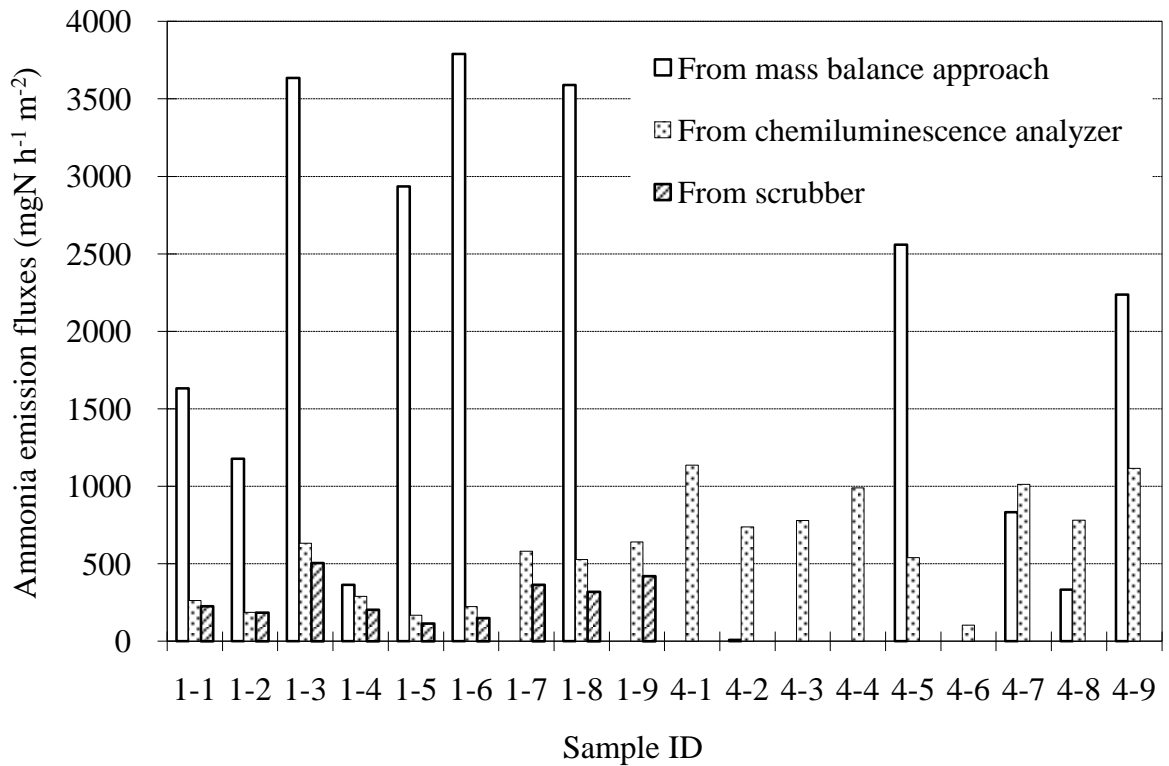


Figure 4-5. Comparisons of ammonia emission fluxes derived using different techniques (Sample ID 1-1 to 1-9 are used to represent the nine samples in set 1, and sample ID 4-1 to 4-9 are used to represent the nine samples in set 4)

As can be seen in Figure 4-5, for nine samples out of the 18 that were tested, the ammonia emission fluxes estimated with the mass balance approach were greater than those estimated from the chemiluminescence analyzer or the acid scrubber measurements. It is suspected that nitrification and denitrification processes may have caused the overestimation of NH_3 fluxes. Further study is needed to quantify other nitrogen losses in order to improve the accuracy of estimating NH_3 fluxes with the mass balance approach. Six negative values were obtained with the mass balance approach; in Figure 4-5, the negative values are treated as zero. The ammonia emission fluxes estimated from the chemiluminescence analyzer measurements were in the range of 104 to 1137 $\text{mg N h}^{-1} \text{m}^{-2}$, which suggested losses of 0.37% to 11.54% of the original total nitrogen content in the litter samples through the tests.

Considering the uncertainty of the TN analysis (standard deviation was 4.2% of the average value), it is believed that the low nitrogen losses during the testing period were the main cause of the great uncertainties in ammonia emission fluxes estimated by the mass balance approach.

The relative errors in ammonia flux estimation by the nitrogen mass balance approach and by the chemiluminescence analyzer measurements are defined by Equation 4-7. In Figure 4-6, these relative errors are plotted against the percentage of total nitrogen losses in the litter samples as estimated from the chemiluminescence analyzer measurements.

$$RE = \frac{(J_1 - J_2)}{J_2} \times 100 \quad (4-7)$$

Where,

RE is relative error, %;

J_1 is ammonia fluxes estimated by the nitrogen mass balance approach, $\text{mgN h}^{-1} \text{m}^{-2}$;

J_2 is ammonia fluxes estimated by the chemiluminescence analyzer measurements, $\text{mgN h}^{-1} \text{m}^{-2}$.

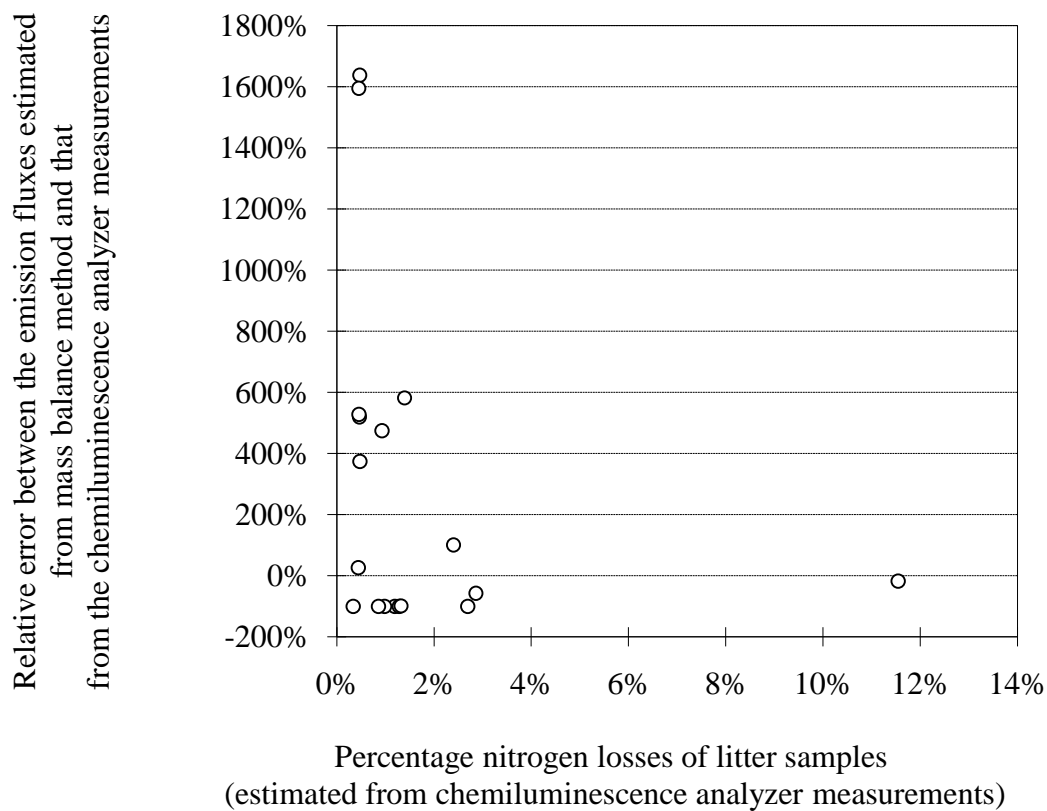


Figure 4-6. Relative errors between ammonia fluxes estimated by the nitrogen mass balance approach and by the chemiluminescence analyzer measurements.

As shown in Figure 4-6, when the percentage of total nitrogen losses in litter samples estimated from the chemiluminescence analyzer measurements was less than 2%, the relative errors between ammonia fluxes estimated by the nitrogen mass balance approach and by the chemiluminescence analyzer measurements can be as high as 1600%. As the percentage of total nitrogen losses increases, the relative errors decrease. For the test with 11.54% nitrogen losses (with a testing time as long as 82 h), the relative error was reduced to 18%.

4.4 CONCLUSION

Three techniques (chemiluminescence ammonia analyzer, acid scrubber, and nitrogen mass balance) were evaluated to estimate ammonia emissions from broiler litter in a dynamic flow-through chamber. The standard wet laboratory analysis with an acid scrubber system is believed to be the most accurate method, but it is usually only able to provide measurements of average concentrations over a relatively long period of time. The chemiluminescence ammonia analyzer is able to measure ammonia concentrations continuously over time. However, experimental results indicated that the chemiluminescence analyzer measurements tended to overestimate ammonia concentrations compared with the acid scrubber measurements, especially when the litter moisture content was high. Through statistical analysis, a p-value of 0.0104 was obtained for the effect of litter moisture content on the ratios of the average chemiluminescence analyzer measurements over the acid scrubber measurements. Further research is needed to find how and why moisture content may contribute to the overestimation of ammonia by the chemiluminescence analyzer.

Considerable uncertainties in ammonia emission flux estimation were observed for the mass balance approach, especially when the percentage of total nitrogen losses in the litter samples was small (less than 2%). In order to apply the mass balance approach to estimate ammonia emissions and to achieve acceptable accuracy, a longer testing period (more than 80 h) is needed under the observed ammonia emission level (104 to 1137 mg N h⁻¹ m⁻²), and more effort is needed to reduce the uncertainties associated with sampling and analyzing litter nitrogen content.

5. EFFECT OF MOISTURE CONTENT ON AMMONIA EMISSIONS

This chapter reports the experimental study to investigate the responses of ammonia emissions to litter moisture content using dynamic flow-through chamber system under laboratory-controlled conditions. It was observed that litter moisture content has a great impact on ammonia emissions from litter. As litter moisture content increased, the total ammoniacal nitrogen content (TAN) in the litter increased, which could potentially increase ammonia emissions. However, measurements of ammonia concentrations in the chamber and total nitrogen losses from litter samples all suggested that water applied to the litter also had an effect of suppressing ammonia emissions for a short time. After enough time (one to two weeks) was allowed, higher moisture content in litter eventually resulted in higher ammonia emissions. It was also noticed that, at very high litter moisture content, even when more time was allowed, ammonia concentrations began to decrease as moisture content further increased.

5.1 RESEARCH OBJECTIVE

As stated in Chapter 2, litter moisture content is one of the important factors that may influence ammonia emissions from broiler litter. However, the comprehensive effect of litter moisture content is complex and still not well known. This chapter investigated the effect of litter moisture content under laboratory-controlled conditions. Understanding of the effect of litter moisture content will be helpful in improving management practices (e.g. litter management, drinker systems, and ventilation systems) and may contribute to practical and cost effective strategies to mitigate ammonia emissions from broiler houses. The ultimate goal is to develop an emission model that combines the effects of temperature, air exchange rate, pH, litter nitrogen content, and litter moisture content.

5.2 METHODOLOGY

5.2.1 Experimental Setup

In order to quantify and compare ammonia emissions from broiler litter with various moisture contents, the dynamic flow-through chamber system was used for measurements of ammonia emissions from broiler litter under various moisture conditions. Design and construction details of the chamber system are given in Chapter 3. The ventilation rates of the chamber (airflow rate through the chamber) in this study were set at 9.8 L min^{-1} , which caused residence time of air in the chamber to be 306 s. The speed of the stirring impeller was kept at 110 revolutions per minute (rpm).

5.2.2 Litter Samples and Moisture Treatments

Litter samples from two commercial broiler farms in North Carolina were tested in this study. The five litter samples were labeled as litter A, B, C, D and E. The two farms use different units for defining the age of litter. Litter A, B, and E were from the same farm with ages of two-year, four-year, and one-year, respectively. Litter C and D were from the other farm with ages of eight-flocks and twelve-flocks respectively. The analyses of litter samples were conducted in the BAE Environmental Analysis Laboratory at North Carolina State University. The analyses methods for the litter samples are provided in Chapter 3.

A known amount of water was applied by uniformly sprinkling and incorporating into the litter to achieve various desired levels of moisture content. All litter moisture contents were expressed on a wet basis by mass in this study. During the test, the moisture content of untreated litter was measured using the standard moisture content measurement method by comparing litter weight before and after oven drying (103°C - 105°C). The moisture content of litter that had been treated with water was calculated from the original untreated litter moisture content and the amount of water added using the following equation.

$$MC_1 = (MC_0 \times W_{\text{Litter}} + W_{\text{H}_2\text{O}}) / (W_{\text{Litter}} + W_{\text{H}_2\text{O}}) \quad (5-1)$$

Where MC_1 is the moisture content of the litter that has been treated with water; MC_0 is the original untreated litter moisture content that measured by standard moisture content measurement; W_{Litter} is weight of litter; and $W_{\text{H}_2\text{O}}$ is weight of water added.

An ECH2O moisture sensor (EC5) was used in each chamber to continuously monitor litter moisture contents during the tests. The ECH2O moisture sensor was calibrated at eight moisture levels using the standard moisture content measurement method by comparing litter weight before and after oven drying. The calibration line has an R-squared of 0.9789. The reading of ECH2O moisture sensor showed very good agreement with the calculated moisture content.

5.2.3 Measurement of Ammonia Concentrations in the Chamber

Three identical chamber systems were built to ensure at least three replicates for each treatment (moisture level) with each experimental run of one hour or so. Room temperatures were kept at 22°C during the tests. Ammonia concentration in each chamber was measured by a boric acid scrubber.

5.2.4 Measurement of Nitrogen Loss of Litter Samples

An alternative method to estimate ammonia emissions from litter involves measuring the nitrogen losses of litter samples after they are exposed to air for a certain amount of time. The total nitrogen losses from litter samples at various moisture levels were determined through analysis of litter samples, and the losses were compared with each other to investigate the effects of litter moisture content.

5.3 RESULTS AND DISCUSSIONS

5.3.1 Effect of Added Water over a Short Period of Time

Four types of pine shaving litter samples (labeled as litter A, B, C and D) were tested in the dynamic flow-through chamber to study the relationships between ammonia concentrations and litter moisture contents. Water was gradually applied to the litter samples to achieve desired moisture contents, and then ammonia concentrations in the chambers were measured at various moisture contents. All the ammonia measurements were taken within two days after water was applied into the litter.

As indicated in Figure 5-1, ammonia concentrations in all four litter samples decreased as litter moisture contents increased. The water applied to the litter obviously suppressed ammonia emissions in the short time range of the experiments (two days). It is believed that the decrease of gas ammonia concentration over a short period of time was mainly due to the dissolving of gas phase ammonia into the added water.

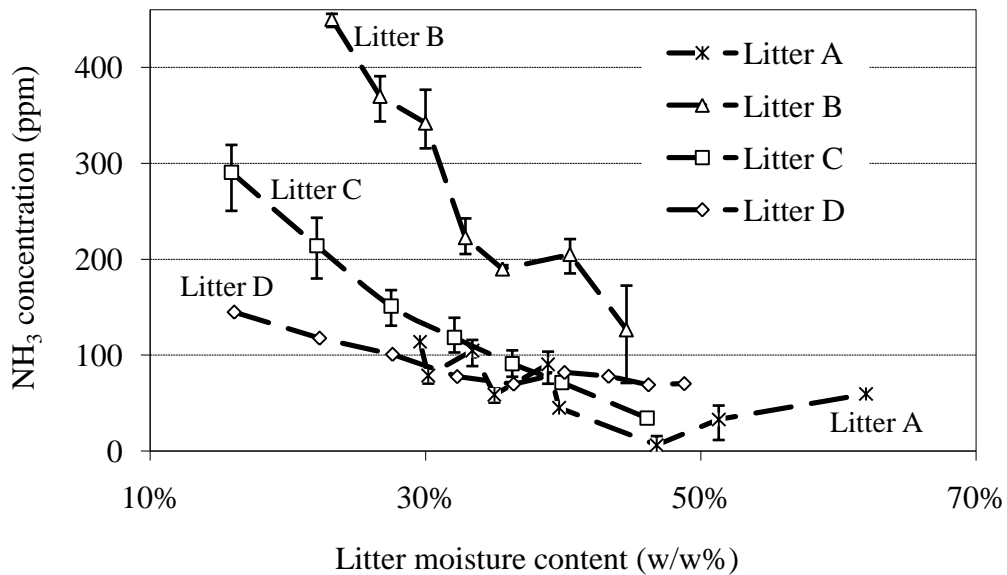


Figure 5-1. Average ammonia concentrations vs. litter moisture content

5.3.2 EFFECT OF LITTER MOISTURE CONTENTS OVER TIME

Water applied to the litter may affect ammonia emissions through various processes in the litter, such as generation of ammonia in the litter as well as mass transfer of ammonia within the litter and from the litter to the air. It was found that time played an important role for the comprehensive effect of the added water. It may take some time for all the effects to be observed. Litter A had a moisture content of 22.8% when no water was applied, and the corresponding ammonia concentration in the chamber was 102 ppm. Right after water was applied and the moisture content of litter A increased to 46.8%, the corresponding ammonia concentration in the chamber was reduced to 6 ppm (Figure 5-1). However, when the ammonia concentration was measured one week after water was applied, the corresponding ammonia concentration in the chamber for litter A with the same moisture content (46.8%) was found to increase to 91 ppm. Litter E was tested in the dynamic flow-through chamber for a time range of 25 days. As days went by, water was gradually added into the litter to achieve increasing moisture content. The resulting moisture contents and the corresponding average ammonia concentrations on each day are plotted in Figure 5-2. It was found that when the ammonia measurements were taken within five days after water was applied into the litter, ammonia concentrations decreased as litter moisture contents increased, which was consistent with what has been reported in previous section of this paper. However, after five days, ammonia concentrations began to increase as moisture contents increased. At day 1, the average ammonia concentration was only 92.9 ppm with litter moisture content of 20.4%. At day 15, the average ammonia concentration reached the highest value, 192.8ppm, with a litter moisture content of 32.9%. It suggested that water applied to litter had an effect of suppressing ammonia emissions in the short term; however, after a longer time, higher moisture contents in litter eventually resulted in higher ammonia emissions. As stated in chapter 2, litter moisture content will affect the conversion rate of uric acid to ammonium-N. As litter moisture content increases, the total ammoniacal nitrogen content (TAN) in the litter will increase, therefore eventually increasing ammonia emissions.

It was also noted that when litter moisture contents were 35.1% or higher, even after a

long time, ammonia concentrations began to decrease as moisture contents further increased. The decrease in ammonia concentrations at high moisture levels has also been reported by Carr et al.(1990), Valentine (1964), and Schefferle (1965). Schefferle (1965) found aerobic bacteria were primarily responsible for uric acid decomposition. It is suspected that at high moisture levels, litter becomes anaerobic thus suppressing ammonia release (Carr et al., 1990).

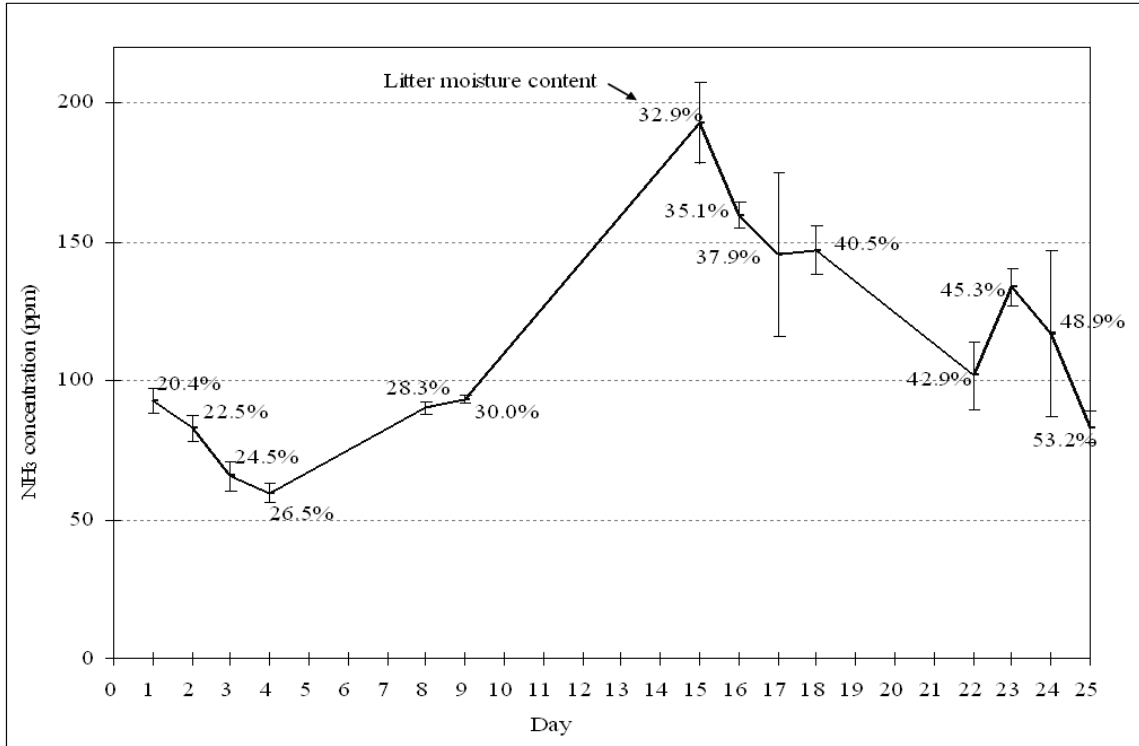


Figure 5-2. Average ammonia concentrations from litter E over time (Each data point is an average of three replicates)

5.3.3 TAN Contents in Litter vs. Ammonia Emissions

Before water was applied to the litter samples, the total nitrogen contents, TAN contents, moisture contents, and pH values of the five litter samples were analyzed as listed in Table 5-1, together with the average ammonia concentration measurements in the chambers for each

of the litter samples. The ratios of TAN content to total nitrogen content were in the range of 5.4% to 14.54% in the five litter samples. It was obvious that the measured ammonia concentrations were positively related with the TAN content in litter. As shown in Figure 5-3, higher TAN contents in litter tend to have higher ammonia concentrations.

Table 5-1. TAN content and ammonia emissions

Litter	Farm	Total nitrogen content in litter ($\mu\text{g g}^{-1}$)	TAN content in litter ($\mu\text{g g}^{-1}$)	Litter moisture content (w/w, %)	pH	Average NH_3 concentration in chamber (ppm)
E (1-year)	1	25020	1980	19.8%	8.48	95.8
A (2-year)	1	30200	1630	22.8%	8.43	102.0
B (4-year)	1	42000	6108	23.2%	8.00	449.9
C (8-flocks)	2	43000	4070	15.9%	7.73	290.6
D (12-flocks)	2	46100	4280	16.1%	7.34	144.5

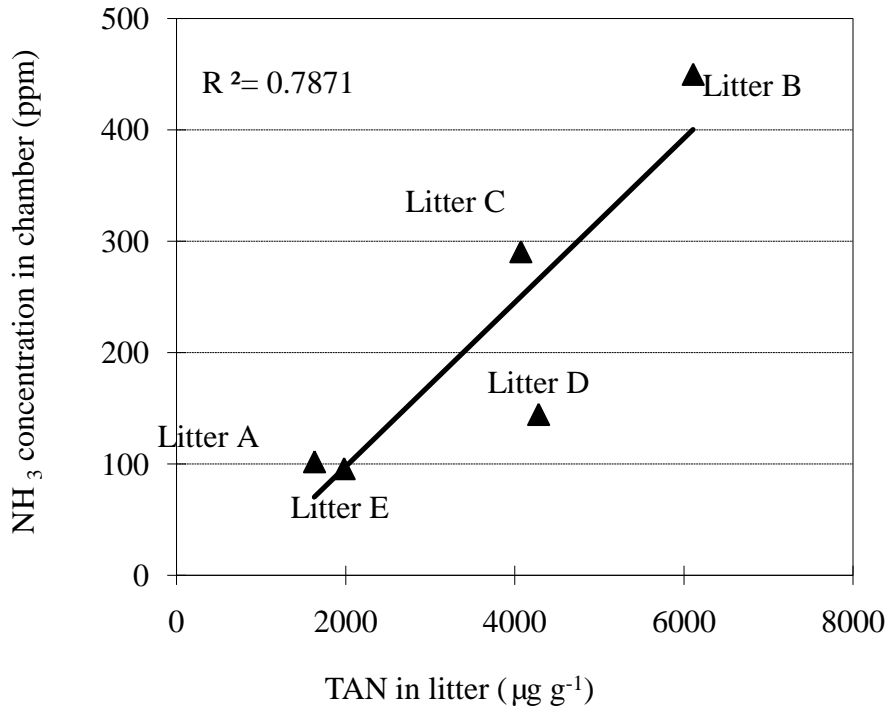


Figure 5-3. Ammonia concentrations vs. TAN contents in the litter samples

5.3.4 Effect of Litter Moisture Contents on TAN Contents

Eight sub-samples of litter A were treated with water to achieve eight various moisture levels from 22.6% to 48.9%. Each of these sub-samples was analyzed for TN, TAN, etc. The ratios of TAN contents to total nitrogen contents at the eight moisture levels for litter A were plotted in Figure 5-4. It was obvious that the TAN contents in litter increased with the litter moisture contents. Therefore, water applied to litter can potentially increase ammonia emissions.

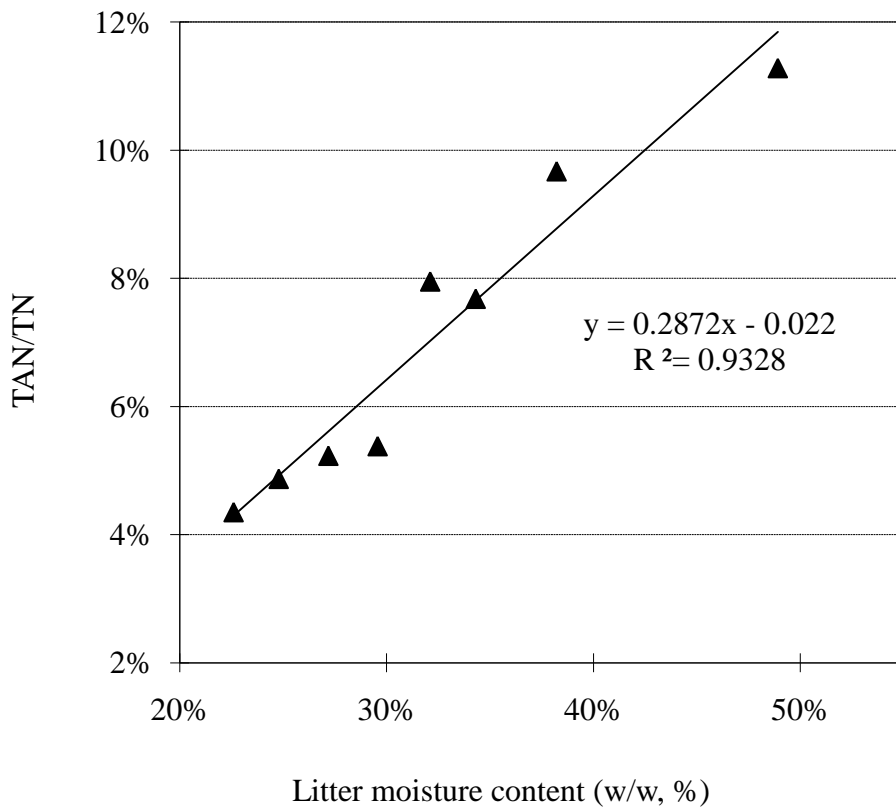


Figure 5-4. TAN contents in litter vs. litter moisture contents (litter A)

5.3.5 Nitrogen Losses from Litter Samples

An alternative method to estimate ammonia emissions from litter is by measuring the nitrogen losses from litter samples. The eight sub-samples of litter A with various moisture levels from 22.6% to 48.9% were put into eight identical uncovered Petri dishes and were allowed to release ammonia for two weeks. After two weeks of ammonia volatilization, each of these sub-samples was analyzed for nitrogen content again. By comparing the litter nitrogen content before and after ammonia volatilization, the nitrogen losses of litter samples at eight moisture levels in these two weeks were obtained. The results are shown in Figure 5-5. It was found that the litter sub-sample that was not treated with water (moisture content

was 22.6%) had the highest nitrogen loss. And the litter sub-samples that were treated with largest amount of water (moisture contents were 38.2% and 48.9%) had the lowest nitrogen losses. These results are consistent with what has been reported in previous sections, which indicated that water applied to the litter had an effect of suppressing ammonia emissions in a short time range. Although increased litter moisture contents resulted in increased TAN contents in litter as was discussed in the previous section, it did not necessarily result in increased ammonia emissions in the time range of the experiments (within two weeks).

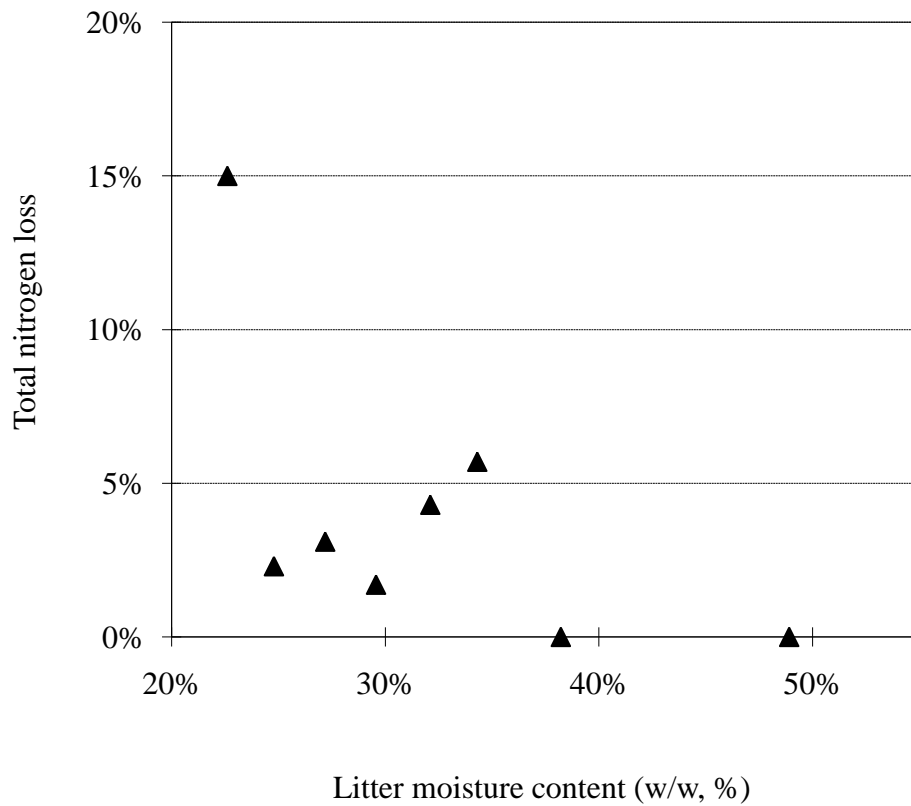


Figure 5-5. Nitrogen losses of litter samples vs. litter moisture contents (litter A)

5.4 CONCLUSION

Ammonia emissions from broiler litter samples were tested at various litter moisture contents under laboratory-controlled conditions. It was observed that ammonia emissions were very sensitive to litter moisture content. Water applied to the litter may affect ammonia emissions through various processes in the litter, such as generation of ammonia within the litter as well as mass transfer of ammonia in the litter and from the litter to the air. It was found that time played an important role for the comprehensive effect of the added water. As water was added to the litter, the TAN contents in litter increased, which could potentially increase ammonia emissions. However, measurements of ammonia concentrations in the chamber and nitrogen loss in the litter all suggested that water applied to the litter also had an effect of suppressing ammonia emissions in the beginning for a short time. After enough time (one to two weeks) elapsed, higher moisture contents in litter eventually resulted in higher ammonia emissions. It was also noted that at very high litter moisture contents, even when more time was allowed, ammonia concentrations began to decrease as moisture contents further increased.

6. MODELING AMMONIA EMISSIONS FROM BROILER LITTER AT LABORATORY

SCALE

This chapter describes the main body of the emission model. In the reported model, the ammonia flux is essentially a function of litter total ammoniacal nitrogen (TAN) content, moisture content, pH, temperature, the Freundlich partition coefficient (K_f), the mass transfer coefficient (K_G), the ventilation rate (Q) and the emission surface area (A). The Freundlich partition coefficient (K_f) was used as a fitting parameter in the model. Both the dynamic flow-through chamber system and the wind tunnel were utilized to measure ammonia fluxes from broiler litter. The dynamic flow-through chamber experiments evaluated the reported model with various litter samples under constant temperature and wind profile. The wind tunnel experiments evaluated the reported model under various temperatures and wind profiles. Model parameters such as K_f and K_G were estimated. The results from the two studies were consistent with each other. The estimated K_G ranged from 1.11 to 27.64 m/h, and the estimated K_f ranged from 0.56 to 4.48 L/kg. A regression sub-model was developed to estimate K_f as function of litter pH and temperature, which indicates that K_f increases with increasing litter pH and decrease with increasing temperature. The reported model was used to estimate the equilibrium gas phase ammonia concentration $C_{g, 0}$ in litter and compared with the observed values. The normalized mean error (NME), the normalized mean square error (NMSE) and fractional bias (FB) were calculated to be 25%, 12% and -0.3% respectively for all the 94 measurements, and the model was able to reproduce 79.86% of the variability of the data. Sensitivity analysis of the model showed that ammonia flux is very sensitive to litter pH followed by temperature, and the relative sensitivity of pH or temperature increases as pH or temperature increases.

6.1 RESEARCH OBJECTIVE

The objective of this study was to develop a mechanistic emission model to estimate ammonia flux from broiler litter, and to evaluate the model at laboratory scale.

6.2 MODEL DEVELOPMENT

6.2.1 The general mass transfer flux equation

The extensive review provided by Ni (1999) suggested a common structure for most ammonia emission models. Although different theories of mass transfer have been used in ammonia emission models, the resulting mass transfer equations tend to be in a form similar to Equation 2-14 in Chapter 2. In broiler houses, considering the fact that broiler chickens generate new manure on the litter surface and chicken activity stirs the litter continuously, it is reasonable to accept the assumption that the ammonia concentration in surface litter is uniformly distributed, and the transfer in the gas phase controls the whole transfer process. For ammonia emission from litter in a broiler house, the general mass transfer flux equation can be expressed as

$$J = K_G (C_{g,0} - C_{g,\infty}) \quad (6-1)$$

In which,

J is ammonia emission flux, $\text{mg m}^{-2} \text{h}^{-1}$;

K_G is overall mass transfer coefficient in gas phase, m h^{-1} ;

$C_{g,0}$ is gas phase ammonia concentration in equilibrium with dissolved ammonia in litter, mg m^{-3} ;

$C_{g,\infty}$ is gas phase ammonia concentration in the free air stream in broiler house, mg m^{-3} .

Mass transfer coefficients reported for ammonia emission models vary widely. The variation is partly due to the physical characteristics of the mass transport process, such as air flow velocity and flow pattern, and partly due to the cumulative effect of various assumed values for the Henry's and dissociation constants used in different models (Montes, 2008). By using the equilibrium gas phase ammonia concentration in Equation 6-1, the chemical equilibrium part of the process is isolated into $C_{g,0}$, and K_G in Equation 6-1 only reflects the physical characteristics of the mass transport process.

Assuming that the ammonia concentration in the air that entering the house are negligible comparing with the ammonia concentration inside the house, from mass balance, the ammonia emission flux J can also be obtained from the following equation:

$$J = (Q/A) C_{g,\infty} \quad (6-2)$$

In which,

Q is ventilation rate of the broiler house, $m^3 h^{-1}$;

A is emission surface area of litter, m^2 .

Combining Equations 6-1 and 6-2, the following equation is obtained,

$$(Q/A) C_{g,\infty} = K_G (C_{g,0} - C_{g,\infty}) \quad (6-3)$$

So,

$$C_{g,\infty} = K_G (K_G + Q/A)^{-1} C_{g,0} \quad (6-4)$$

Combining Equation 6-4 into Equation 6-2, the core emission flux model can be obtained as

$$J = ((Q/A)^{-1} + K_G^{-1})^{-1} C_{g,0} \quad (6-5)$$

Defining the overall emission coefficient K_e ,

$$K_e = [(Q/A)^{-1} + K_G^{-1}]^{-1} \quad (6-6)$$

Then the emission flux J can be expressed as

$$J = K_e \times C_{g, 0} \quad (6-7)$$

The overall emission coefficient K_e has units of velocity, and it is determined by the mass transfer coefficient K_G and the Q/A ratio as shown in Equation 6-6. Influence of the relative magnitude of Q/A and K_G values on K_e is summarized in Table 6-1.

Table 6-1. Influence of the relative magnitude of Q/A and K_G value on K_e

	K_e	$C_{g, \infty}$	J	Example condition
When $Q/A \gg K_G$	$K_e \approx K_G$	$C_{g, \infty} \approx 0$;	$J \approx K_G \times C_{g, 0}$	Open field
When $Q/A \ll K_G$	$K_e \approx Q/A$	$C_{g, \infty} \approx C_{g, 0}$;	$J \approx Q/A \times C_{g, 0}$	Closed house

In the core emission flux model (Equation 6-5), the ammonia flux is a function of the mass transfer coefficient K_G , the gas phase ammonia concentration in equilibrium with dissolved ammonia in litter ($C_{g, 0}$), the ventilation rate (Q) and the emission surface area (A). To estimate the ammonia flux, the most important task is to determine $C_{g, 0}$ and K_G . Determination of K_G is largely empirical. The reported values of these coefficients vary widely, ranging from 0.005 to 42 m/h (Ni, 1999). Review of the existing ammonia emission models showed that the mass transfer coefficients were usually calculated as a function of air velocity and temperature (Ni, 1999; Zhang, 1992). Sometimes surface roughness, air density and air viscosity were also considered. Determination of $C_{g, 0}$ is more complex, and a sub-model was developed for it.

6.2.2 Sub-model of the equilibrium gas phase ammonia concentration ($C_{g, 0}$)

The value of $C_{g, 0}$ depends on the equilibrium between gas phase ammonia and the total ammoniacal nitrogen (TAN) content in the litter. Because of litter moisture content, TAN in litter partitions into the adsorbed and dissolved phases. Dissolved ammonia in litter can exist in the form of ammonium ions (NH_4^+) and free ammonia (NH_3), and adsorbed ammonia is mainly in the form of NH_4^+ . The processes related to ammonia emissions from broiler litter are illustrated in Chapter 2, Figure 2-1.

Using mass balance, TAN mass in litter can be expressed as:

$$[\text{TAN}] = \text{Adsorbed } \text{NH}_4^+\text{-N} + \text{dissolved } \text{NH}_3\text{-N} + \text{dissolved } \text{NH}_4^+\text{-N} \quad (6-8)$$

Where $[\text{TAN}]$ is the TAN content in litter on a dry basis ($\mu\text{g g}^{-1}$). The NH_4^+ in the dissolved phase and adsorbed phase are in equilibrium. The Freundlich isotherm is widely used for NH_4^+ partitioning between solid phase and aqueous phase (Bolt, 1976). It may be expressed as:

$$\text{Adsorbed } \text{NH}_4^+\text{-N} = K_f \times [\text{NH}_4^+\text{-N}]_l^{1/n} / 1000 \quad (6-9)$$

Where adsorbed $\text{NH}_4^+\text{-N}$ is expressed on a dry basis ($\mu\text{g g}^{-1}$), K_f is the Freundlich partition coefficient (L kg^{-1}), and $[\text{NH}_4^+\text{-N}]_l$ is the concentration of dissolved phase $\text{NH}_4^+\text{-N}$ ($\mu\text{g L}^{-1}$). For solutions with low concentrations, the Freundlich isotherm can be simplified to a linear isotherm by setting $1/n$ in equation equal to one. In the linear isotherm the parameter K_f (L kg^{-1}) is expressed by the ratio between the adsorbed $\text{NH}_4^+\text{-N}$ on the solid ($\mu\text{g g}^{-1}$) and the dissolved phase $\text{NH}_4^+\text{-N}$ concentration in liquid ($\mu\text{g L}^{-1}$).

The dissolved phase $\text{NH}_3\text{-N}$ and $\text{NH}_4^+\text{-N}$ in litter are in aqueous equilibrium. The ratio of $[\text{NH}_4^+\text{-N}]_l / [\text{NH}_3\text{-N}]_l$ is determined by the pH value and the dissociation constant K_{d0} .

$$[\text{NH}_4^+\text{-N}]_l / [\text{NH}_3\text{-N}]_l = 10^{-\text{pH}} / K_d \quad (6-10)$$

Where $[\text{NH}_3\text{-N}]_l$ is the concentration of dissolved phase $\text{NH}_3\text{-N}$ ($\mu\text{g L}^{-1}$), and K_{d0} is the dissociation constant in water (dimensionless).

Combining Equations 6-8, 6-9, 6-10, and using a linear isotherm, the following model can be obtained to estimate the concentration of dissolved phase $\text{NH}_3\text{-N}$ in litter:

$$[\text{NH}_3\text{-N}]_l = 1000 \times [\text{TAN}] / \{K_f \times 10^{-\text{pH}} / K_{d0} + \text{MC} \times (1 + 10^{-\text{pH}} / K_{d0}) / \rho_{\text{H}_2\text{O}}\} \quad (6-11)$$

Where MC is the moisture content of litter on a dry basis (w/w %), and $\rho_{\text{H}_2\text{O}}$ is the density of water (kg L^{-1}). During the ammonia release process, only free ammonia can be released into air stream. The fraction of free ammonia nitrogen over TAN can be calculated using the following equation.

$$F_c = \frac{\text{dissolved NH}_3\text{-N}}{\text{TAN}} = \frac{1}{1 + \frac{10^{-\text{pH}}}{K_{d0}} (1 + K_f \frac{\rho_{\text{H}_2\text{O}}}{\text{MC}})} \quad (6-12)$$

Where F_c is the corrected fraction of free ammonia nitrogen over TAN (dimensionless)

In Equation 6-12, it can be seen that introducing K_f reduces the fraction of free ammonia nitrogen over TAN in litter as compared with that in water.

The dissociation constant in water solution K_{d0} is a function of temperature (K). It can be expressed with the following semi-empirical equation (Kamin et al., 1979). At 25°C, $K_{d0} = 10^{-9.3}$.

$$\text{Log } K_{d0} = -0.0918 - 2729.92/T \quad (6-13)$$

As stated in Chapter 2, the dissociation constant in manure K_d was often expressed by multiplying K_{d0} with a ratio α that incorporates the effect of solids and ions. Therefore, the fraction of free ammonia nitrogen over TAN in manure was calculated using the following equation.

$$F_c = \frac{1}{1 + \frac{10^{-\text{pH}}}{\alpha K_{d0}}} \quad (6-14)$$

Comparing Equations 6-12 and 6-14, it can be seen that in this sub-model, α is related with K_f and litter moisture content, and it can be calculated by:

$$\alpha = \left(1 + K_f \frac{\rho_{\text{H}_2\text{O}}}{[\text{MC}]}\right)^{-1} \quad (6-15)$$

[TAN], MC, and pH are all measurable variables. Once $[\text{NH}_3\text{-N}]_l$ is determined using Equation 6-11. The gas phase ammonia concentration in equilibrium with dissolved ammonia in litter ($C_{g, 0}$) can be estimated from $[\text{NH}_3\text{-N}]_l$ and Henry's constant (K_h).

$$K_h = [\text{NH}_3\text{-N}]_l / (14/17 \times C_{g, 0}) \quad (6-16)$$

The equation of Hales and Drewes (1979) was used in the sub-model. It calculated K_h in non-dimensional form as function of temperature (K).

$$\text{Log } K_h = -1.69 + 1477.7/T \quad (6-17)$$

In summary, $C_{g, 0}$ can be estimated from [TAN], MC and pH of litter material using a sub-model described in Equations 6-11 through 6-17.

6.3 EXPERIMENTAL METHODS

The dynamic flow-through chamber system and the wind tunnel were used to measure ammonia emissions from broiler litter and to evaluate the model performance.

6.3.1 Dynamic flow-through chamber

Design and construction details of the chamber system are given in Chapter 3.

Litter samples were placed on the chamber bottom to a depth of about 0.025 m.

Ammonia emission fluxes at steady state from the litter were measured under various ventilation rates (airflow rates through the chamber) from 8.3 to 40.9 min⁻¹.

The general mass transfer flux equation can be rearranged as:

$$C_{g, \infty} = C_{g, 0} - (1/K_G) J \quad (6-18)$$

The speed (RPM) of the stirring impeller in the chamber was set at 110 rpm, and the room temperature was kept at 22 °C. Assuming that the mass transfer coefficient (K_G) is constant, the concentration of gas phase ammonia in the chamber ($C_{g, \infty}$) and the ammonia emission flux (J) should have a negative linear relationship. The values of measured $C_{g, \infty}$ versus J were plotted, and a linear regression was performed. The slope of the regression line provided the estimated value of $(-1/K_G)$, from which K_G was calculated. Once K_G was determined, $C_{g, 0}$ was obtained from the measured ammonia flux. The $C_{g, 0}$ values for ten different litter samples were obtained at $T = 22$ °C. For each litter sample, three replicate measurements were taken.

6.3.2 The Wind tunnel

Design and construction details of the wind tunnel are given in Chapter 3.

In the wind tunnel experiments, $C_{g, 0}$ was obtained by measuring the equilibrium concentration of gas phase ammonia at the litter surface directly, in absence of air exchange, by closing the wind tunnel and allowing zero airflow. Since values of $C_{g, 0}$ were usually higher than 100 ppm, which was the full-scale reading of the chemiluminescence ammonia analyzer; a dilution system was fabricated and employed upstream of the analyzer. The dilution ratio was calibrated using standard ammonia gas (400 ppm, $\pm 2\%$, National Specialty Gases, Durham, N.C.). The dilution ratio was determined to be 15.18 with a standard deviation of 0.62 ($n = 10$). In order to investigate the influence of temperature, the $C_{g, 0}$ was measured at various temperatures. Two litter samples with different TAN and moisture contents were tested. Ammonia fluxes (J) in the wind tunnel were measured at various

combinations of air velocities and air temperatures. After J and $C_{g,0}$ were determined, the mass transfer coefficient (K_G) was calculated using the core emission flux equation (Equation 6-1).

6.3.3 Litter samples

Litter samples were taken from multiple locations of a broiler farm in North Carolina during the clean-out period. The litter material consisted of wood shavings. Each of the litter samples were well mixed together before tests. For each test, sub-samples of litter were taken from the same well-mixed litter sample and put into the chamber or the emission section inside the wind tunnel to make a constant ammonia emission sources. The analyses of litter samples were conducted in the BAE Environmental Analysis Laboratory at North Carolina State University. The analyses methods for the litter samples are provided in Chapter 3.

6.3.4 Model evaluation parameters

Normalized mean error (NME), normalized mean square error (NMSE), and fractional bias (FB) were calculated to evaluate the performance of the model:

$$NME = \frac{\sum |C_{Pi} - C_{Oi}|}{\sum C_{Oi}} \quad (6-19)$$

$$NMSE = \frac{\sum (C_{Pi} - C_{Oi})^2}{(n C_p C_O)} \quad (6-20)$$

$$FB = \frac{2(C_P - C_O)}{(C_P + C_O)} \quad (6-21)$$

Where,

C_{Pi} is model-predicted value of $C_{g,0}$, mg m^{-3} ;

C_{Oi} is observed value of $C_{g,0}$, mg m^{-3} ;

n is number of corresponding pairs of observed and predicted values.

C_p is mean predicted value of $C_{g,0}$, mg m^{-3} ;

C_o is mean observed value of $C_{g,0}$, mg m^{-3} .

6.3.5 Sensitivity analysis

In order to assess the relative importance of critical parameters, a sensitivity analysis was performed to evaluate the relative changes in model-predicted ammonia flux with respect to changes in the model input variables, such as litter TAN content, moisture content, pH, temperature, K_f , and K_G . Although some variables are not totally independent of each other (such as K_G vs. temperature), only the variable of interest was changed in the sensitivity analysis. The relative sensitivity indicates the percent change in flux for each percent change in the input variable in the range being considered. It was calculated using the method described by Zerihun et al. (1996) and Liang et al. (2002) and is defined as:

$$S_r = (\Delta J/J)/(\Delta x/x) \quad (6-22)$$

Where,

S_r is relative sensitivity, dimensionless;

ΔJ is change of ammonia emission flux, $\text{mg h}^{-1} \text{m}^{-2}$;

J is ammonia emission flux when all variables using baseline values, $\text{mg h}^{-1} \text{m}^{-2}$;

Δx is change of the variable of interest over the range being considered;

x is baseline value of the variable of interest.

6.4 RESULTS AND DISCUSSIONS

6.4.1 $C_{g,0}$ of different litter samples at constant temperature

In the dynamic flow-through chamber experiments, it was observed that as ventilation rate increased, the concentration of gas phase ammonia in the chamber ($C_{g,\infty}$), decreased, while the ammonia flux (J) increased (Figure 6-1).

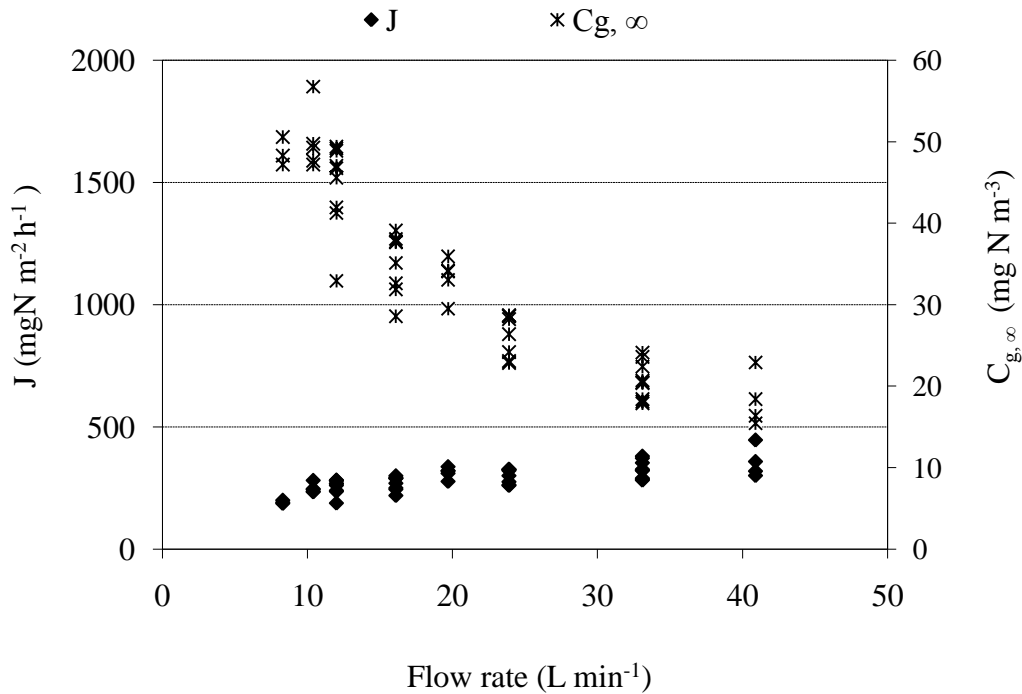


Figure 6-1. Flux and concentration vs. flow rate

The values of measured $C_{g,\infty}$ versus J were plotted and a linear regression was performed (Figure 6-2). The slope was estimated to be -0.1233 with a standard deviation of 0.027. An average value of 8.11 m h^{-1} was obtained for K_G . The average value of $C_{g,0}$ for each litter sample and corresponding litter properties are presented in Table 6-2, in which TAN and litter moisture contents were expressed on a dry basis.

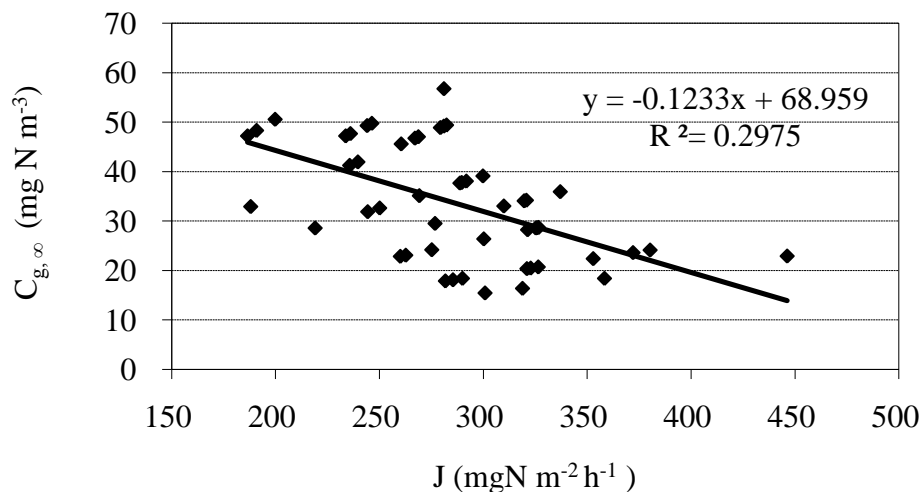


Figure 6-2. $C_{g,\infty}$ vs. emission flux J

Table 6-2. $C_{g,0}$ for various litter samples (T=22 °C)

Litter sample No.	TAN ($\mu\text{g g}^{-1}$)	pH	Moisture content (w/w, %)	$C_{g,0}$ (mg m ⁻³)	K_d ratio α
1	3787	8.90	33.4	162.7	0.069
2	1751	9.02	29.6	118.6	0.074
3	3961	7.59	35.1	27.2	0.232
4	2605	8.72	21.8	142.9	0.087
5	4650	8.14	21.7	86.3	0.110
6	3405	7.45	28.1	13.2	0.144
7	4607	7.79	36.9	81.0	0.399
8	3033	8.13	32.9	63.7	0.194
9	4795	6.26	22.9	1.1	0.109
10	1908	8.81	34.4	133.6	0.146

Applying Henry's law (Equation 6-15), the concentrations of dissolved phase $\text{NH}_3\text{-N}$ in litter were estimated to be in the range of 1.9 to 278 mg L^{-1} . The dissociation constant (K_d) was estimated and compared with that in water. The K_d ratio α was calculated and the results are listed in Table 6-2. The estimated K_d ratio α has an average value of 0.157 with standard deviation of 0.095, which is comparable with one-sixth as reported by Hashimoto and Ludington (1971) and one-fifth as reported by Zhang (1992) in their study of chicken and pig manure. It was also noticed that the K_d ratio α was positively related with litter moisture content as shown in Figure 6-3, which is expected from Equation 6-15.

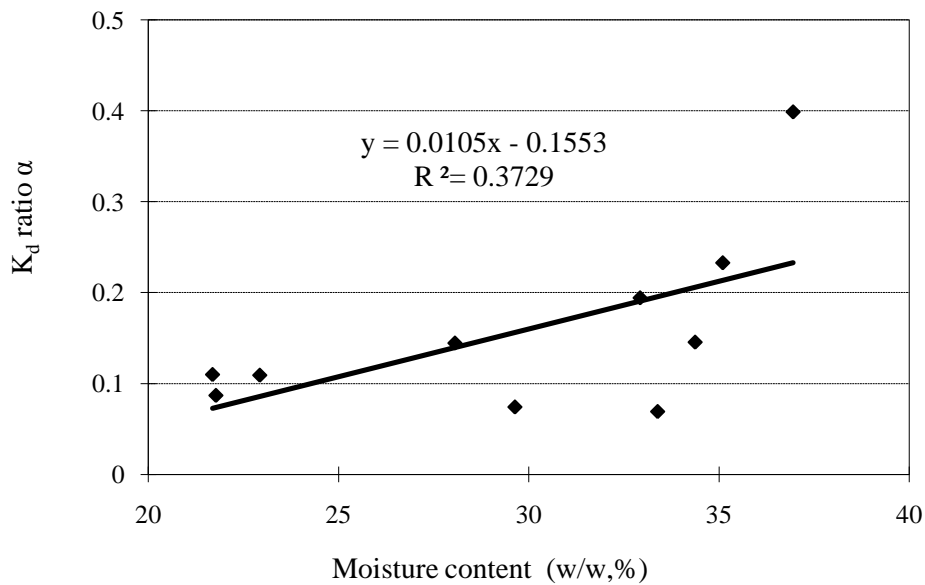


Figure 6-3. The K_d ratio α vs. litter moisture content

Griffin et al. (1976) reported that K_f of ammonia in Montmorillonite sand was 0.24 to 2.00 L kg^{-1} . Freewood et al. (2001) reported that K_f of ammonia in Colliery spoil was 0.6 to 19.3 L kg^{-1} . No values of K_f have been reported for broiler litter in the available literature. Therefore, K_f was used as a fitting parameter. The K_f value can be estimated using Equation 6-15. The estimated K_f value is in fact a lumped parameter accounting for all the effects (solid adsorption, ionic interaction, etc.) that contribute to the deviation of K_d from that of

water. The K_f of ammonia in litter was estimated to have an average value of 2.11 L kg^{-1} for the nine tested litter samples. The result of the litter sample which has a pH value of 6.26 was omitted because of its' unrealistically low pH value.

The distribution of TAN content of the tested ten samples was calculated and the results were illustrated in Figure 6-4. It was estimated that the dissolved phase $\text{NH}_3\text{-N}$ was only 0.01% to 4.11% of TAN in litter, and the adsorbed phase $\text{NH}_4^+\text{-N}$ was 59.5% to 90.8% of TAN in litter.

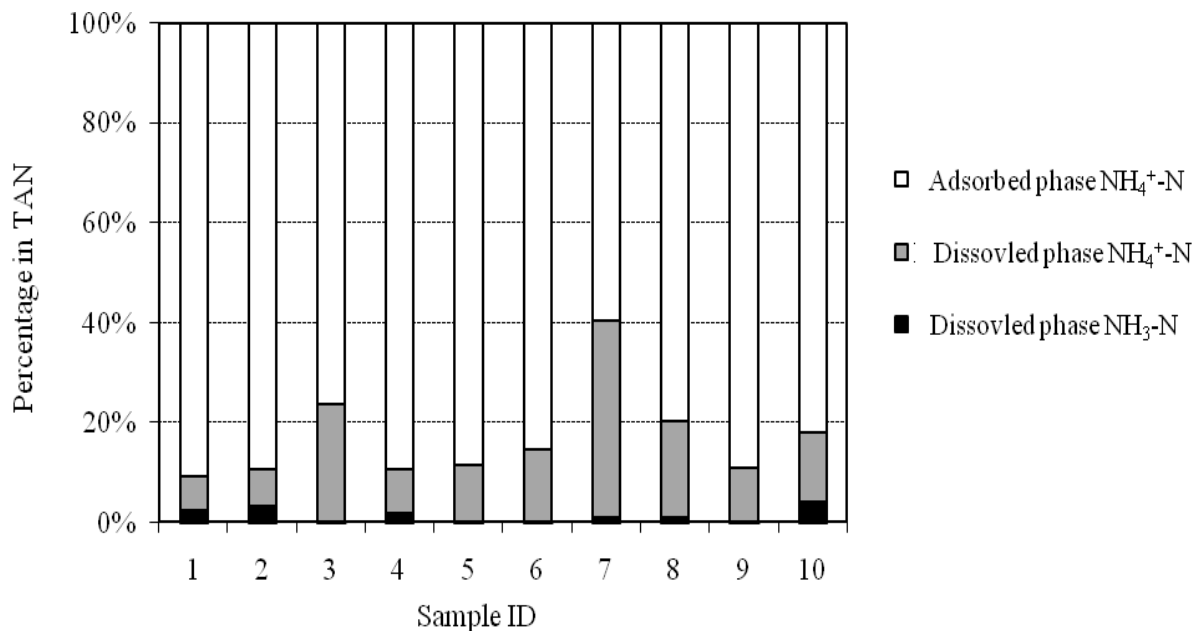


Figure 6-4. Estimated distribution of TAN content of the tested ten litter samples

The $C_{g,0}$ can then be calculated using the sub-model described in Equations 6-11 through 6-17 and the estimated average K_f value (2.11 L kg^{-1}). The model predicted values of $C_{g,0}$ were compared with the observed values in Figure 6-5. It can be seen that the sub-model was able to simulate $C_{g,0}$ as function of pH. It has also been observed that the K_f of ammonia in litter was positively related with litter pH value as shown in Figure 6-6. The effect of pH on K_f may explain why the sub-model tends to overestimate $C_{g,0}$ at higher pH values when using a constant K_f (2.11 L kg^{-1}) as shown in Figure 6-5.

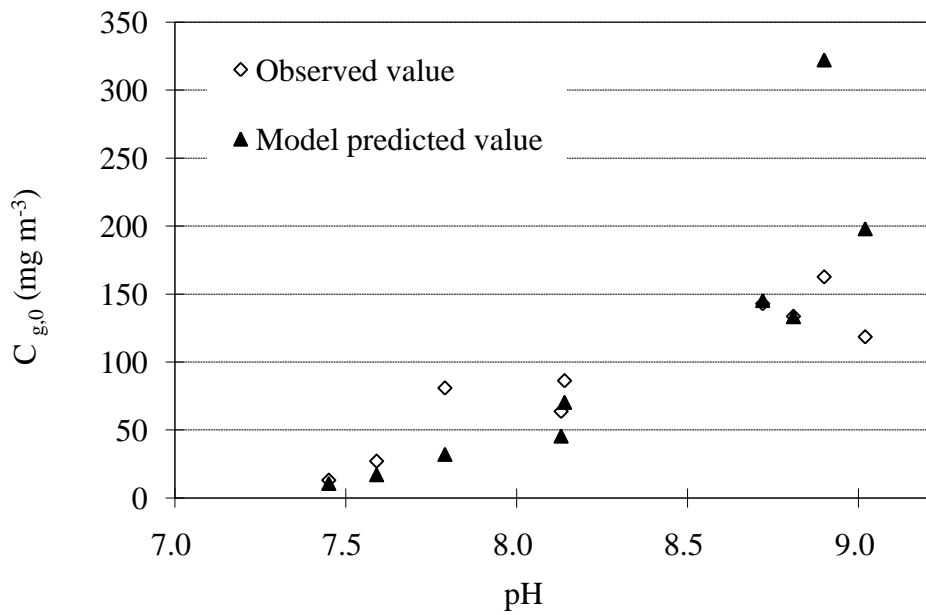


Figure 6-5. The model predicted values and the observed values of $C_{g,0}$ of the tested nine litter samples ($T=22^{\circ}\text{C}$)

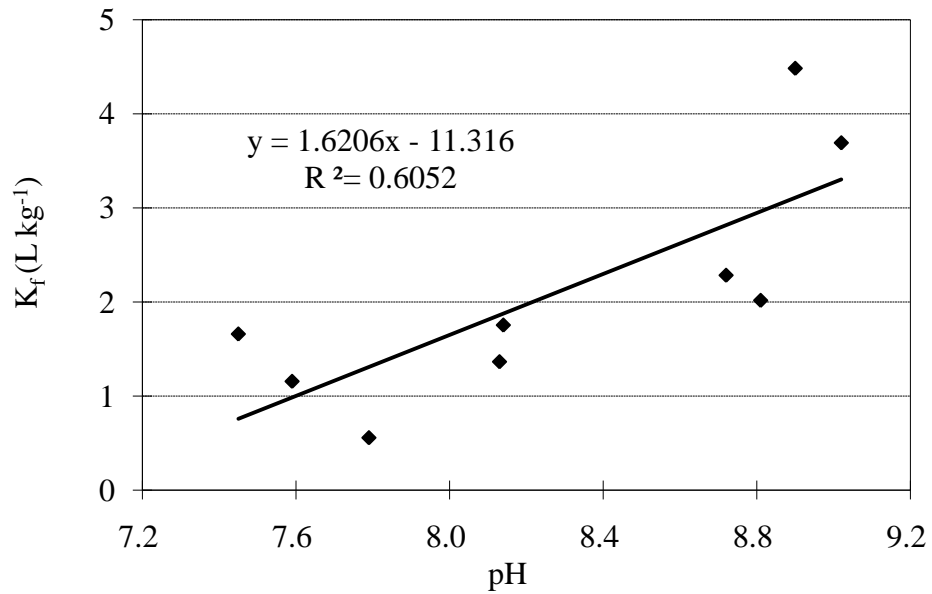


Figure 6-6. K_f vs. pH

6.4.2 $C_{g,0}$ at various temperatures

In the wind tunnel experiments, two litter samples were tested at various temperatures. Properties of the two litter samples are listed in Table 6-3, in which TAN and litter moisture contents are expressed on a dry basis.

Table 6-3. Properties of the two litter samples

Litter sample label	TAN ($\mu\text{g g}^{-1}$)	pH	Moisture content (w/w, %)
A	4501	8.49	29.8
B	9176	8.62	56.7

Thirty measurements were taken for litter A at various temperatures from 8.2 °C to 27.2 °C. The estimated K_d ratio α has an average value of 0.145 with standard deviation of 0.032 for litter A. An average value of 1.87 L kg⁻¹ was obtained for K_f , with a standard deviation of 0.52 L kg⁻¹.

Fifty four measurements were taken for litter B at various temperatures from 8.4 °C to 30.0 °C. The estimated K_d ratio α has an average value of 0.192 with standard deviation of 0.075 for litter B, and an average value of 2.15 L kg⁻¹ was obtained for K_f , with a standard deviation of 0.99 L kg⁻¹.

The $C_{g,0}$ can then be calculated using the sub-model described in Equations 6-11 through 6-17 and the estimated average K_f value for each litter sample. The model predicted values of $C_{g,0}$ are compared with the observed values in Figure 6-7 and Figure 6-8. It can be seen that the sub-model was able to simulate $C_{g,0}$ as function of temperature. It has also been observed that K_f has a tendency to decrease with increasing temperature for both litter A and B as shown in Figure 6-9 and Figure 6-10. The effect of temperature on K_f may explain why the sub-model tends to underestimate $C_{g,0}$ at higher temperatures when using a constant K_f as shown in Figure 6-7 and Figure 6-8. The difference of K_f values between litter A and litter B can be explained by their different pH value.

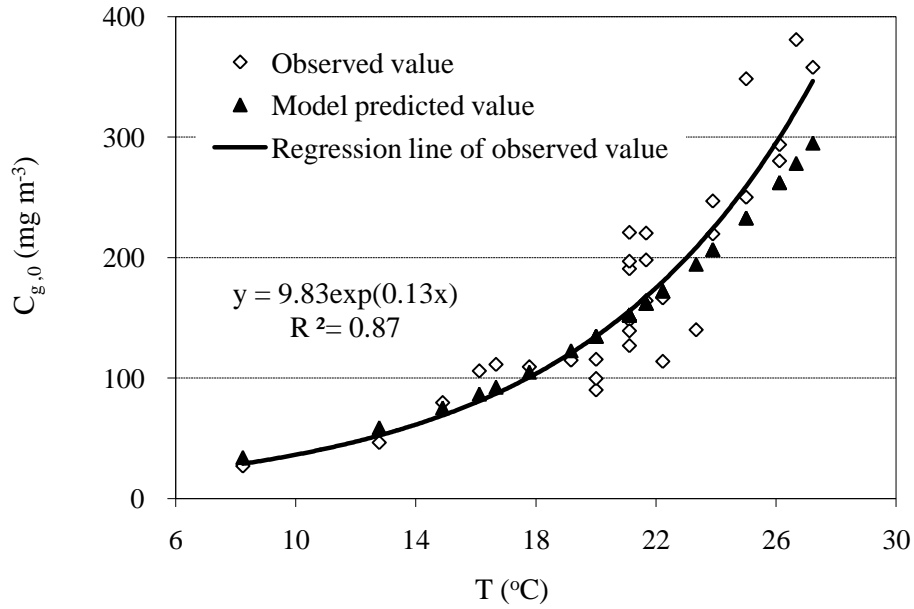


Figure 6-7. The model predicted values and the observed values of $C_{g,0}$ for the litter A at various temperatures (using $K_f=1.87 \text{ L kg}^{-1}$ in model)

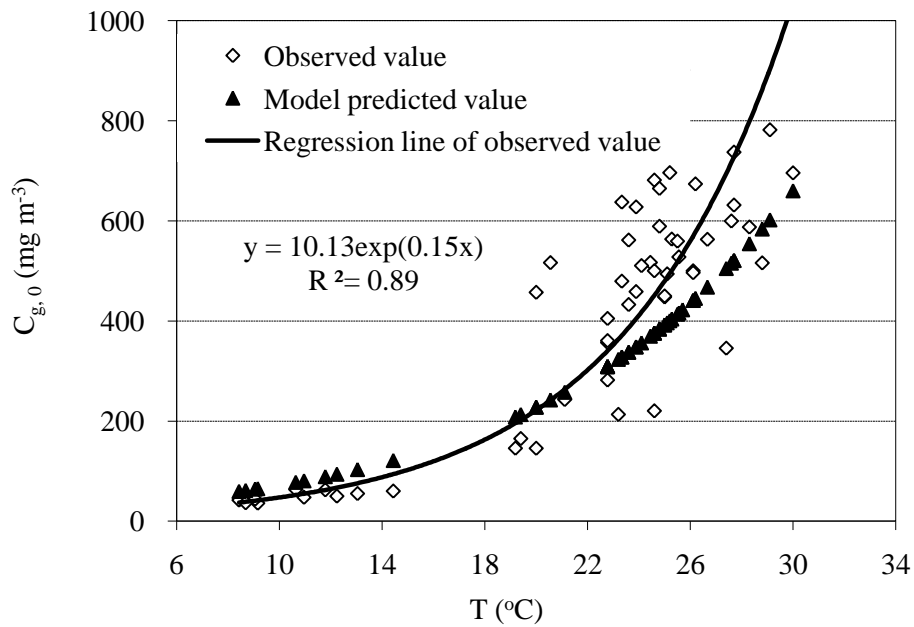


Figure 6-8. The model predicted values and the observed values of $C_{g,0}$ for the litter B at various temperatures (using $K_f=2.15 \text{ L kg}^{-1}$ in model)

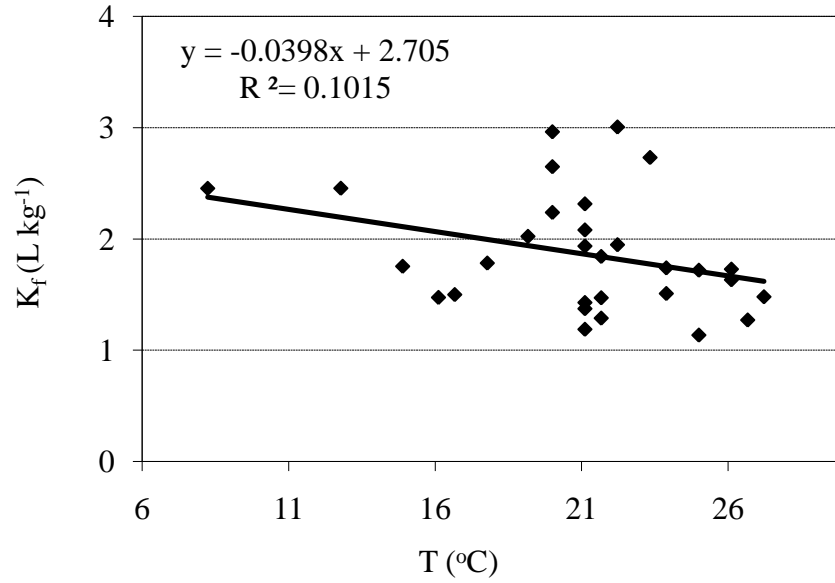


Figure 6-9. K_f vs. temperature for the litter A

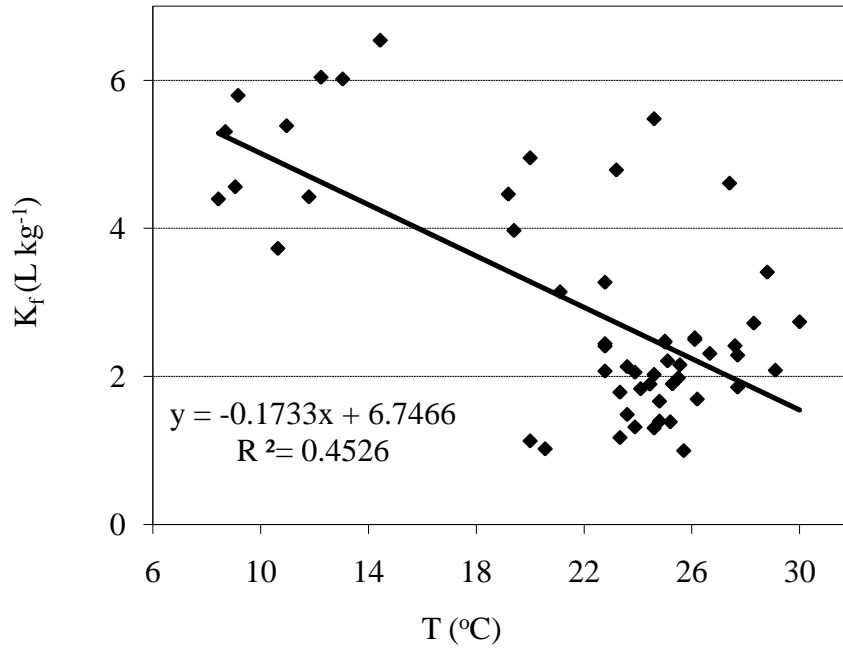


Figure 6-10. K_f vs. temperature for the litter B

The model predicted values and the observed values of the fraction of free ammonia nitrogen over TAN for litter A and B are shown in Figure 6-11. The fraction of free ammonia nitrogen over TAN was obviously higher in litter B than that in litter A due to its higher moisture content and higher pH value.

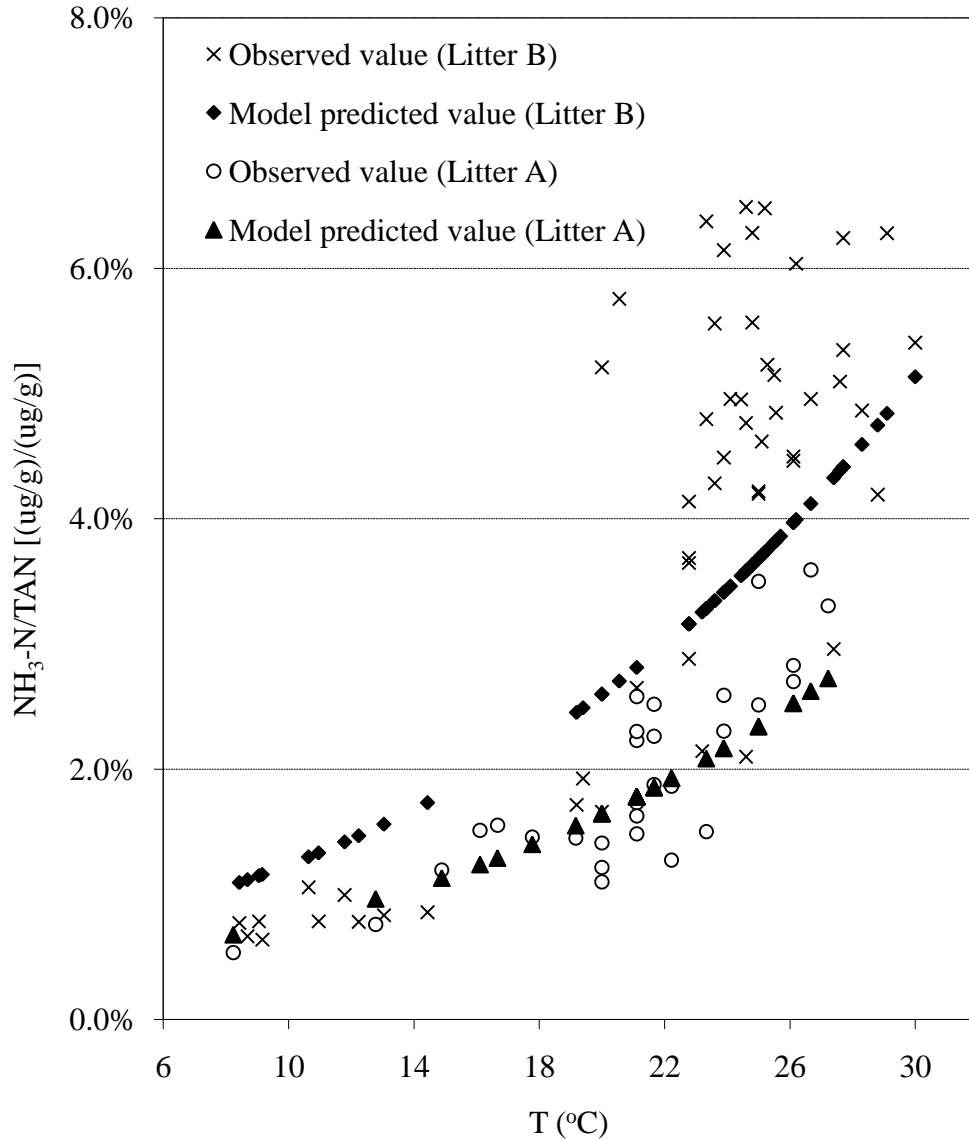


Figure 6-11. The model predicted values and the observed values of fraction of free ammonia nitrogen over TAN for litter A and B

6.4.3 Regression model of K_f

Based on the measurements from both the dynamic flow-through chamber and the wind tunnel study, the following regression model of K_f as function of litter pH value (concentration of hydrogen ion $[H^+]$) and temperature ($^{\circ}C$) was obtained.

$$K_f = C_k [H^+]^a T^b \quad (6-23)$$

Where C_k , a , b are regression coefficients. $a = -0.412 \pm 0.085$, $b = -0.759 \pm 0.135$, $C_k = 0.00672$. Effect of $[H^+]$ and T both have a P-value smaller than 0.001.

6.4.4 Evaluation of the model

The value of $C_{g, 0}$ can be calculated using the sub-model described in Equations 6-11 through 6-17 and the regression model of K_f . The model predicted values of $C_{g, 0}$ were compared with the observed values in Figure 6-12 for all 94 measurements from both the dynamic flow-through chamber and the wind tunnel study. It can be seen that the model was able to reproduce 80% of the variability of the data. For all the 94 measurements, the NME was calculated to be 25%; the NMSE was 13%; and the FB was only -0.3%.

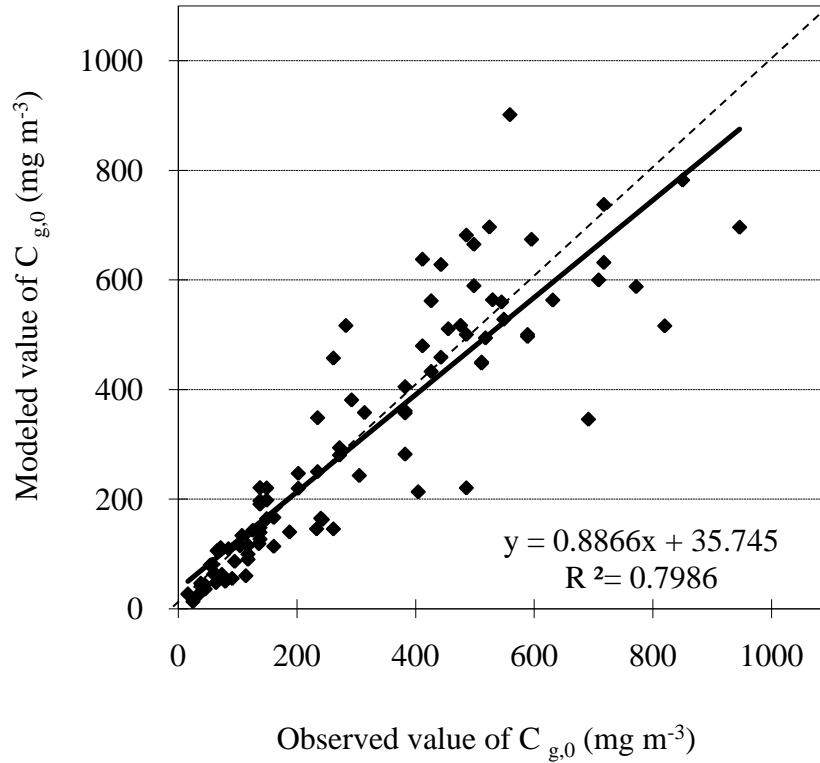


Figure 6-12. The model predicted values and the observed values of $C_{g,0}$

6.4.5 Simulation of $C_{g,0}$ in time series

The equilibrium ammonia concentration $C_{g,0}$ of litter B and ambient air temperature was continuously measured from 12:00pm on 2008/08/27 to 6:00pm on 2008/09/02. Data were recorded at one minute intervals. Figure 6-13 shows the comparison of the model predicted $C_{g,0}$ and observed $C_{g,0}$ in time series. It can be seen that the variation of observed $C_{g,0}$ correlated with ambient temperatures, and the sub-model performed well in simulating the expected variation of $C_{g,0}$ that due to the variation of temperatures.

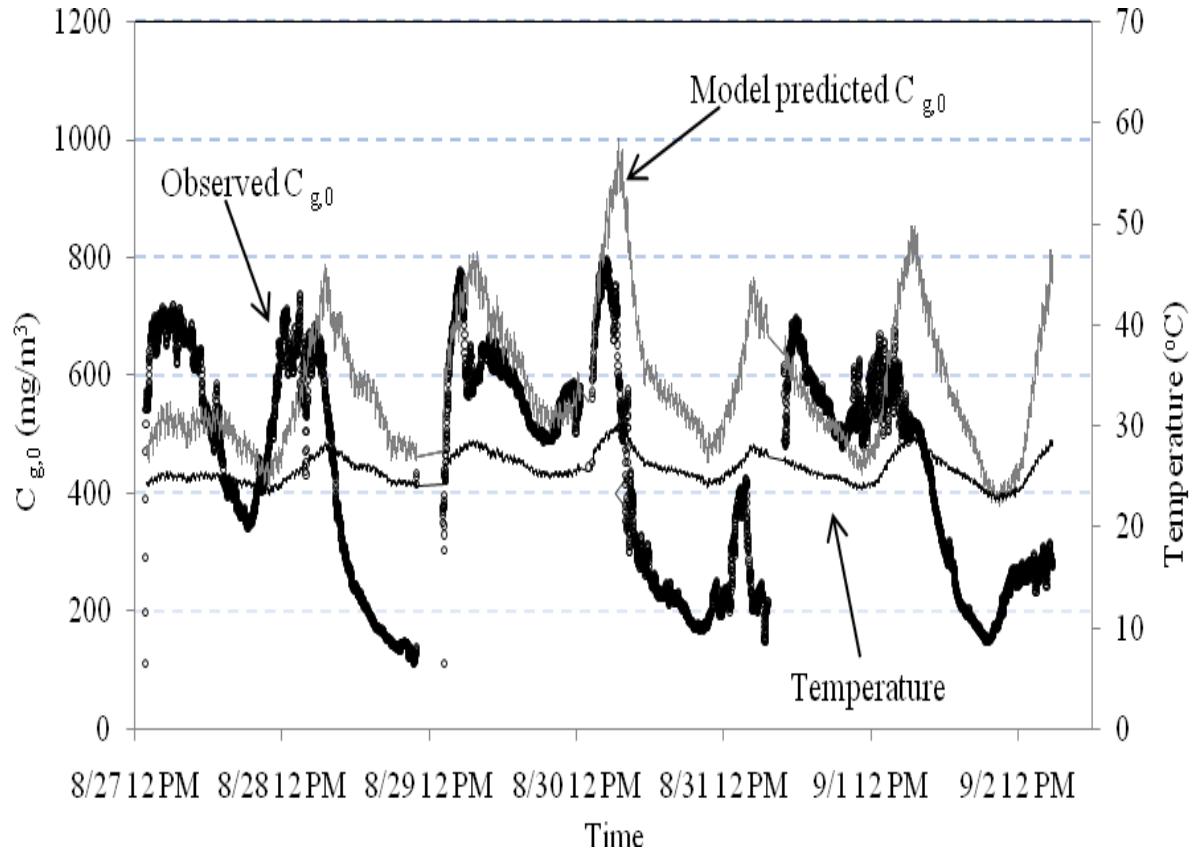


Figure 6-13. Comparison of the model predicted $C_{g,0}$ and observed $C_{g,0}$ in time series

6.4.6 The mass transfer coefficient (K_G)

The mass transfer coefficient (K_G) in the wind tunnel was measured at various combinations of air velocities and air temperatures. In 188 measurements, the K_G ranged from 1.11 to 27.64 m h^{-1} with an average value of 9.10 m h^{-1} . It was found that the K_G was a function of air velocity and air temperature, and the results are discussed in detail in Chapter 7. When air temperature was 22°C and air velocity was 0.80 m s^{-1} , a K_G value of 9.82 m h^{-1} was obtained, which is comparable with what was obtained from the dynamic flow-through chamber experiments ($K_G = 8.11 \text{ m h}^{-1}$).

6.4.7 Model predicted ammonia flux

Combining the sub-model for calculating $C_{g,0}$ and the core emission flux model (Equation 6-5), the ammonia flux is essentially a function of litter TAN content, moisture content, pH, temperature, the Freundlich partition coefficient K_f , the mass transfer coefficient K_G , the ventilation rate Q and the emission surface area A . Furthermore, K_f can be estimated from pH and temperature using regression Equation 6-19. The model predicted ammonia fluxes under various temperatures and pH values are plotted in Figure 6-14. Baseline values were used for all other input variables. It can be seen that ammonia fluxes increased sharply as either pH or temperature increased.

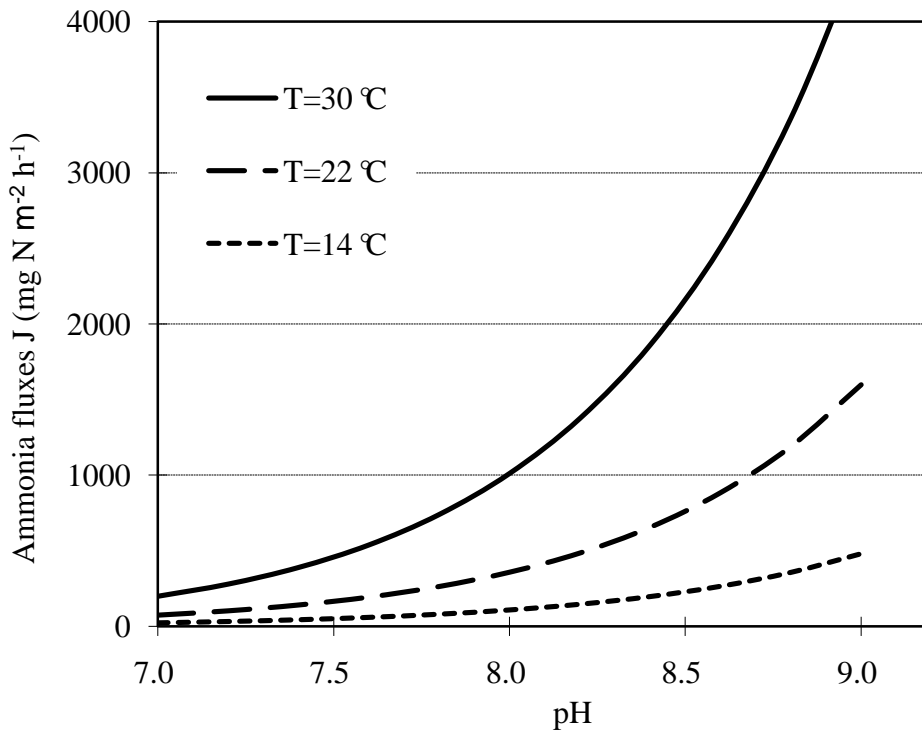


Figure 6-14. The model predicted ammonia fluxes under various temperatures and pH values (baseline values, all on dry basis: TAN = 3553 μ g g⁻¹, moisture content = 32.94 w/w%, $K_G = 8.11$ m h⁻¹, $Q/A = 100$ m h⁻¹)

6.4.8 Sensitivity analysis

Ammonia flux was calculated to be $446 \text{ mgN m}^{-2} \text{ h}^{-1}$ when using baseline values in Table 6-4 for all variables. For a 10% increase of the variable of interest from the baseline value, the resulting percentage changes of ammonia flux are also presented in Table 6-4. It can be seen that ammonia flux is very sensitive to litter pH and temperature. In fact, an increase of 0.2 in pH or an increase of 2°C in temperature can result in more than 20% increase in flux. The resulting percentage change of ammonia flux due to the variation of K_f or K_G has the same order of magnitude of the percentage change of the parameter itself. As indicated before, sensitivity of K_G is dependent on the relative magnitude of Q/A and K_G baseline values. The choice of 100 m h^{-1} as the baseline value for Q/A was based on actual tunnel-ventilated broiler house measurements (Lacey et al. 2003).

Table 6-4. Baseline values and percentage change of ammonia flux for 10% increase of variables

Variables of interest	Baseline values	Percentage change of ammonia flux for 10% increase of the variable of interest from baseline value
TAN ($\mu\text{g g}^{-1}$)	3553	+10%
pH	8.11	+509.6%
Moisture content (w/w, %)	32.94	-1.9%
Temperature ($^\circ\text{C}$)	22	+27.3%
K_f (L kg^{-1})	1.44	-7.4%
K_G (m h^{-1})	8.59	+9.1%
Q/A (m h^{-1})	100	+0.7%

The relative sensitivity indicates the percent change in flux for each percent change in the input variable in the range being considered. The results are presented in Table 6-5. It was observed that the relative sensitivity of pH or temperature increases as pH or temperature increases.

Table 6-5. Relative sensitivity S_r for ammonia emission flux from litter with respect to litter pH and temperature at different pH and temperature ranges

pH		Temperature	
Range	S_r	Range ($^{\circ}\text{C}$)	S_r
7.0-7.2	20.49	14-16	1.83
7.9-8.1	22.88	22-24	2.70
8.8-9.0	23.74	30-32	3.45

6.5 CONCLUSION

An emission model was developed to estimate ammonia flux from broiler litter. The model inputs include the litter TAN content, litter pH value, litter moisture content, the Freundlich partition coefficient (K_f), mass transfer coefficient (K_G), ventilation rate (Q), and emission surface area (A). The model was evaluated based on experimental results from a dynamic flow-through chamber and a wind tunnel. The results from the two experimental facilities are comparable with each other. Model parameters such as K_f and K_G were estimated. Based on the experimental results, it was estimated that the dissolved phase $\text{NH}_3\text{-N}$ was only 0.01% to 4.11% of the TAN in litter, and the Freundlich partition coefficient (K_f) of ammonia in litter was estimated to be in the range from 0.56 to 4.48 L kg^{-1} . A regression sub-model was developed to estimate K_f as a function of litter pH and temperature, which indicates that K_f increases with increasing litter pH and decreases with increasing temperature. The reported model was used to estimate the equilibrium gas phase ammonia concentration ($C_{g,0}$) in litter, which were then compared with the observed values. The normalized mean error (NME), the normalized mean square error (NMSE), and fractional bias (FB) were calculated to be 25%, 12%, and -0.3%, respectively, for all 93 measurements. And the model was able to reproduce 80% of the variability of the data. Sensitivity analysis of the model showed that ammonia flux is very sensitive to litter pH followed by temperature, and the relative sensitivity of pH or temperature increases as pH or temperature increases.

7. MASS TRANSFER COEFFICIENT OF AMMONIA EMISSIONS

In this chapter, the mass transfer coefficient (K_G) of ammonia was measured in the wind tunnel under various air velocities (0.2 to 2.0 m s⁻¹) and temperatures, and a regression sub-model for calculating K_G was developed. The estimated K_G was in the range from 1.10 to 27.64 m h⁻¹ for 179 measurements. It was observed that under turbulent conditions the K_G increased with increasing air velocity, while under laminar conditions K_G decreased with increasing air velocity. The results also showed that the K_G value negatively related with the air temperature, and the sensitivity of K_G to air temperature was influenced by air velocity. Two groups of measurements were taken. A regression model was developed for K_G based on one group of measurements and the other group was used to validate the model. The model was able to reproduce 58.6% of the variability of the independent group of measurement data. Through dimensionless analysis, equations were developed to calculate K_G as function of air velocity, the characteristic length that influences the air flow, the kinematic viscosity of air, the molecular diffusivity of ammonia in air, and air temperature. It is expected that these equations can be used for systems that have a different scale. The results of this study may be used in emission models to estimated ammonia flux from broiler litter.

7.1 RESEARCH OBJECTIVE

Determination of the mass transfer coefficient is empirical. The gaseous phase mass transfer is usually dominated by convective transfer except for the cases when there was almost no air movement. Review of existing ammonia emission models showed that the mass transfer coefficients were closely related to air velocity and temperature (Ni, 1999; Zhang, 1992). Sometimes surface roughness was also considered (Rachhpal-Singh and Nye, 1986). The mass transfer coefficients obtained in different experiments which measured ammonia emission from manure are very important for emission modeling. A mechanistic emission

model has been developed to simulate the variation of ammonia emissions from broiler litter under various conditions. In the model, the ammonia emission flux was essentially a function of the convective mass transfer coefficient and the equilibrium concentration of gas phase ammonia at the litter surface. The objective of this part of study was to investigate the mass transfer coefficient under various environmental conditions and to develop a regression model.

7.2 EXPERIMENTAL METHOD

7.2.1 The wind tunnel

The mass transfer coefficient K_G was measured using the wind tunnel. Design and construction details of the wind tunnel are given in Chapter 3.

7.2.2 Litter samples

Two litter samples with different TAN and moisture content were used: litter A and litter B. Properties of the two litter samples are listed in Chapter 6, Table 6-3. Measurements of litter A were used to develop the regression model of K_G , and measurements of litter B was used to validate the model. Collection of litter samples, their compositions, and analyses were discussed in Chapter 3 and Chapter 6.

7.2.3 Measurements of ammonia emission and the mass transfer coefficient K_G

Ammonia fluxes were measured for the nominal air velocity values of 0.05, 0.10, 0.15, 0.25, 0.50, 0.80, 1.00, 1.30, 1.60, and 2.00 m s^{-1} . At each velocity, measurements were taken at various air temperatures from 9.1 °C to 29.6 °C. For each test, about 3 kg sub-samples of litter were taken from the same well-mixed litter sample and put into the emission section inside the wind tunnel to make a constant ammonia emission source. It usually took 15 to 30

minutes for the wind tunnel to reach steady state. After steady state was reached, measurements of ammonia concentration were taken using 30-minute average values.

In order to calculate the mass transfer coefficient K_G , the equilibrium concentrations of gas phase ammonia at the litter surface $C_{g,0}$ were measured by closing the wind tunnel and allowing zero airflow. The $C_{g,0}$ was measured at various temperatures. Ammonia fluxes J in the wind tunnel were measured at various combinations of air velocities and air temperatures. After J and $C_{g,0}$ were measured; the mass transfer coefficient K_G was calculated using the core emission flux equation (Equation 6-1 in Chapter 6).

7.3 RESULTS AND DISCUSSION

7.3.1 Ammonia concentration at outlet and emission flux

Measurements of ammonia emission from litter A in the wind tunnel were taken from April 1st to April 30th, and September 22th to November 22th, 2008. In total, 98 measurements were taken. Figure 7-1 shows measurements of ammonia concentration at the outlet of the wind tunnel at various air velocities for litter A. Nominal air velocity was measured at height of 0.13m above litter on the start point of the emission section in the wind tunnel. Measurements for each air velocity value were taken at various temperatures from 9.1 °C to 27.2 °C. It can be seen that ammonia concentration decreased exponentially as air velocity increased. Emission flux is a function of the ammonia concentration at the outlet and the airflow rate of the wind tunnel. Figure 7-2 shows that the airflow rate of the wind tunnel measured by the AV-2 rotating vane anemometer linearly related with the nominal air velocity in the wind tunnel measured by a hotwire anemometer as expected. The calculated emission fluxes from litter A are presented in Figure 7-3, which were in the range from 285 to 2831 mgN m⁻² h⁻¹ with an average value of 1111 mgN m⁻² h⁻¹.

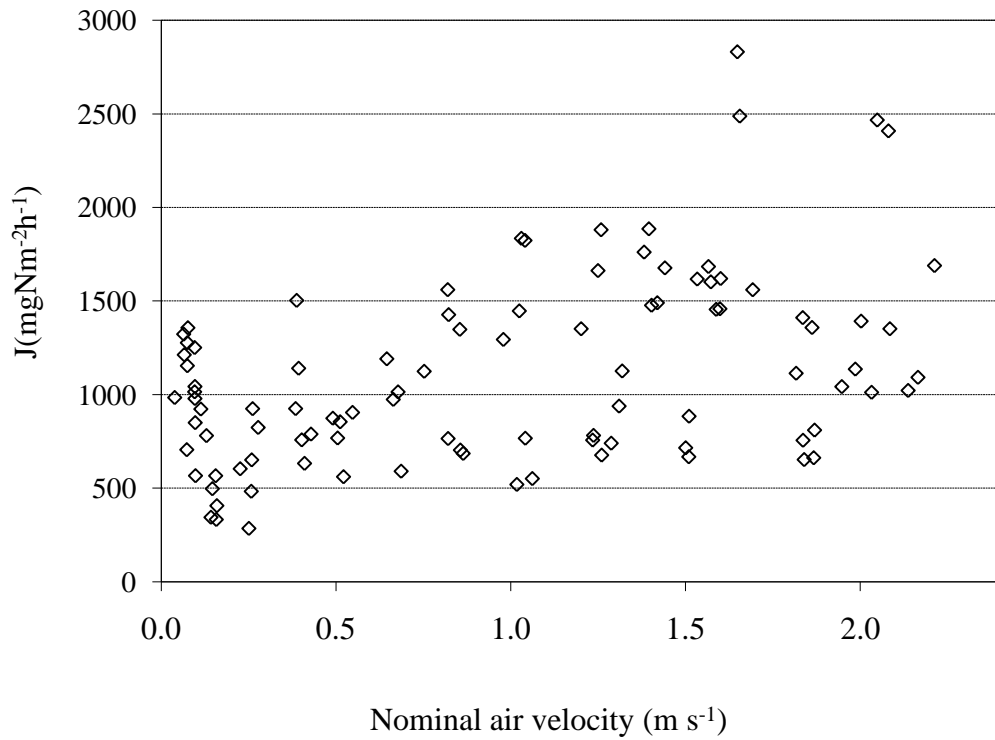


Figure 7-3. Ammonia emission fluxes at various air velocities (Litter A)

7.3.2 Effect of air temperature and air velocity on mass transfer coefficient K_G

The mass transfer coefficient K_G was obtained in the range from 2.20 to 25.80 m h^{-1} with an average value of 11.60 m h^{-1} for measurements of litter A. Statistical analyses show that K_G correlated negatively with air temperature, and the effect of temperature had a P-value less than 0.001. Figure 7-4 presents the obtained K_G value at various temperatures.

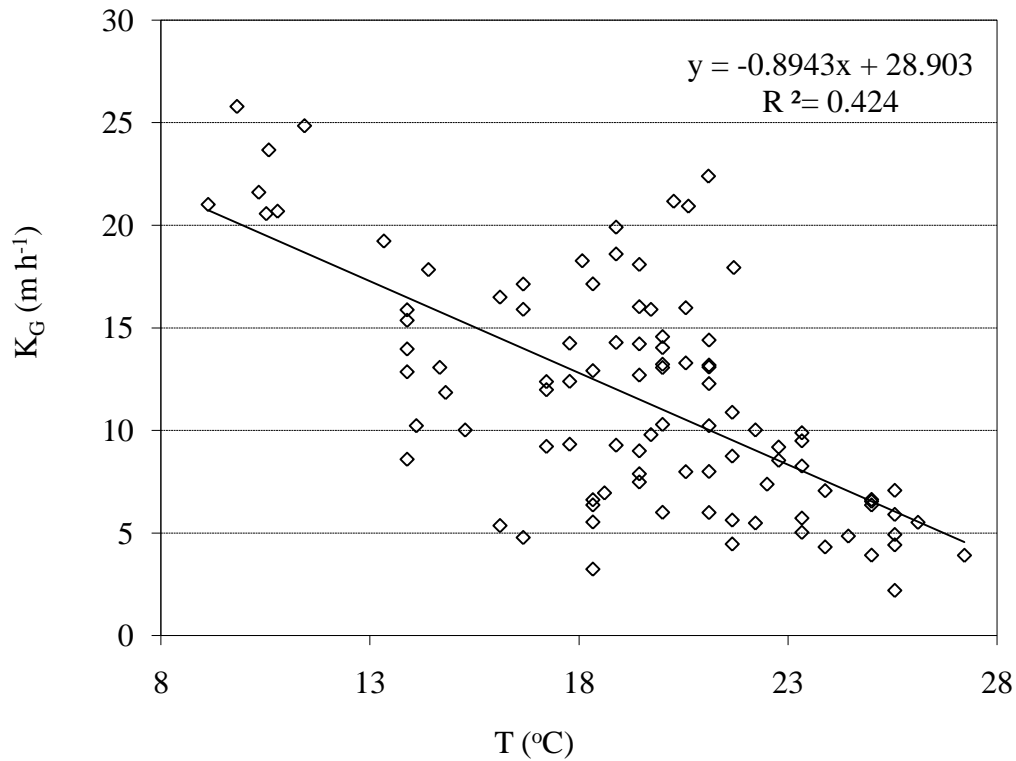


Figure 7-4. K_G value at various air temperatures (Litter A)

In order to investigate the pattern of influence of air temperature and air velocity on K_G, data points were grouped for each air velocity level and the K_G values were plotted against temperature in each group. Figure 7-5 shows that, at all air velocities in the range from 0.05 m s⁻¹ to 2.00 m s⁻¹, the magnitude of K_G decreased as the air temperature increased. The observed negative effect of air temperature on K_G agrees with what has been reported by Arogo, et al. (1999) in their study of mass transfer coefficient in liquid swine manure.

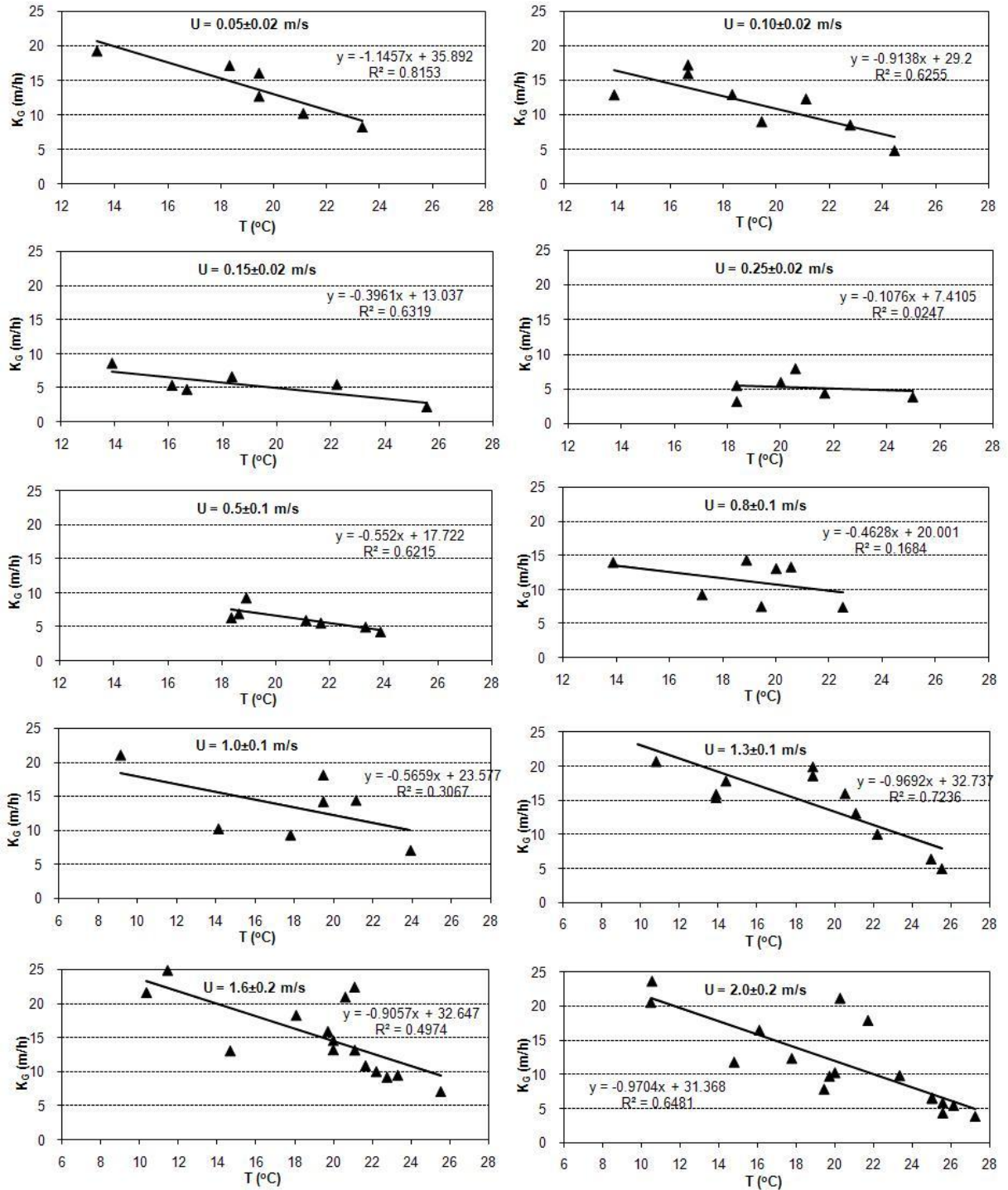


Figure 7-5. Effect of air temperature on the mass transfer coefficient K_G at various air velocities

It was also observed that the sensitivity of K_G over air temperature (i.e., $\Delta K_G/\Delta T$) was influenced by air velocity. Figure 7-6 presents the K_G values at $T=20^\circ\text{C}$ which were estimated from the regression line of K_G over air temperature at various air velocities. The absolute values of the slope of regression line ($\Delta K_G/\Delta T$) are also presented in the figure. It can be seen that, when air velocities were in the range of 0.15 to 0.25 m s^{-1} , the K_G reached its lowest value, and it was also least sensitive to air temperature.

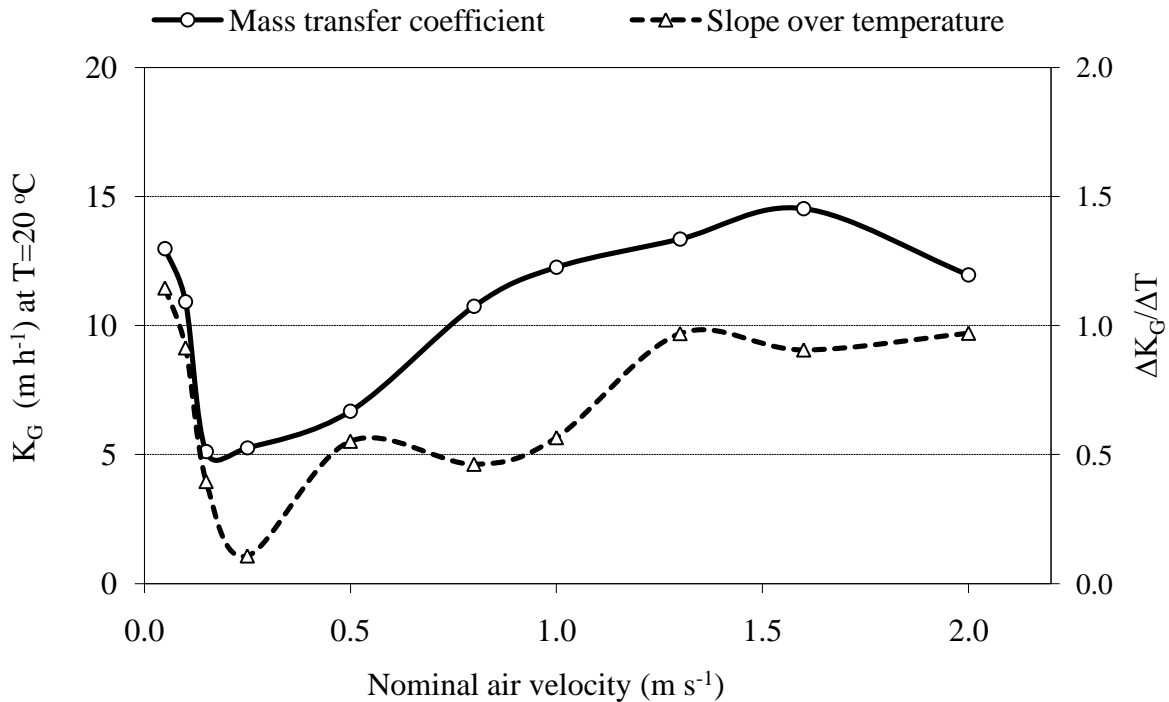


Figure 7-6. K_G value at $T=20^\circ\text{C}$ and the slope of regression line of K_G over air temperature at various air velocities

Figure 7-7 presents the K_G values at three temperatures. It was observed that the K_G was more sensitive to air velocity at lower temperatures. At higher temperature ($T > 25^\circ\text{C}$), the K_G was less affected by air velocity.

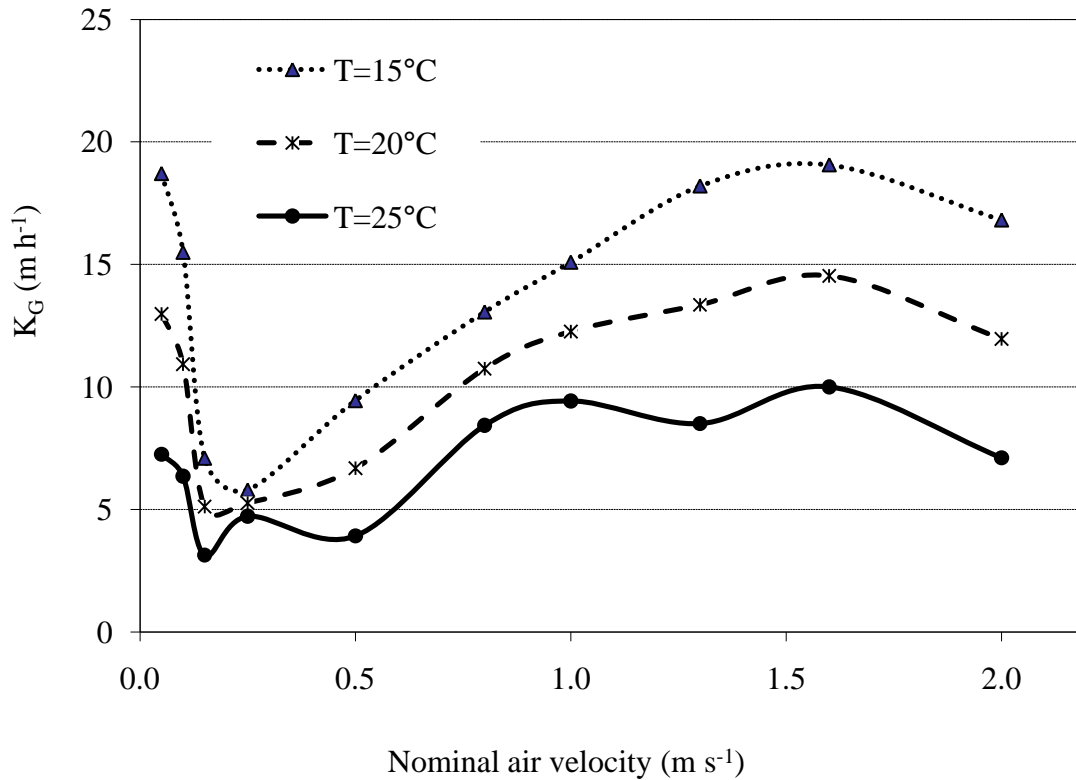


Figure 7-7. Effect of air velocity on mass transfer coefficient K_G at three air temperatures

It is believed that effect of air velocity on mass transfer coefficient K_G was influenced by the airflow pattern in the wind tunnel. The width and height of the wind tunnel (L) are 0.203m, and the kinematic viscosity of air $\nu=1.56 \times 10^{-5} \text{ m}^2 \text{ s}^{-1}$ in standard air condition (25 °C). Therefore, when air velocity in the wind tunnel was 0.15 to 0.25 m s^{-1} , the Reynolds number ($Re=UL/\nu$) was estimated to be 2000 to 3300, while the critical value of Reynolds number is 3000 for transition from laminar to turbulent flow in ducts. When the air velocity was less than 0.15 m s^{-1} , the air in the wind tunnel was in laminar flow, and K_G decreased as air velocity increased as shown in Figure 7-7. When the air velocity was greater than 0.25 m s^{-1} , the air in the wind tunnel was in turbulent flow. As air velocity further increased, the turbulence intensity increased and therefore leading to a larger value of K_G . However, it was also observed that, the K_G values at 2.0 m s^{-1} air velocity was smaller than that at 1.6 m s^{-1} air

velocity. This may be caused by significant loss of nitrogen and moisture from litter surface at high air velocity level. The overall model assumed constant TAN and moisture content in litter. As air velocity increased to certain level, emission fluxes increased and the loss of nitrogen and moisture from litter were not negligible any more, and therefore resulted in reduced measurement of emission fluxes and K_G .

7.3.3 Regression model of K_G

Based on the 81 measurements from litter A (the data at 2.0 m s^{-1} air velocity were excluded), the following regression model of K_G as function of air velocity and air temperature was obtained.

$$K_G = C_k (U)^a (T)^b \quad (7-1)$$

In which, temperature is measured in $^{\circ}\text{C}$. C_k , a , b are regression coefficients.

The results for the constant C_k and exponents a , b are reported in Table 7-1.

Table 7-1. Constant C_k and exponents a , b in Equation 7-1

Regression coefficients	Value	
	When $U \leq 0.25 \text{ m s}^{-1}$, $Re < 3300$ (laminar condition)	When $U > 0.25 \text{ m s}^{-1}$, $Re > 3300$ (turbulent condition)
C_k	84.73	247.88
a	-1.01 ± 0.14	0.48 ± 0.07
b	-1.56 ± 0.35	-1.05 ± 0.17

According to the regression model, under laminar conditions, K_G decreases with increasing air velocity. Under turbulent conditions, K_G increases with increasing air velocity. Under both laminar and turbulent conditions, K_G decreases with increasing air temperature. In the regression model, the effect of pH and T both have P-values smaller than 0.001. The negative power of the temperature has also been reported by other researchers (Haslam et al., 1924; Arogo et al; 1999, Zhao and Chen, 2003; Elzing and Monteny, 1997a, b; and Monteny et al., 1998).

Figure 7-8 presented results of the comparison between model predicted K_G and observed K_G for measurements of litter A. The model is able to reproduce 64.4% of the variability of the data.

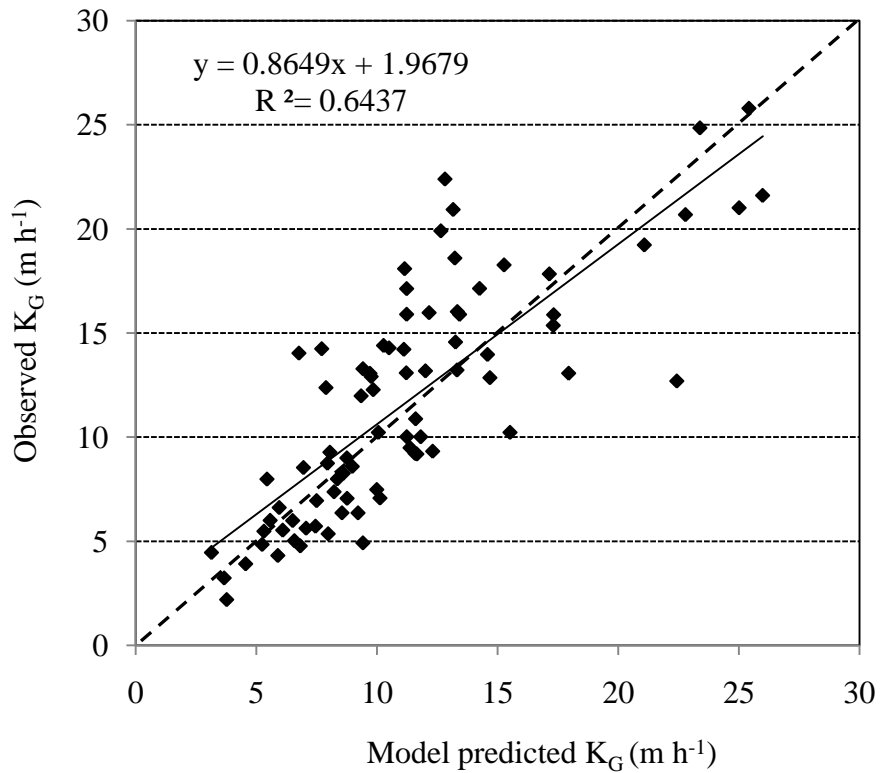


Figure 7-8. Observed K_G vs. model predicted K_G (litter A)

Figures 7-9 to 7-11 presented the residual plots of the model. Figure 7-9 and Figure 7-10 showed essentially random scatter of the residuals, suggesting no significant violation of assumptions. However, Figure 7-11 indicates that the model tends to underestimate K_G at higher K_G levels.

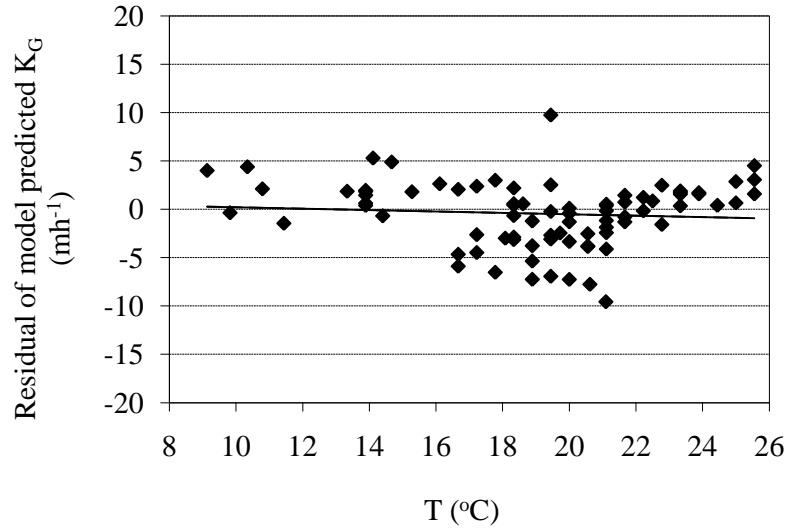


Figure 7-9. Residual vs. temperature (litter A)

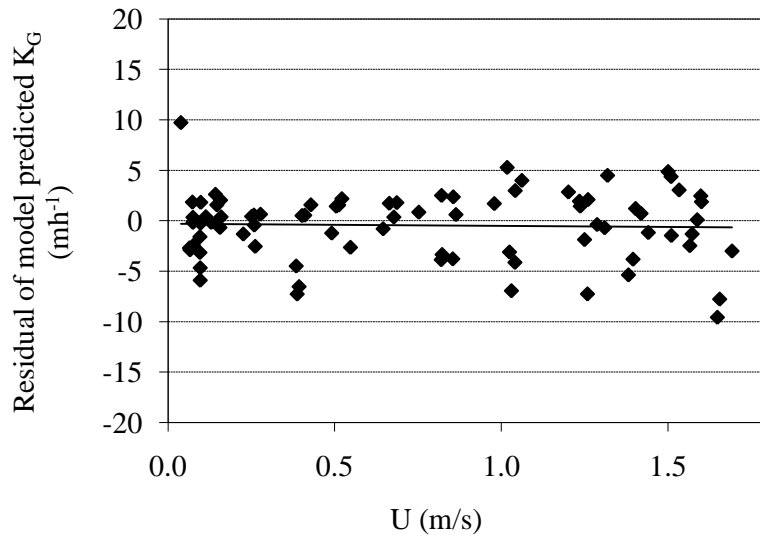


Figure 7-10. Residual vs. air velocity (litter A)

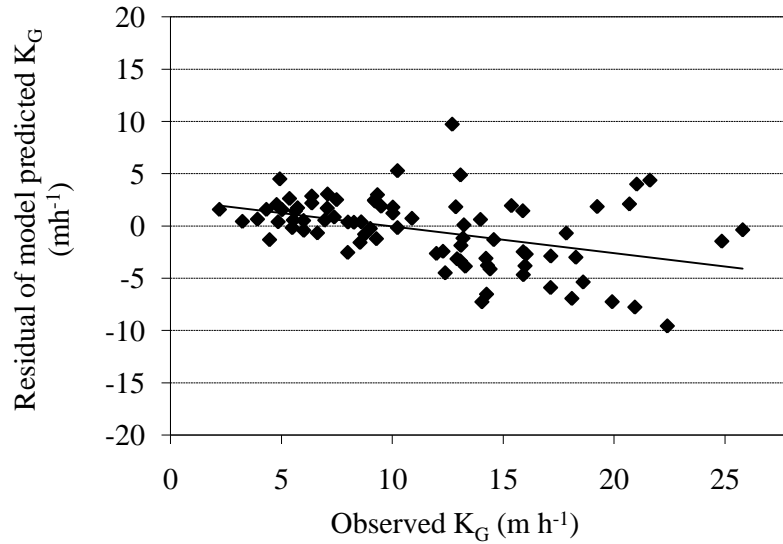


Figure 7-11. Residual vs. observed K_G (litter A)

7.3.4 Validation of the K_G regression model with independent experimental data set

In order to validate the K_G regression model, an independent group of measurements of ammonia emission from litter B in the wind tunnel were taken from August 27th to December 3rd, 2008. The model was validated by comparing model output with measured data.

In total, 81 measurements were taken for litter B. Measurements at each air velocity level were taken at various temperatures from 18.5 °C to 29.6 °C. The mass transfer coefficient K_G obtained from litter B was in the range from 1.11 to 27.64 $m h^{-1}$ with an average value of 6.08 $m h^{-1}$. It was observed that K_G values obtained from litter B were also negatively related with air temperature, which agrees with what was found in the study of litter A. Figure 7-12 presents results of the comparison between model predicted K_G and observed K_G for measurements of litter B. The model is able to reproduce 58.6% of the variability of the data.

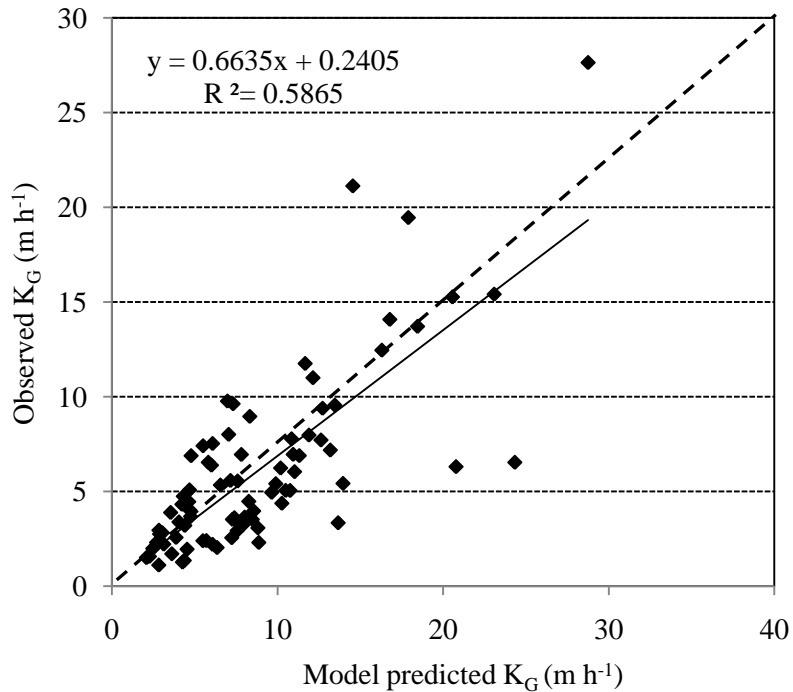


Figure 7-12. Observed K_G vs. model predicted K_G (litter B)

When treating the study of litter A and litter B as two blocks, air velocity and air temperature as two predictor variables, the block effect on K_G can be investigated through the GLM procedure. The P-value of the block effect was found to be 0.6, which indicated no significant block effect. Also, during the study of litter B, relative humidity (RH) of ambient air was also measured along with the ammonia emission measurement to investigate the possible influence of RH on K_G . The measured RH of air was in the range from 50.0% to 65.5%. It was found that for the three predictor variables, RH has a P-value of 0.52 while air temperature and air velocity both have P-values less than 0.005, which indicated no significant effect of RH on K_G .

7.3.5 Dimensionless analysis

Assuming that the resistance to ammonia emission from litter is controlled by the gas phase, the mass transfer coefficient is mainly determined by air properties, such as air

velocity, air viscosity, air density, as well as diffusivity of ammonia in air. Then mass transfer process is obviously influenced by the flow pattern, so system geometry is also an important factor. Dimensional analysis has been used to quantify the combined effects of these factors on the mass transfer process (Montes et al., 2008; Incropera et al., 2007; Arago et al., 1999; Cussler, 1997). The advantage of using dimensionless numbers is that, once they are defined, they can be used for systems that have different scales.

The dimensionless numbers that have been used to describe the mass transfer process include the Sherwood number (Sh), the Schmidt number (Sc) and the Reynolds number (Re). They are defined in Equations 7-2 to 7-4 respectively.

$$\text{Sh} = K_G L/D \quad (7-2)$$

$$\text{Sc} = \nu/D \quad (7-3)$$

$$\text{Re} = UL/\nu \quad (7-4)$$

In which,

K_G is mass transfer coefficient, m s^{-1} ;

L is the characteristic length that influences the air flow, m ;

D is the molecular diffusivity of ammonia in air, $\text{m}^2 \text{s}^{-1}$;

ν is the kinematic viscosity of air, $\text{m}^2 \text{s}^{-1}$, which equals air viscosity divided by air density.

The Sherwood number represents the ratio of convective to diffusive mass transport. The Schmidt number represents the ratio of viscous to diffusive effects. The Reynolds number represents the ratio of inertial to viscous effects. The three dimensionless numbers can be related as in Equation 7-5 (Cussler, 1997) through dimensional reasoning.

$$Sh = C_k (Re)^a (Sc)^b \quad (7-5)$$

In Equation 7-5, C_k , a , b are parameters that depend on the characteristics of the flow and are commonly determined experimentally. Values of a available in the literature range from 0.3 to 0.85 (Arogo et al., 1999; Schwarzenbach et al., 2003; Incropera et al., 2007; Cussler 1997; Perry et al., 1997). The most commonly used number for b is 1/3 (Perry et al., 1997). By applying an error analysis methodology proposed by Taylor (1997) and Holman (1994) to Equation 7-5, it is possible to demonstrate that the expected variation due to changes in temperature from 0 °C to 30 °C is less than 15% (Montes et al., 2008). However, larger variation of K_G associated with temperature was observed in this study. In order to include the large influence of temperature, Murphy (1950) developed the following relationship through dimensional reasoning.

$$K_G L/D = C_k (UL/\nu)^a (\nu/D)^b (T/T_0)^c \quad (7-6)$$

The kinematic viscosity of air is influenced by air temperature, and the following empirical equations have been developed (Cortus et al., 2006).

$$\nu = 4 \times 10^{-10} \times (T+273.15)^{1.859} \quad (7-7)$$

The diffusivity of ammonia in air is calculated using the following equation developed by Fuller et al (1966).

$$D = \frac{10^{-7} (273.15+T)^{1.75} \left[\frac{1}{MW_{NH_3}} + \frac{1}{MW_{air}} \right]^{1/2}}{P \left[(\Sigma v)_{NH_3}^{1/3} + (\Sigma v)_{air}^{1/3} \right]^2} \quad (7-8)$$

In Equations 7-7 and 7-8, T is air temperature in °C. MW_{NH_3} and MW_{air} are molecular weights of ammonia and air, respectively. P is pressure in atmospheres. $(\Sigma v)_{NH_3}$ and $(\Sigma v)_{air}$ are atomic diffusion volumes of ammonia and air, respectively. And their values were taken from Liley et al. (1984) ($20.1 \text{ cm}^3 \text{ mol}^{-1}$ for air, $14.9 \text{ cm}^3 \text{ mol}^{-1}$ for ammonia).

Using the width of the wind tunnel as the characteristic length L (0.2032 m), all the

dimensionless numbers in Equation 7-6 were calculated. Let $b=1/3$ and the reference temperature $T_0 = 22^\circ\text{C}$, then the constant C_k and exponents a, c were obtained from experimental data. The results are reported in Table 7-2.

Table 7-2. Constant C_k and exponents a, c in Equation 7-6

Regression coefficients	Value	
	When $Re \leq 3300$ (laminar condition)	When $Re > 3300$ (turbulent condition)
C_k	23094	0.3453
a	-1.01 ± 0.14	0.43 ± 0.07
c	-1.26 ± 0.22	-1.69 ± 0.14

Using the values in Table 7-2, the following equations for calculating K_G were obtained from Equation 7-6.

When $Re \leq 3300$ (laminar condition),

$$K_G = 1.13 \times 10^6 U^{-1.01} L^{-2.01} v^{1.34} D^{0.67} T^{-1.26} \quad (7-9)$$

When $Re > 3300$ (turbulent condition),

$$K_G = 64.1 U^{0.43} L^{-0.57} v^{-0.10} D^{0.67} T^{-1.69} \quad (7-10)$$

In Equations 7-9 and 7-10, K_G has units of m s^{-1} . Figure 7-20 presents results of the comparison between the observed K_G and the K_G calculated by Equation 7-9 and 7-10.

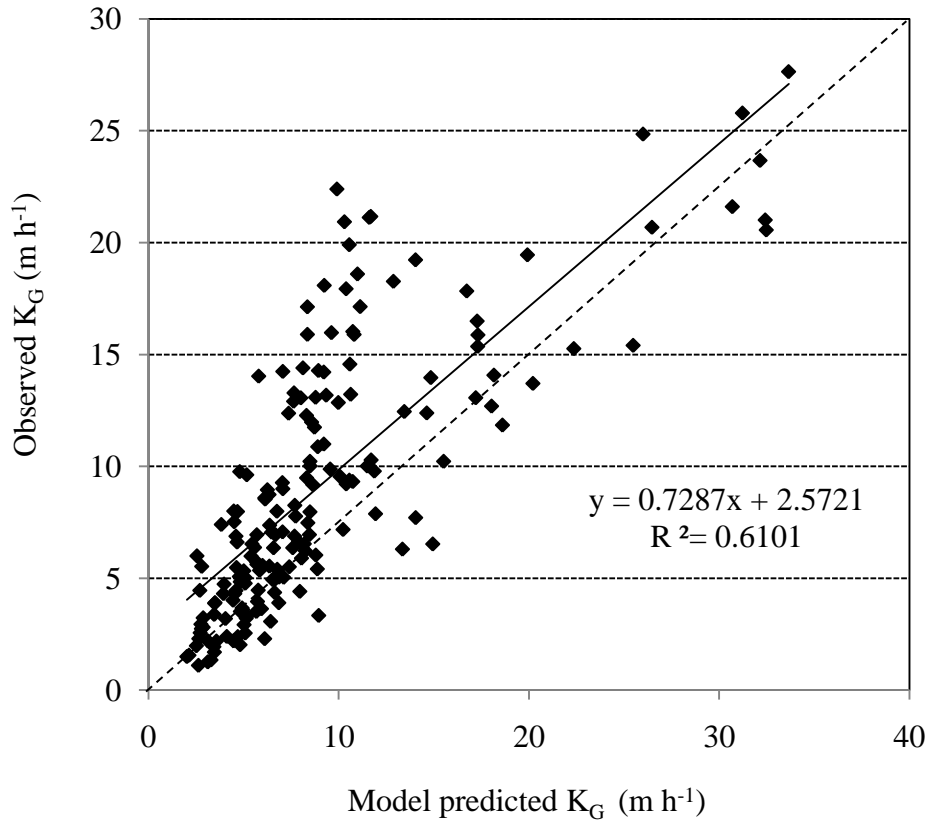


Figure 7-13. Observed K_G vs. K_G calculated by Equation 7-9 and 7-10

7.4 CONCLUSION

The mass transfer coefficient of ammonia emission from broiler litter was investigated in a wind tunnel under various combinations of air velocities and temperatures. The estimated K_G was in the range from 1.10 to 27.64 m h^{-1} in 179 measurements. It was observed that under turbulent conditions, the K_G increased with increasing air velocity, while under laminar conditions, K_G decreased with increasing air velocity. K_G decreased as the air temperature increased. When air velocities were in the range of 0.15 to 0.25 m s^{-1} , the K_G reached its lowest value, and it was also least sensitive to air temperature. When air velocities were less than 0.15 m s^{-1} or larger than 1.0 m s^{-1} , the values of K_G were larger, and K_G was also more

sensitive to air temperature.

Based on measurements for litter A, a regression model of K_G as function of air velocity and air temperature was obtained. The model was able to reproduce 58.6% of the variability of the independent group of measurements for litter B.

Through dimensionless analysis, equations were developed to calculate K_G as function of air velocity, the characteristic length that influences the air flow, the kinematic viscosity of air, the molecular diffusivity of ammonia in air, air temperature, and litter temperature. It is expected that these equations can be used for systems that have a different scale. The results of this study can be used in emission models to estimate ammonia flux from broiler litter.

8. VALIDATION AND UNCERTAINTY ANALYSIS OF THE MODEL

A mechanistic emission model was developed at laboratory scale to estimate ammonia emission fluxes from broiler litter as reported in Chapter 6. The overall model inputs include air temperature, air velocity, and litter properties such as litter nitrogen content, moisture content and pH. The model outputs are predicted ammonia emission fluxes from litter. Considerable uncertainty may exist in measurement values of model inputs and outputs as well as model parameters. The purpose of this study was to perform model validation in the presence of measurement and model parameter uncertainties. A validation metric based on the mean and covariance in the measurement and in the model parameters were used to validate the ammonia emission model of broiler litter. The core model was validated given the uncertainties in the model prediction due to uncertainties of parameters (the Freundlich partition coefficient K_f and the mass transfer coefficient K_G), and the uncertainties in the measurements. The significant level for the core model validation was 17.8%. The K_f sub-model was validated at the given uncertainties of pH and temperature, and the significant levels were from 12.0% to 49.4%, which provided high confidence on the K_f sub-model. At the given uncertainty levels of air velocity and temperature, the K_G sub-model passed the validation test ($P > 5\%$) when air velocities were low, and failed the validation test ($P < 5\%$) when air velocities were high. The failure of K_G sub-model at high air velocity levels may be caused by significant loss of nitrogen and moisture content from litter surface.

8.1 INTRODUCTION

A mechanistic emission model was developed at laboratory scale to estimate ammonia emission fluxes from broiler litter (Chapter 6). The overall model inputs include air temperature, air velocity, and litter properties such as litter nitrogen content, moisture content and pH. The model outputs are the predicted ammonia emission fluxes from litter. Model validation is generally a recurrent activity in a phase of model development (Ni, et al., 2000).

A common method of validation is the simple comparison of model predictions to experimental measurements through graph. However, there has been an increased concern on the role of uncertainty in model validation in literature (Warren-Hicks et al., 2002; Hills and Trucano, 1999; Easteling, 2003). Considerable uncertainty may exist in measurement values of model inputs and outputs as well as model parameters. The presence of uncertainty complicates the model validation process. Because of these uncertainties, big difference may be observed between the model predictions and the experimental measurements, even for actually valid models.

8.2 RESEARCH OBJECTIVE

The objective of this part of study was to perform validation on the emission model for broiler litter in the presence of measurement and model parameter uncertainty. A validation metric, introduced by Hills (2006), based on the mean and covariance in the measurement and in the model parameters was used to quantify and evaluate the distance between model predictions and experimental measurements.

8.3 MODEL STRUCTURE

The overall broiler litter ammonia emission model includes the core emission flux equation, the $C_{g,0}$ sub-model, the K_f regression sub-model, and the K_G regression sub-model. The overall model structure is shown in Figure 8-1. The inputs for the overall model include: litter TAN content, litter pH, litter moisture content, ambient temperature, air velocity at litter surface and Q/A ratio. Model predicted fluxes were compared with observed fluxes from experimental measurements. The overall model was able to reproduce 52.6% of the variability of the data. The Normalized Mean Error (NME) was calculated to be 34.1%.

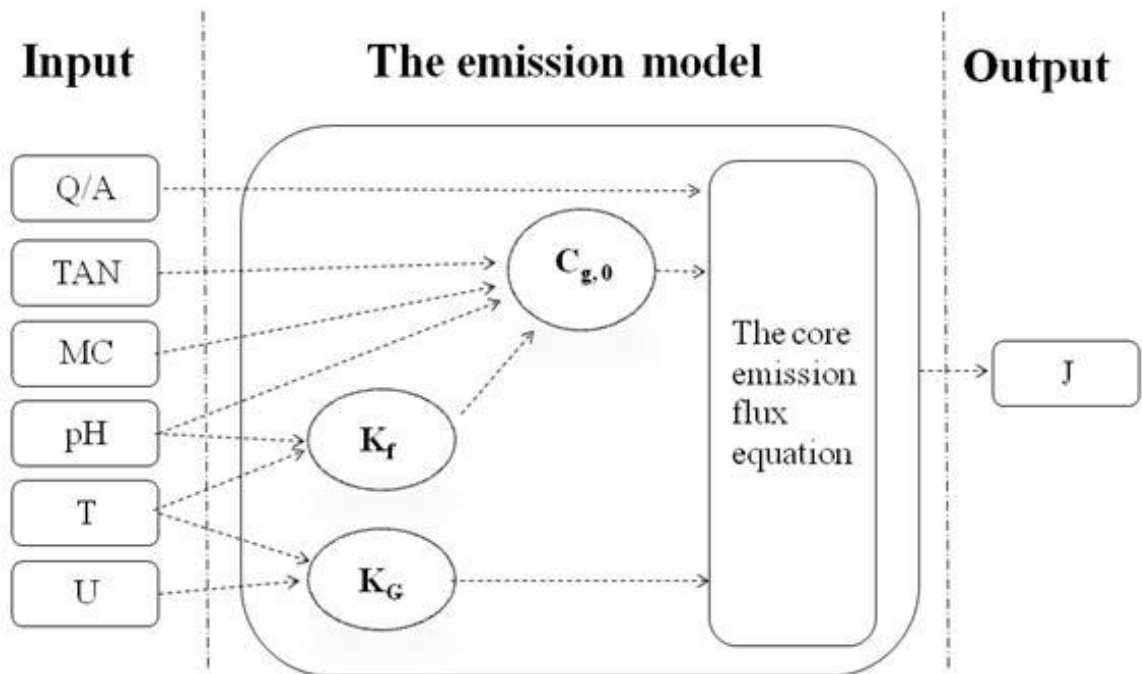


Figure 8-1. The overall model structure

8.4 VALIDATION METRICS

8.4.1 Uncertainties in model validation

The sources of uncertainty in model validation practices mainly include: (1) Measurement uncertainties; (2) Model parameter uncertainties; (3) Uncertainties associated with the model form error (Hills, 2006). In order to perform model validation in the presence of measurement and model parameter uncertainties, we need to evaluate whether the effects of uncertainties associated with the model form error are significant as compared with that of measurement uncertainties and model parameter uncertainties.

To quantitatively test for model validity, a measure of distance between the model predictions and the experimental measurements is needed. In an n dimensional space, the n

measurements and the corresponding n model predictions can be represented by two points. The effects of uncertainties from measurements and model parameters can be plotted around the two points respectively in the form of isoprobability density function (PDF) surfaces, which can be estimated and propagated through the model using a multivariate, first-order sensitivity analysis presented by Hills and Trucano (2001).

When using a statistical test to evaluate the distance between the model predictions and the experimental measurements in the presence of uncertainties, it is common practice that one does not reject the model unless one has less than a 5% probability of rejecting a valid model (Type I error). In other words, the model is rejected if the significance level is less than 5%. Hills (2006) also suggested that one has confidence in the model if the significance level is larger than 33% (approximately one standard deviation for a normal distribution).

8.4.2 The r^2 metric

A validation metric based on the mean and covariance in the measurement and in the model parameters, which was introduced by Hills (2006), was used to quantify the distance between the model predictions and the experimental measurements in n -dimensional space, where n is the number of measurements and corresponding predictions. It is the weighted least squares metric defined as follows.

$$r^2 = (\mathbf{X}_{\text{model}} - \mathbf{X}_{\text{exp}})^T [\text{cov}^{-1}(\mathbf{X}_{\text{model}} - \mathbf{X}_{\text{exp}})] (\mathbf{X}_{\text{model}} - \mathbf{X}_{\text{exp}}) \quad (8-1)$$

In which, $\mathbf{X}_{\text{model}}$ is the vector of model predictions and \mathbf{X}_{exp} is the corresponding vector of experimental measurements. The matrix $\text{cov}(\mathbf{X}_{\text{model}} - \mathbf{X}_{\text{exp}})$ is the covariance of the difference between model predictions and experimental measurements. The advantage of this metric is it measures distance based on the correlation structure of uncertainties in the model predictions and the experimental measurements (Hills, 2006). Assuming that the differences between the model predictions and the experimental measurements are normally distributed, and the covariance matrix for these differences is adequately represented, r^2 will be

distributed as a $\chi^2(df)$ distribution where df is the degrees of freedom. If no parameters were estimated in the process, the degree of freedom is the number of measurements and corresponding predictions.

Assuming the uncertainties in the measurements are independent of the uncertainties in the model predictions, the covariance matrix for the difference between model predictions and experimental measurements is the sum of the covariance matrices for each.

$$\text{cov}(\mathbf{X}_{\text{model}} - \mathbf{X}_{\text{exp}}) = \text{cov}(\mathbf{X}_{\text{model}}) + \text{cov}(\mathbf{X}_{\text{exp}}) \quad (8-2)$$

The uncertainties in the model prediction can be estimated and propagated through the model using a multivariate, first-order sensitivity analysis presented by Hills and Trucano (2001). Therefore, the covariance matrix for the model prediction $\text{cov}(\mathbf{X}_{\text{model}})$ can be estimated using the following equation.

$$\text{cov}(\mathbf{X}_{\text{model}}) = \nabla_{\theta} \mathbf{X} \text{cov}(\theta) [\nabla_{\theta} \mathbf{X}]^T \quad (8-3)$$

In which,

θ is the vector of model parameters;

$\nabla_{\theta} \mathbf{X}$ is the sensitivity matrix with n measurements for a model with p parameters, which is given by:

$$\nabla_{\theta} \mathbf{X} = \begin{bmatrix} \frac{\partial X_1}{\partial \theta_1} & \frac{\partial X_1}{\partial \theta_2} & \dots & \frac{\partial X_1}{\partial \theta_p} \\ \frac{\partial X_2}{\partial \theta_1} & \frac{\partial X_2}{\partial \theta_2} & \dots & \frac{\partial X_2}{\partial \theta_p} \\ \vdots & \vdots & \ddots & \vdots \\ \frac{\partial X_n}{\partial \theta_1} & \frac{\partial X_n}{\partial \theta_2} & \dots & \frac{\partial X_n}{\partial \theta_p} \end{bmatrix} \quad (8-4)$$

8.5 VALIDATION OF THE EMISSION MODEL

8.5.1 Validation of core model considering uncertainties of K_f and K_G

Combining the core emission flux model and the sub-model for calculating $C_{g, 0}$, the ammonia flux is essentially a function of litter TAN content, moisture content, pH, temperature, the Freundlich partition coefficient K_f , the mass transfer coefficient K_G , the ventilation rate Q and the emission surface area A . In which, estimation of K_f and K_G are usually associated with substantial uncertainties.

The measurement uncertainty of the emission fluxes may include instrumental noises and errors due to nuisance factors. It is assumed to be normally distributed, with a mean of zero. The standard deviation was estimated from the experimental measurements when all design factors were kept at constant values. The standard deviation of ammonia fluxes $\sigma_J = 233 \text{ mg m}^{-2} \text{ h}^{-1}$.

The ammonia emission fluxes from ten different litter samples were measured in the dynamic flux chamber, and for each litter samples, three replicate measurements were taken and the average values were used in the validation of the model. The average value of K_f was 2.08 L kg^{-1} for the ten litter samples, and the standard deviation of K_f value $\sigma_{Kf} = 1.12 \text{ L kg}^{-1}$. The average value of K_G was estimated to be 8.11 m h^{-1} , and the standard deviation of K_G value $\sigma_{KG} = 1.86 \text{ m h}^{-1}$. The measured and model predicted ammonia emission fluxes for the tested ten litter samples were compared in Figure 8-2.

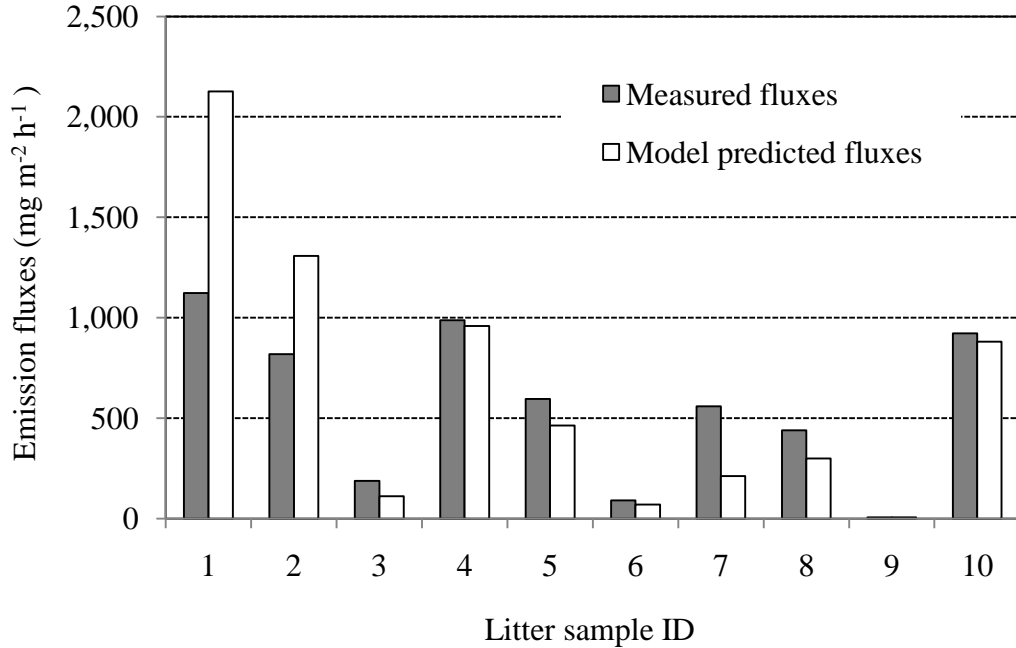


Figure 8-2. Comparison of measured and model predicted ammonia emission fluxes for the tested ten litter samples ($K_f = 2.08 \text{ L kg}^{-1}$, $K_G = 8.11 \text{ m h}^{-1}$)

The metric defined in Equation 8-1 to 8-4 can now be used to validate the emission model in the presence of uncertainties of K_f and K_G . Assuming K_f and K_G are uncorrelated and normally distributed, the covariance matrices of the experimental measurements and the model parameters are

$$\text{cov}(X_{\text{exp}}) = \text{cov}(J) = \begin{bmatrix} 233^2 & 0 & \dots & 0 \\ 0 & 233^2 & \dots & 0 \\ \vdots & \vdots & \ddots & \vdots \\ 0 & 0 & \dots & 233^2 \end{bmatrix} \quad (8-5)$$

$$\text{cov}(\theta) = \text{cov} \begin{pmatrix} K_f \\ K_G \end{pmatrix} = \begin{bmatrix} 1.12^2 & 0 \\ 0 & 1.86^2 \end{bmatrix} \quad (8-6)$$

Since K_f value was estimated from the ten measurements, the total degree of freedom is $10-1=9$. Therefore, r^2 was distributed as a $\chi^2(9)$ distribution. The sensitivity matrix was approximated through finite differences. The results give

$$r^2 = 12.68 \quad (8-7)$$

$$P(r^2 > 12.68) = 0.178 \quad (8-8)$$

The significance level is 17.8%, which means, given the uncertainties in the model prediction due to parameter uncertainties of K_f and K_G , and the uncertainties in the measurements, the probability of a valid model given this large or larger value in the weighted distance squared is 17.8%. This is more significant than 5% specified earlier to outright reject the model.

8.5.2 Validation of the k_f sub-model considering uncertainties of pH and temperature

The sub-model of K_f as function of litter pH value (concentration of hydrogen ion $[H^+]$) and temperature ($^{\circ}C$) (Equation 6-19) was tested in the wind tunnel, and the validation metric r^2 was calculated at various combinations of pH and temperature. The sub-model was evaluated under the following measurement uncertainty level of pH and temperature: $\sigma_{pH} = 0.1$; $\sigma_T = 0.5^{\circ}C$.

The validation results were presented in Table 8-1. It can be seen that, for all the 6 groups of measurements, the K_f sub-model passed the validation test ($P > 5\%$) at the given uncertainty level of pH and temperature.

Table 8-1. Validation results of the K_f sub-model

pH	Temperature (°C)	Model predicted K_f (L kg ⁻¹)	Standard deviation of measured K_f (L kg ⁻¹)	Number of measurements	Validation metric r^2	Significant level P
8.49	20.0	2.18	0.36	3	4.17	0.244
8.49	21.1	2.09	0.45	6	6.74	0.345
8.49	21.7	2.05	0.28	3	5.83	0.120
8.62	22.8	2.23	0.51	4	3.86	0.425
8.62	24.6	2.10	2.23	3	2.40	0.494
8.62	27.7	1.92	0.29	3	2.98	0.394

8.5.3 Validation of the K_G sub-model considering uncertainties of air velocity and temperature

The sub-model of K_G as function of air velocity and temperature was tested in the wind tunnel, and the validation metric r^2 was calculated at various combinations of air velocity and temperature. A hotwire anemometer (Dwyer Model 641-18-LED; range: 0-10 m s⁻¹; accuracy: 3% full scale) was used to measure air velocity. The sub-model was evaluated under the following measurement uncertainty level of air velocity and temperature: $\sigma_u = 0.1$ m s⁻¹; $\sigma_T = 0.5$ °C.

(1) Validation of the first regression sub-model of K_G

Based on all the 97 measurements from litter A, the following first regression sub-model of K_G as function of air velocity and air temperature has been obtained.

When $U \leq 0.25 \text{ m s}^{-1}$,

$$K_G = 84.73 U^{-1.01} T^{-1.56} \quad (8-9)$$

When $U > 0.25 \text{ m s}^{-1}$,

$$K_G = 456.36 U^{0.31} T^{-1.28} \quad (8-10)$$

The validation results of first regression sub-model of K_G are presented in Table 8-2. It can be seen that, for 6 out of 12 groups of measurements, the sub-model passed the validation test ($P > 5\%$) at the given uncertainty level of air velocity and temperature. Two different litter samples were used in the tests. The measurement data of litter A have been used in the development of the K_G sub-model. The measured and model predicted K_G for litter A at selected combinations of air velocity and temperature were compared in Figure 8-3. For litter A, at air velocity of 1.24 m s^{-1} and 1.56 m s^{-1} , the sub-model failed the validation test, and the sub-model underestimated the emission fluxes. At air velocity of 1.73 m s^{-1} and 1.99 m s^{-1} , the sub-model failed the validation test, and the sub-model overestimated the emission fluxes.

Table 8-2. Validation results of the first sub-model of K_G

Litter	Air velocity (m s ⁻¹)	Temperature (°C)	Model predicted K_G (m h ⁻¹)	Average value of measured K_G (m h ⁻¹)	Standard deviation of measured K_G (m h ⁻¹)	Number of measurements	Validation metric r^2	Significant level P
A	0.07	19.4	12.13	12.58	3.52	3	2.00	0.572
A	0.12	16.7	8.95	12.60	6.81	3	2.41	0.492
A	1.20	14.1	16.33	14.83	3.25	4	3.68	0.451
A	1.24	21.1	9.84	13.56	0.73	3	45.14	<0.001
A	1.56	20.8	10.77	19.77	3.36	3	22.69	<0.001
A	1.72	20.0	11.67	12.70	2.19	3	2.60	0.457
A	1.73	10.5	26.67	21.95	1.58	3	8.48	0.037
A	1.99	25.8	8.81	5.28	0.77	3	49.64	<0.001
B	0.16	24.6	3.65	3.02	1.82	3	2.13	0.546
B	0.39	25.4	5.42	3.68	2.82	4	5.06	0.281
B	0.62	24.0	6.73	3.67	1.65	3	11.01	0.012
B	1.20	27.8	6.85	3.60	0.33	3	119.29	<0.001

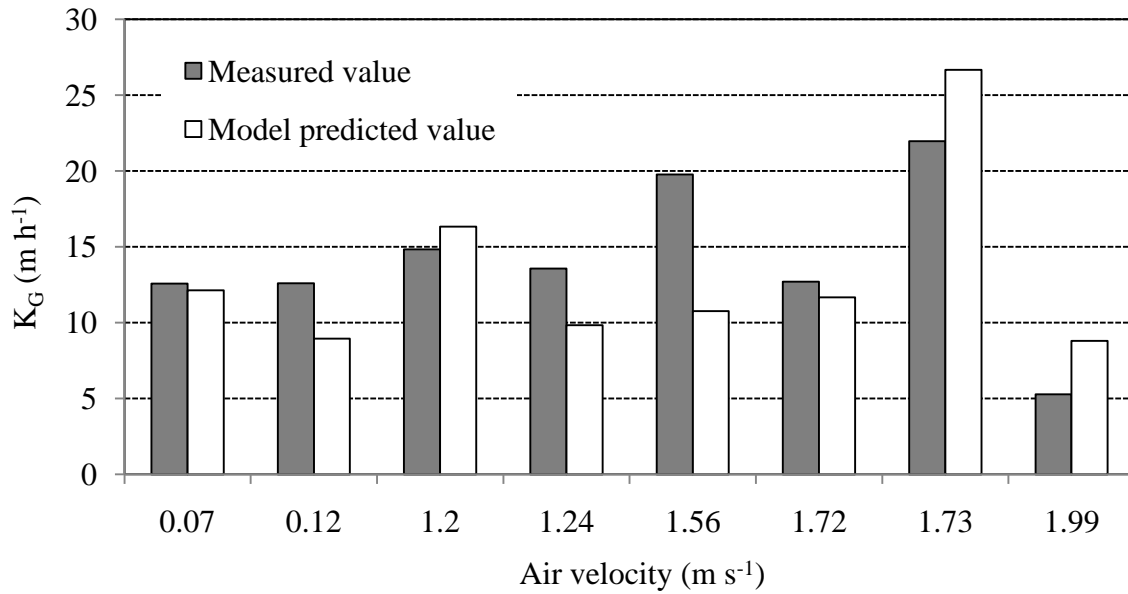


Figure 8-3. Comparison of measured and model predicted K_G for litter A at selected combinations of air velocity and temperature

The measured and model predicted K_G for litter A at $T=25^{\circ}\text{C}$ were compared in Figure 8-4. It can be seen that, as air velocity increased, the measured emission fluxes had a “decreasing effect” compared with the model predicted values. This may be caused by significant loss of nitrogen and moisture from litter surface at high air velocity level. The overall model assumed constant TAN and moisture content in litter. As air velocity increased to a certain level, emission fluxes increased and the loss of nitrogen and moisture from litter were not negligible any more, and therefore resulted in reduced measurement of emission fluxes and K_G .

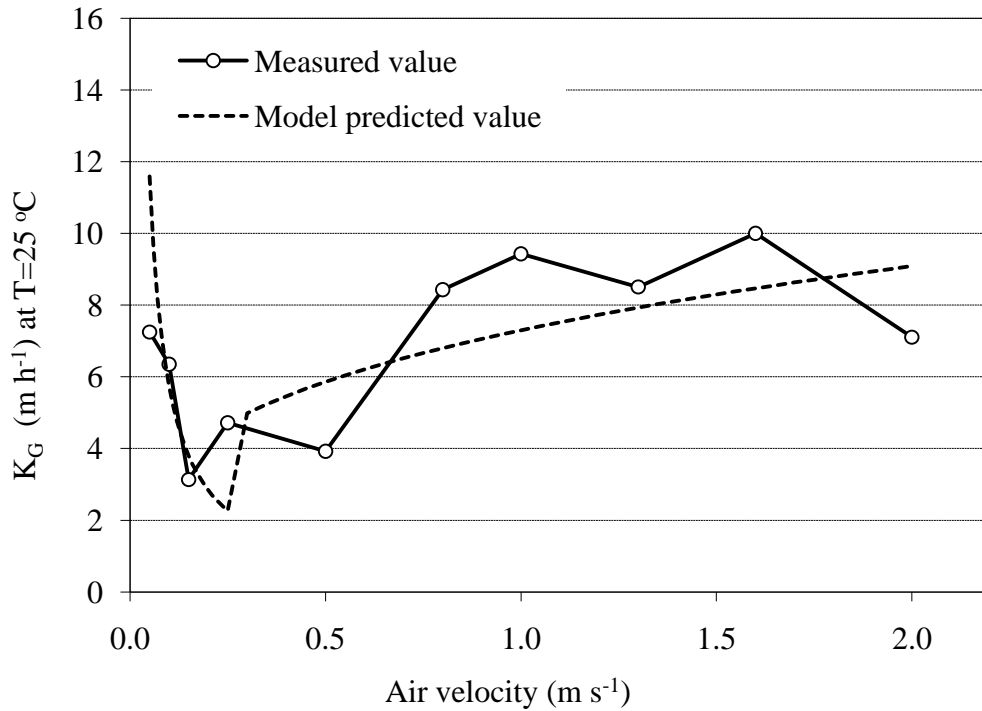


Figure 8-4. Comparison of measured and model predicted K_G for litter A at $T=25^\circ\text{C}$

Measurement data of litter B are independent from the development of the K_G sub-model. Litter B had a much higher TAN content than litter A and the measured emission fluxes from litter B were much higher than from litter A. Therefore, the “decreasing effect” caused by loss of nitrogen from litter was more obvious. The measured and model predicted K_G for litter B at selected combinations of air velocity and temperature were compared in Figure 8-5. As can be seen in Table 8-2 and Figure 8-5, at air velocity of 0.62 m s^{-1} and 1.20 m s^{-1} , the sub-model failed the validation test, and the sub-model overestimated the emission fluxes and therefore the K_G value.

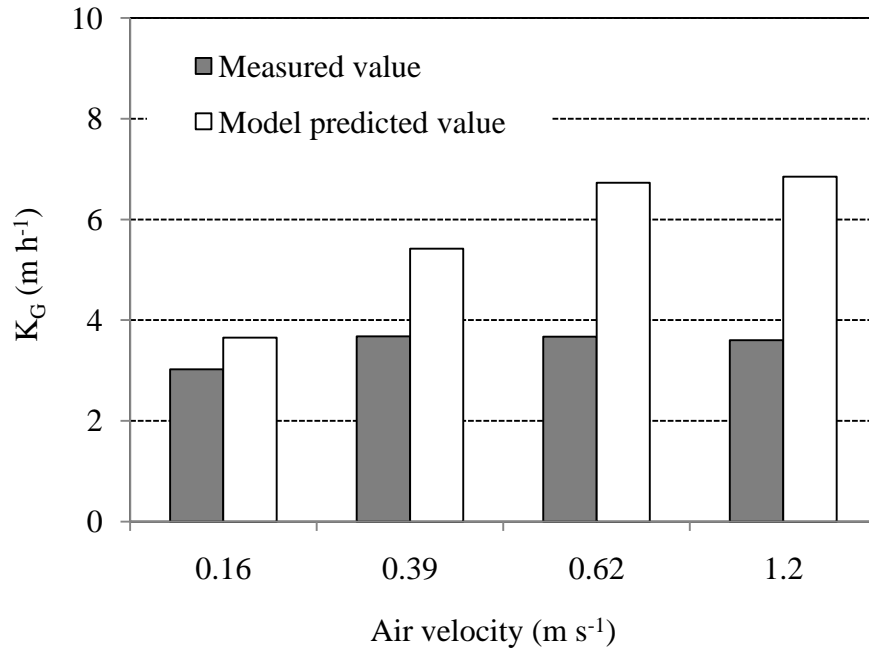


Figure 8-5. Comparison of measured and model predicted K_G for litter B at selected combinations of air velocity and temperature

(2) Validation of the second regression sub-model of K_G

In order to avoid the effect of significant loss of nitrogen and moisture from litter surface at high air velocity level, the second regression sub-model was developed on the 81 measurements from litter A, excluding the data points at 2.0 m s⁻¹ air velocity).

When $U > 0.25$ m s⁻¹, the regression sub-model becomes:

$$K_G = 247.88 U^{0.48} T^{-1.05} \quad (8-11)$$

The validation results of second regression sub-model of K_G are presented in Table 8-3. It can be seen that, for 9 out of 11 groups of measurements, the sub-model passed the validation test ($P > 5\%$) at the given uncertainty level of air velocity and temperature.

Table 8-3. Validation results of the second sub-model of K_G

Litter	Air velocity ($m s^{-1}$)	Temperature ($^{\circ}C$)	Model predicted K_G ($m h^{-1}$)	Average value of measured K_G ($m h^{-1}$)	Standard deviation of measured K_G ($m h^{-1}$)	Number of measurements	Validation metric r^2	Significant level P
A	0.07	19.4	12.13	12.58	3.52	3	2.00	0.572
A	0.12	16.7	8.95	12.60	6.81	3	2.41	0.492
A	1.20	14.1	16.81	14.83	3.25	4	3.35	0.501
A	1.24	21.1	11.18	13.56	0.73	3	3.50	0.319
A	1.56	20.8	12.68	19.77	3.36	3	8.34	0.039
A	1.72	20.0	13.84	12.70	2.19	3	2.51	0.530
A	1.73	10.5	21.73	21.95	1.58	3	3.39	0.335
B	0.16	24.6	3.65	3.02	1.82	3	2.13	0.546
B	0.39	25.4	5.28	3.68	2.82	4	4.02	0.404
B	0.62	24.0	7.00	3.67	1.65	3	5.62	0.132
B	1.20	27.8	8.24	3.60	0.33	3	12.74	0.005

8.6 CONCLUSION

A validation metric based on the mean and covariance in the measurement and in the model parameters were used to validate the ammonia emission model of broiler litter. The core model was validated given the uncertainties in the model prediction due to parameter uncertainties of K_f and K_G , and the uncertainties in the measurements. The significant level for the core model validation was 17.8%. The K_f sub-model was validated at the given uncertainties of pH and temperature, and the significant levels were from 12.0% to 49.4%, which provided high confidence on the K_f sub-model. At the given uncertainty levels of air velocity and temperature, the K_G sub-model passed the validation test ($P > 5\%$) when air velocities were low, and failed the validation test ($P < 5\%$) when air velocities were high. The failure of K_G sub-model at high air velocity levels may be caused by significant loss of nitrogen and moisture content from litter surface. The K_G sub-model was improved by excluding the data points at high air velocity levels.

9. FUTURE DIRECTION

The reported model provided estimates for ammonia emission under controlled laboratory conditions, but extrapolation of the model to actual broiler houses still requires more work. External validation need to be performed using actual broiler house measurement data. The results of external validation should provide an assessment of overall model validity, and provide a consistent method of assessing uncertainty of model predictions, so that the capability of the model as an efficient tool for ammonia emission estimation can be confirmed.

It is suggested that the future direction for improvement of the model may include:

Extend the basic model to the dynamic situation of broiler houses.

Include more sub-models (such as ventilation, N-excretion and pH sub-models) to further simplify the overall model inputs so that the model only uses commonly available or easy obtainable input data.

REFERENCES

- Aarnink A J A. 1997. Ammonia emission from houses for growing pigs as affected by pen design, indoor climate and behaviour. PhD Thesis, Institute of Agricultural and Environmental Engineering, the Wageningen Institute of Animal Sciences and the Agricultural University Wageningen.
- Anderson G.A.; Smith R.J.; Bundy D.S.; Hammond E.G. 1987. Model to predict gaseous contaminants in swine confinement buildings. *Journal of Agricultural Engineering Research*, 37, 235-253
- Aneja, V.P., J.P. Chauhan and J.T. Walker. 2000. Characterization of atmospheric ammonia emissions from swine waste storage and treatment lagoons. *Journal of Geophysical Research* 105, 11535-11545.
- Aneja, V.P. 1976. Dynamic studies of ammonia uptake by selected plant species under flow reactor conditions. Ph. D. Thesis, NC State University. Raleigh, NC. p. 216.
- AOAC. 1995. Official method 990.03: Protein (crude) in animal feed: Combustion method.. In *Official Methods of Analysis*. 16th edition, 4:18-19, Gaithersburg, Md.: AOAC International.
- APHA. 1998. Standard method 4500 NH₃ G: Automated phenate method. In *Standard Methods for the Examination of Water and Wastewater*. 20th edition. Washington, D.C.: APHA, AWWA, WEF.
- Applegate, T. J., L.P.V. Potturi, and R. Angel. 2003. Model for estimating poultry manure nutrient excretion: a mass balance approach. Proc. of the Ninth International Symposium on Animal, Agricultural, and Food Processing Manures (ISAAFPW). October 12-15. Raleigh, NC. pp. 296-309.

- Agaro, J., P.W. Westerman, A.J. Heber, W.P. Robarge and J.J. Classen. 2002. Ammonia emissions from animal feeding operations. National Center for Manure and Animal Waste Management White Papers, North Carolina State University, Raleigh NC (available from Midwest Plan Service, Ames IA).
- Arogo J., D. L. Day, L. L. Christianson, G. L. Riskowski, and R. Zhang. 1996. Evaluation of mass transfer coefficient of ammonia from liquid swine manure. First International Conference on Air Pollution from Agricultural Operation. Kansas City, Missouri, USA, 111-118.
- Arogo, J., P., R.H. Zhang, G.L. Riskowski, L.L. Christianson, D.L. Day. 1999. Mass transfer coefficient of ammonia in liquid swine manure and aqueous solutions. *J. Agric. Engng Res.* 73,77-86.
- Arogo, J. P. W. Westerman, A. J. Heber, W. P. Robarge and J. J. Classen. 2001. Ammonia in animal production. Paper No. 01-4089, present at the 2001 ASAE Annual International Meeting in Sacramento, CA, St. Joseph, MI.
- Arogo, J., P. Westerman and A. Heber. 2003. A Review of ammonia emissions from confined swine feeding operations. *Trans. ASAE* 46(3):805-817.
- Arogo, J., P. Westerman, A. Heber, W. Robarge and J. Classen. 2006. Ammonia emissions from animal feeding operations. *Animal Agriculture and the Environment: National Center for Manure and Animal Waste Management White Papers*. p. 41-88. J. M. Rice, D. F. Caldwell, F. J. Humenik, eds. Pub. Number 913C0306. St. Joseph, Michigan: ASABE.
- Arogo, J., P. Westerman and A. Heber. 2003. A Review of ammonia emissions from confined swine feeding operations. *Trans. ASAE* 46(3):805-817.
- ASABE. 2005. Manure production and characteristics, D384.2, Mar. 2005.

- Asman, W.A.H., 1992. Ammonia Emission in Europe: Updated Emission and Emission Variations. Report No. 228471008 for National Institute of Public Health and Environmental Protection, Bilthoven, The Netherlands
- Barthelmie, R.J., and S.C. Pryor. 1998. Implications of ammonia emissions for fine aerosol formation and visibility impairment: A case study from the Lower Fraser Valley, British Columbia. *Atmospheric Environment* 32(3): 345-352.
- Battye, R., W. Battye, C. Overcash, S. Fudge. 1994. Development and Selection of Ammonia Emission Factors. 68-D3-0034. US Environmental Protection Agency, Washington, DC
- Battye, W., V. P. Aneja and P. A. Roelle. 2003. Evaluation and improvement of ammonia emissions inventories. *Atmospheric Environment* 37(27): 3873-3883.
- Bolt, G. H., 1976. Transport and accumulation of soluble soil components, In: Bolt, G. H., Bruggenwert, M.G.M. (Eds), *Soil Chemistry. A. Basic elements*. Elsevier, New York. pp. 126-140.
- Brewer, S.K. and T.A. Costello. 1999. In situ measurement of ammonia volatilization from broiler litter using an enclosed air chamber. *Transaction of ASAE*, Vol. 42(5), 1415-1422.
- Bussink, D.W. and O. Oenema. 1998. Ammonia volatilization from dairy farming systems in temperate areas: a review. *Nutrient Cycling in Agroecosystems*. 51: 19-33.
- Carlile, F. S. 1984. Ammonia in poultry houses: A literature review. *World's Poultry Science J.* 40: 99-113.
- Carr, L.E. F. W. Wheaton and L. W. Douglas. 1990. Empirical models to determine ammonia concentrations from broiler chicken litter. *Transaction of the ASAE*, Vol. 33(4): 1337-1342

- Casey, K.D., R.S. Gates, E.F. Wheeler, J.S. Zajackowski, P.A. Topper, H. Xin and Y. Liang. 2003. Ammonia Emissions from Broiler Houses in Kentucky during Winter. International Symposium on GASEOUS AND ODOUR EMISSIONS FROM ANIMAL PRODUCTION FACILITIES. Scandic Hotel Bygholm Park Horsens June. 1-4.
- Chaoui, H., F. Montes, C.A. Rotz, T.L. Richard. 2008. Dissociation and mass transfer coefficients for ammonia volatilization models. ASABE Paper No. 083802. St. Joseph, Mich.: ASABE.
- CIGR, 2002. Climatization of animal houses. Heat and moisture production at animal and house levels. S. Pedersen and K S älvik (eds). pub Danish Institute of Agricultural Sciences, Bygholm, Denmark.
- Cortus, E.L., Lemay, S.P., Barber, E.M., Hill, G., Godbout, S. 2006. Modeling ammonia emission from urine puddles. ASABE Paper No 064107, St. Joseph, Mich: ASABE.
- Cussler, E. 1997. Diffusion, Mass transfer in Fluid Systems. Second Edition. Cambridge University Press.
- Cumby, T. R.; B. S. O. Moses; E. Nigro. 1995. Gases from livestock slurries: emission kinetics. In: Proceedings of the Seventh International Symposium on Agricultural and Food Processing Wastes (ISAFPW95) (Ross C C, ed.), Hyatt Regency Chicago, Chicago, Ills. ASAE, 230-240.
- Da Borso and Chiumenti. 1999. Poultry housing and manure management systems: recent development in Italy as regards ammonia emissions. Proceedings of the 8th International Conference of the FAO ESCORENA Network on Recycling of Agricultural, Municipal and Industrial Residues in Agriculture, RAMIRAN 98, Vol. 2, Posters Presentation. pp 15-21.

- Dammgen, U, M. Luttich, H. Dohler, B. Eurich-Menden, B. Osterburg. 2002. GAS-EM—a procedure to calculate gaseous emissions from agriculture. *Landbauforschung Volkenrode* 52, 19–42.
- De Visscher, A., L. Harper, P. Westerman, Z. Liang, J. Arogo, R. Sharpe and O. Van Cleemput. 2001. Ammonia emissions from anaerobic swine lagoons: model development. *J. Applied Meteorology* 41(April 2002): 426-433.
- Easterling, R. C., 2003, Statistical Foundations for Model Validation: Two Papers, SAND2003-0287, Sandia National Laboratories, Albuquerque.
- Elliott, H.A. and N. E. Collins. 1982. Factors affecting ammonia release in broiler houses. *Trans. ASAE* 25(2): 413–424.
- Elwinger K. and L. Svensson. 1996. Effect of dietary protein content, litter and drinker types on ammonia emission from broiler house. *Journal of Agricultural Engineering Research*, 64, 197-208
- Elzing, A. and G.J. Monteny. 1997 (a). Ammonia emission in a scale model of a dairycow house. *Transactions of the ASAE*, Vol. 40 (3): 713-720.
- Elzing, A. and G.J. Monteny. 1997 (b). Modeling and experimental determination of ammonia emissions rates from a scale model dairy-cow house. *Transactions of the ASAE*, Vol. 40 (3): 721-726.
- EPA. 1979. Method 351.2:Nitrogen, Kjeldahl, Total. Colorimetric, semi-automated block digester, AAII.. In *Methods for Chemical Analysis of Water and Wastes*. Environmental monitoring and support laboratory, Cincinnati, OH. EPA-600/4-79-020. Gates, R. S., K. D. Casey, E. F. Wheeler, H. Xin, A. J. Pescatore, J. L. Zajaczkowski, J. R. Bicudo, P. A. Topper, Y. Liang, and M. Ford. 2004. Broiler house ammonia emissions: U.S. baseline data. In *Proc. Multi-State Poultry Feeding*

- and Nutrition and Health and Management Conference and Degussa Corporation's Technical Symposium*. Available at: www.bae.uky.edu/ifafs/timeline.htm.
- Faulkner, W.B., J.J. Powell, J.M. Lange, B.W. Shaw, Lacey, and C.B. Parnell. 2006. Comparison of Dispersion Models for Ammonia Emissions from a Ground Level Area Source. Proceedings of Workshop on Agricultural Air Quality: State of the science, Bolger conference center, Potomac, Maryland, USA, June 5-8.
- Fuller E. N., P. D. Schelter, J. C. Giddings. 1966. A new method for prediction of binary gas-phase diffusion coefficients. *Industrial and Engineering Chemistry*. 58(5), 19-27.
- Freewood, R.J., J. C. Cripps, C. C. Smith. 2001. Leachate attenuation characteristics of colliery spoils. In: Thornton, S.F., Oswald, S.E., (Eds.) *Groundwater Quality: Natural and Enhanced Restoration of Groundwater Pollution*. IAHS Publication 275. Cited in: Buss S.R., Herbert, A.W., Morgan, P., Thornton, S.F., 2003. Review of ammonium attenuation in soil and groundwater. NGWCLC report NC/02/49. Published by Environment Agency UK. ISBN: 1 84432 110 1.
- Gates, R. S., K. D. Casey, E. F. Wheeler, H. Xin, A. J. Pescatore, J. L. Zajackowski, J. R. Bicudo, P. A. Topper, Y. Liang and M. Ford. 2004. Broiler house ammonia emissions: U.S. baseline data. Proc of Multi-State Poultry Feeding and Nutrition and Health and Management Conference and Degussa Corporation's Technical Symposium. May 25-27, 2004. Indianapolis, IN. Available at <http://www.bae.uky.edu/ifafs/timeline.htm>.
- Gates, R. S., K. D. Casey, E. F. Wheeler, H. Xin, A. J. Pescatore, J. L. 2008. U.S. broiler housing ammonia emissions inventory. *Atmospheric Environment*.42, 3342-3350.
- Givens, G.H. and J.P. Hughes. 1995. Model validation and assessment of uncertainty in a deterministic model for gonorrhoea.
- Griffin, R.A., N.F. Shimp, J.D Steele, R.R.Ruch, W.A.White, G.M.Hughes. 1976. Attenuation of pollutants in municipal landfill leachate by passage through clay. In:

- Environmental Science and Technology*, vol. 10, pp. 1262 – 1268. Cited in: Buss S.R., Herbert, A.W., Morgan, P., Thornton, S.F., 2003. Review of ammonium attenuation in soil and groundwater. NGWCLC report NC/02/49. Published by Environment Agency UK. ISBN: 1 84432 110 1.
- Guiziou, F. and F. Beline. 2005. In situ measurement of ammonia and green house gas emissions from broiler houses in France. *Bioresource Technology*, 96, 203-207.
- Hales, J.M. and D.R., Drewes. 1979. Solubility of ammonia at low concentrations. *Atmospheric Environment* 13, pp. 1133–1147.
- Hargreaves, K.J. and Atkins, D.H.F. 1987. The measurement of ammonia in the outdoor environment using passive diffusion samplers. United Kingdom Atomic Energy Authority Report AERE-12668, Harwell Laboratory, Oxfordshire
- Harper, L. 2005. Ammonia: Measurement Issues. *Micrometeorology in Agricultural Systems*. p.345-379. V.M., Hatfield J. and J. Baker (eds). Agronomy Series No. 47 American Society of Agronomy. Crop Science Society of America. Soil Science Society of America.
- Hashimoto A G and D. C. Ludington. 1971. Ammonia desorption from concentrated chicken manure slurries. *Livestock Waste Management and Pollution Abatement, Proceedings of the International Symposium on Livestock Wastes*. St. Joseph, MI: ASAE, 117-121.
- Haslam, R.T.; Hershey, R.L.; Keen, R.H. 1924. Effect of gas velocity and temperature on rate of absorption. *Industrial and Engineering Chemistry*. 16(12), 1224–1230
- Hills, R.G. 2006. Model validation: model parameter and measurement uncertainty. *Journal of Heat Transfer*. Vol. 128, 339-351.

- Hills, R. G., and Trucano, T. G., 1999, Statistical Validation of Engineering and Scientific Models: Background, SAND99-1256, Sandia National Laboratories, Albuquerque.
- Hills, R. G., and Trucano, T. G., 2001, Statistical Validation of Engineering and Scientific Models with Application to CTH, SAND2001-0312, Sandia National Laboratories, Albuquerque.
- Holman, J. 1994. Experimental Methods for Engineers. Sixth Edition. McGraw-Hill Inc. Series in Mechanical Engineering.
- Husted, S.; Jensen, L.S.; Jorgensen, S.S. 1991. Reducing ammonia loss from cattle slurry by the use of acidifying additives – the role of the buffer system. *Journal of the Science of Food and Agriculture*, 57(3), 335–350
- Hutchings, N. H. Fagerli, W. Asman¹, T. Misselbrook, R. Pinder and J. Webb. 2006. Modeling and Regulating Ammonia Emissions. Proceedings of Workshop on Agricultural Air Quality: State of the science, Bolger conference center, Potomac, Maryland, USA, June 5-8
- Hutchings, N. J., S. G. Sommer, J. M. Andersen and W. A. H. Asman. 2001. A detailed ammonia emission inventory for Denmark. *Atmospheric Environment* 35(11): 1959-1968.
- Hyde, B. P., O. T. Carton, P. O'Toole and T. H. Misselbrook. 2003. A new inventory of ammonia emissions from Irish agriculture. *Atmospheric Environment* 37(1): 55-62.
- Incropera, F., DeWitt, D., T. Bergman and A. Lavine. 1997. Fundamentals of Heat and Mass Transfer. Wiley, Sixth Edition. John Wiley & Sons.
- Jayaweera, G.R. and Mikkelson, D.S. 1990. Ammonia volatilization from flooded soil systems: A computer model. I. Theoretical aspects. *Soil Science Society of America Journal*, 54, 1447–1455

- Kamin, H., J.C. Barber, S.I. Brown, C.C. Delwiche, D. Grosjean, J.M. Hales, J.L.W. Knapp, E.R. Lemon, C.S. Martens, A.H. Niden,; R.P. Wilson and J.A. Frazier. 1979. *Ammonia*. Baltimore: University Park Press
- Keener, H. M. and L. Zhao. 2006. Predicting NH₃ Emissions from Manure N for Livestock Facilities and Storages: A Modified Mass Balance Approach. Proceedings of the Workshop on Agricultural Air Quality: State of the Science. June 5-8, Bolger Center, Potomac, MD, USA.
- Koelliker J K; Miner J R. 1973. Desorption of ammonia from anaerobic lagoons. *Transactions of the ASAE*, 16, 148-151
- Koerkamp, G., J.H.M. Metz, G.H. Uenk, V.R. Phillips, M.R. Holden. et al.1998. Concentrations and emissions of ammonia in livestock buildings in northern Europe. *J. Agric. Eng. Res.* 70:79-95
- Kohn, R.A., Z. Dou, J.D. Ferguson, and R.C. Boston. 1997. A sensitivity analysis of nitrogen losses from dairy farms. *Journal of Environmental Management* 50:417-428.
- Lacey, R.E., J.S. Redwine and C.B. Parnell, Jr. 2003. Particulate matter and ammonia emission factors for tunnel-ventilated broiler production houses in the Southern U.S. *Transactions of ASAE*, Vol. 46(4): 1203-1214.
- Latenser B.A. and T.A. Loucktong . 2000. Anhydrous ammonia burns: case presentation and literature review. *J Burn Care Rehabil* 21:40-42.
- Leduce D. et al. 1992. Acute and long-term respiratory damage following inhalation of ammonia. *Thorax* 46:755-757.
- Lee, Y. H. and S. U. Park. 2002. Estimation of ammonia emission in South Korea. *Water Air and Soil Pollution* 135(1-4): 23-37.

- Liang Y., H. Xin, A. Tanaka, S. H. Lee, H. Li, E. F. Wheeler, R. S. Gates, J. S. Zajackowski, P. Topper and K. D. Casey. 2003. Ammonia emissions from U.S. poultry houses: Part II - Layer houses. Pp: 147-158, *Proceedings of Third International Conference on Air Pollution from Agricultural Operations*, Raleigh, NC.
- Liang, Z. S., P. W. Westman, J. Arogo. 2002. Modeling ammonia emission from swine anaerobic lagoons. *Transaction of ASAE*, Vol. 45(3), 787-798.
- Liley, P.E., R.C. Reid, and E. Buck. 1984. Physical and chemical data. Perry's Chemical Engineering Handbook. 6th Edition. McGraw-Hill. pp. 2408.
- Liu, Z., L. Wang, D. B. Beasley, and B. S. Shah. 2008. Mass Transfer Coefficient of Ammonia Emissions from Broiler Litter, Paper number 084368, 2008 ASABE Annual Meeting, Providence, Rhode Island. June 29 – July 2.
- Liu, Z., L. Wang, D. B. Beasley, and E. Oviedo. 2007a. Effect of moisture content on ammonia emissions from broiler litter: A laboratory study. *J. Atmos. Chem.* 58(1): 41-53.
- Liu, Z., L. Wang, D. B. Beasley, and E. Oviedo. 2007b. Modeling ammonia emissions from broiler litter with a dynamic flow-through chamber system. ASABE Paper No. 074090. St. Joseph, Mich.: ASABE.
- Lockyer, D.R. 1983. A system for the measurement in the field of losses of ammonia through volatilization. *Journal of the Science of Food and Agriculture*, 35, 837 – 848
- Loubet, B., P. Cellier, S. Genermont, and D. Flura. 1999b. An Evaluation of the wind-tunnel technique for estimating ammonia volatilization from land: part 2. Influence of the tunnel on transfer processes. *J. Agric. Engng Res.* 72: 83-92.

- Marshall, Valin G., and Dean S. DeBell. 1980. Comparison of four methods of measuring volatilization losses of nitrogen following urea fertilization of forest soils. *Can. J. Soil Sci.* 60: 549-563.
- Misselbrook, T.H. 2000. Inventory of Ammonia Emissions from UK Agriculture 1999. Contract Report AM0108 Department for Environment Food and Rural Affairs, UK
- Misselbrook, T. H., F. Nicholson, B. J. Chambers, and R. A. Johnson. 2005. Measuring ammonia emissions from land applied manure: An intercomparison of commonly used samplers and techniques. *Environ. Pollut.* 135(3): 389-397.
- Monteny, G.J.; Schulte, D.D.; Elzing, A.; Lamaker, E.J.J. 1996. Prediction modeling of ammonia emissions from cubicle dairy cow houses. Proceedings of the 1st International Conference on Air Pollution from Agricultural Operations. Kansas City, Missouri, USA, pp. 215–220
- Monteny G J and E J J. Lamaker. 1997. Factors influencing air velocity in and ammonia volatilization from a slurry pit in cubicle houses for dairy cows. In: International Symposium on Ammonia and Odor Control from Animal Production Facilities. (Voermans J A M; Monteny G J, eds.), Vinkeloord, The Netherlands, 57-67
- Monteny, G.J., D.D. Schulte, A. Elzing and E.J.J. Lamaker. 1998. A conceptual mechanistic model for the ammonia emissions from free stall cubicle dairy cow houses. *Transactions of the ASAE*, Vol. 41 (1): 193-201.
- Montes, F., A. Rotz, H. Chaoui. 2008. Process modeling of ammonia volatilization from ammonium solution and manure surfaces. ASABE paper No. 083584. St. Joseph, Mich.: ASABE.
- Moore Jr., P. A., T.C. Daniel, D.R. Edwards and D.M. Miller. 1996. Evaluation of chemical amendments to reduce ammonia volatilization from poultry litter. *Poul. Sci.* 75(3): 315-320

- Muck R E; Steenhuis T S. 1982. Nitrogen losses from manure storages. *Agricultural Wastes*, 4, 41-54
- Mukhtar,S., J.L. Ullman, J.B Carey, R.E. Lacey. 2004. A review of literature concerning odors, ammonia, and dust from broiler production facilities: 3. Land application, processing, and storage of broiler litter. *J. Appl. Poult. Res.* 13:514-52.
- Murphy G. 1950. *Similitude in Engineering*. New York. Ronald Press Company.
- National Research Council (NRC). 2003. *Air emissions from Animal Feeding Operations: Current Knowledge, Future Needs*. National Academies Press, Washington, DC.
- Nicholson, F.A., B. J. Chambers, A. W. Walker. 2004. Ammonia emissions from broiler litter and laying hen manure management systems, *Biosystems Engineering*, 89(2), 175-185.
- Ni, J. 1998. Emission of carbon dioxide and ammonia from mechanically ventilated pig house. PhD Thesis. Catholic University of Leuven, February, 227 pp
- Ni, J. 1999. Mechanistic models of ammonia release from liquid manure: a review. *J. Agric. Engng Res.* 72, 1-17.
- Ni, J., J. Hendriks, C. Vinckier and J. Coenegrachts. 2000. Development and validation of a dynamic mathematical model of ammonia release in pig house. *Environment International* 26(2000):105-115.
- Ni, J. and A. Heber. 2001. Sampling and measurement of ammonia concentration at animal facilities: a review. Paper Number: 01-4090. St Joseph, Mich.: ASABE.
- Olesen J E and S.G. Sommer. 1993. Modeling effects of wind speed and surface cover on ammonia volatilization from stored pig slurry. *Atmospheric Environment. Part A. General Topics*, 27(16), 2567-2574.

- Pinder, R. W., N.J. Pekney, C.I. Davidson, and P.J. Adams. 2004. A process-based model of ammonia emissions from dairy cows: improved temporal and spatial resolution. *Atmospheric Environment* 38 (9):1357-1365.
- Perry, R., D. Green and J. Maloney. 1997. Perry's Chemical Engineering Handbook. 7th Edition. McGraw-Hill.
- Raupach M. R., R. A. Antonia, and S. Rajagopalan. 1991. Rough-wall turbulent boundary layers, *Applied Mechanical Review*, 44(1), 1-24.
- Rachhpal-Singh; Nye P H.1986. A model of ammonia volatilization from applied urea. I. Development of the model. *Journal of Soil Science*, , 37, 9-20
- Redwine, J.S., R.E. Lacey, S. Mukhtar, and J.B. Carey. 2002. Concentration and emissions of ammonia and particulate matter in tunnel-ventilated broiler houses under summer conditions in Texas. *Transactions of ASAE*, Vol. 45(4): 1101-1109.
- Reece, F.N., B. D. Lott and B. J. Bates. 1985. The performance of a computerized system for control of broiler-house environment. *Poult. Sci.* 64:261-265
- Reidy, B., U. Dämmgen, H. Döhler, B. Eurich-Menden, F.K. van Evert, N.J. Hutchings, H.H. Luesink, H.T. Menzi, H. Misselbrook, G.J. Monteny, J. Webb. 2006. Comparison of Models Used for the Calculation of National Ammonia Emission Inventories from Agriculture in Europe. Proceedings of Workshop on Agricultural Air Quality: State of the science, Bolger conference center, Potomac, Maryland, USA, June 5-8
- Reidy, B. and H. Menzi. 2006. DYNAMO: An ammonia emission calculation model and its application for the Swiss ammonia emission inventory. Proceedings of the Workshop on Agricultural Air Quality: State of the Science. June 5-8, Bolger Center, Potomac, MD, USA.

- Roelle, P. and V. Aneja. 2005. Modeling ammonia emissions from soils. *Environ. Engineering Sci.* 22(1):58-72.
- Roelle, P. A., V. P. Aneja, J. O'Connor, W. Robarge, D.-S. Kim, and J. S. Levine. 1999. Measurement of nitrogen oxide emissions from an agricultural soil with a dynamic chamber system. *J. Geophysical Res.* 104(D17): 1609-1619.
- Ruxton, G.D. 1995. Mathematical modeling of ammonia volatilization from slurry stores and its effect on *Cryptosporidium* oocyst viability. *Journal of Agricultural Science*, Cambridge, 124, 55-56
- Ryden, J. C. and D. R. Lockyear. 1985. Evaluation of a system of wind tunnels for field studies of ammonia loss from grassland through volatilization. *J. Sci. Food Agric.* 36:781-788.
- Schecfferle, H.E. 1965. The decomposition of uric acid in built-up poultry litter. *J. Appl. Bact.* 28: 412-420.
- Schulze, E.-D., de Vries, W., Hauhs, M., Rosehn, K., Rasmussen, L., Tamm, C. O., Nilsson, J., 1989. Critical loads for nitrogen deposition on forest ecosystems. *Water Air and Soil Pollution* 48, 451-456.
- Schuman, G. E., M. A. Stanley, and D. Knudsen. 1973. Automated total nitrogen analysis of soil and plant samples. *SSSA Proc.* 37(3): 480-481.
- Schwarzenbach, R., P. Gschwend and D. Imboden. 2003. Environmental organic chemistry. Second Edition. Wiley-Interscience.
- Shah, S. B., G. L. Grabow, and P. W. Westerman. 2006. Ammonia adsorption in five types of flexible tubing materials. *Applied Eng. in Agric.* 22(6): 919-923.

- Shah, S. B., T. K. Marshall, E. P. Harris, P. W. Westerman, and R. D. Munilla. 2007. An innovative wind tunnel for evaluating gaseous emissions from agricultural land or liquid surfaces. Paper number 074005, 2007 ASABE Annual Meeting, Minneapolis, Minnesota. 17-20 June.
- Siefert, R.L., J.R. Scudlark, A.M. Potter, K.A. Simonsen, and K.B. Savidge. 2004. Characterization of atmospheric ammonia emissions from a commercial chicken house on the Delmarva Peninsula. *Environ. Sci. Technol.* 38:2769-2778.
- Sims, J.T. and D.C. Wolf. 1994. Poultry waste management: agricultural and environmental issues. *Advances in Agronomy.* 52, 1-83.
- Srinath E. G. and R. C. Loehr. 1974 Ammonia desorption by diffused aeration. *Journal of Water Pollution Control Federation.* 46 (8), 1937-1957.
- Stumm, W. and J. Morgan. 1996. *Aquatic Chemistry.* Third Edition. Wiley Interscience.
- Sutton, M. A., C. J. Place, M. Eager, D. Fowler and R. I. Smith. 1995. Assessment of the magnitude of ammonia emissions in the United Kingdom. *Atmospheric Environment* 29(12): 1393-1411.
- Taylor, J. 1997. An introduction to error analysis: The study of uncertainties in physical measurements. Second Edition. University Science Books.
- Teye, F.K. and M. Hautala. 2008. Adaptation of an ammonia volatilization model for a naturally ventilated dairy building. *Atmospheric Environment.* 42, 4345-4354.
- Tucker, S. and A.W. Walker. 1992. Hock burn in broilers. In: Garnsworthy, P.C., Haresign, W., Cole, D.J.A. (Eds.), *Recent Advances in Animal Nutrition.* Butterworth-Heinemann Ltd. Oxford, Oxford. pp. 33-49.

- Townsend A. A. 1976. The structure of turbulent shear flow, Cambridge University Press, Cambridge.
- Valentine, H. 1964. A study of the effect of different ventilation rates on the ammonia concentrations in the atmosphere of broiler houses. *Brit. Poul. Sci.* 5: 149-159.
- Van Breemen, N., P. A. Burrough, E. J. Velthorst, H. F. van Dobben, T. de Wit, T. B. Ridder, and H. F. Reijnders. 1982. Soil acidification from atmospheric ammonium sulphate in forest canopy throughfall. *Nature* 299(5883): 548-550.
- Van der Hoek, K. W. 1991. Emission factors for ammonia in The Netherlands. IIASA Workshop on Ammonia Emissions in Europe: Emission Factors and Abatement Costs, Luxemburg, Austria.
- van der Molen J., Beljaars A. C. M., Chardon W. J., Jury W. A., Vanfaassen H. G. 1990. Ammonia volatilization from arable land after application of cattle slurry. 2. Derivation of a transfer model. *Netherlands Journal of Agricultural Science*, 38 (3), 239-254.
- Warren-Hicks, W., Carbone, J.P., and Havens, P.L. 2002. Using Monte Carlo Techniques to Judge Model Prediction Accuracy: Validation of the Pesticide Root Zone Model 3.12, *Envir. Toxicol. Chem.* 21 (8), pp. 1570-1577.
- Webba, J. and T.H. Misselbrook. 2004. A mass-flow model of ammonia emissions from UK livestock production, *Atmospheric Environment* 38 (2004) 2163–2176
- Welty J R., C. E. Wicks, R. E. Wilson. 1984. Fundamentals of Momentum, Heat, and Mass Transfer. 3rd edition. New York: Wiley.
- Wheeler, E. F., K. D. Casey, J. D. Zajackowski, P. A. Topper, R. S. Gates, H. Xin, Y. Liang, and A. Tanaka. 2003. Ammonia emissions from U.S. poultry houses: Part III. Broiler

- houses. In *Proc. 3rd Intl. Conf. Air Pollution from Agricultural Operations*, 159-166. St. Joseph, Mich.: ASABE.
- Wheeler, E.F., K.D. Casey, R.S. Gates, J.S. Zajackowski, P. A. Topper, R. S. Gates, H. Xin, Y. Liang. and D. Brown. 2004. Ammonia Emissions from U.S. Broiler Houses in Kentucky and Pennsylvania. Written for presentation at the 2004 ASAE/CSAE Annual International Meeting Sponsored by ASAE/CSAE Fairmont Chateau Laurier, The Westin, Government Centre Ottawa, Ontario, Canada. August 1-4.
- Whitehead, D.C. and N. Raistrick. 1993. Nitrogen in the excreta of dairy cattle: changes during the short-term storage. *Journal of Agricultural Science* 121: 73-81.
- Witter, E. and Kirchmann. H. 1989. Effects of addition of calcium and magnesium salts on ammonia volatilization during manure decomposition. *Plant & Soil* 115(1): 53-58.
- Wolpert, R.L., K.H. Rechow, and L.J. Steinberg. 1992. Bayesian hierarchical models for transport and fate modeling. In J.S. Hodges et al. (Eds) *Bayesian Statistics in Science and Technology: Case Studies*, Newyork: Springer-Verlag, pp. 241-96.
- Xin, H., Y. Liang, A. Tanaka, R. S. Gates, E. F. Wheeler, K. D. Casey, A. J. Heber, J. Ni and H. Li. 2003. Ammonia emissions from U.S. poultry houses: Part I – Measurement system and techniques. Pp: 106-115, *Proceedings of Third International Conference on Air Pollution from Agricultural Operations*, Raleigh, NC.
- Zerihun, D., J. Feyen, and J. M. Reddy. 1996. Sensitivity analysis of furrow-irrigation performance parameters. *J. Irrigation and Drainage Eng.* 122(1): 49-57
- Zhang R. H.1992. Degradation of swine manure and a computer model for predicting the desorption rate of ammonia from an under-floor pit. PhD dissertation. Library, University of Illinois, Urbana IL.

Zhang, R., J. Fadel, T. Rumsey, H. Xin, J. Arogo, Z. Wang and G. Mansell. 2005 An Improved Process Based Ammonia Emission Model for Agricultural Sources – Model Development. Prepared for presentation at the 14th International Emission Inventory Conference. Las Vegas, NV. March.

Zhang, R., T.R. Rumsey, J.G. Fadel, J. Arogo, Z. Wang, G.E. Mansell, H. Xin. 2006. A Process-Based Ammonia Emission Model for Confinement Animal Feeding Operations – Model Development, technical paper, http://www.ladco.org/reports/rpo/MWRPOprojects/Emissions/Technical_Paper2.pdf, accessed July, 2006

Zhao B. and S. Chen. 2003. Ammonia volatilization from dairy manure under anaerobic and aerated conditions at different temperature. ASABE Paper No. 034148. St. Joseph, Mich.: ASABE.

Zhao, D. W. and A. P. Wang. 1994. Estimation of anthropogenic ammonia emissions in Asia. *Atmospheric Environment* 28(4): 689-694.

APPENDIX

APPENDIX A. SUMMARY OF LITTER ANALYSIS DATA

No	Sample code	Litter age	Analysis date	pH	Wet basis					Dry basis					TAN/T KN
					Moisture Content (w/w,%)	TKN (µg/g)	TAN (µg/g)	Total Carbon (%)	Total Nitrogen (%)	Moisture Content (w/w, %)	TKN (µg/g)	TAN (µg/g)	Total Carbon (%)	Total Nitrogen (%)	
1	A	2 years	5/3/2006	8.43	22.79	29800	1630	31.96	3.02	29.52	38596	2111	41.39	3.91	5.5%
2	B	4 years	5/23/2006	8.00	23.2	38002	6108	28.44	4.2	30.21	49482	7953	37.03	5.47	16.1%
3	C	8 flocks	3/29/2006	7.73	15.86	43848	4070	23.52	4.3	18.85	52113	4837	27.95	5.11	9.3%
4	D	12 flocks	3/29/2006	7.34	16.07	46507	4280	26.14	4.61	19.15	55412	5099	31.15	5.49	9.2%
5	E	1 year	3/20/2006	8.48	19.82	24731	1980	31.77	2.502	24.72	30844	2469	39.62	3.12	8.0%
6		3 flocks	3/29/2006	7.62	17.92	34604	3940	31.56	3.67	21.83	42159	4800	38.45	4.47	11.4%
7		4 flocks	3/29/2006	8.42	31.69	39165	5800	26.35	3.73	46.39	57334	8491	38.57	5.46	14.8%
8		5 flocks	3/29/2006	8.10	21.16	30972	3140	29.7	3.2	26.84	39285	3983	37.67	4.06	10.1%
9		6 flocks	3/29/2006	8.14	27.87	35801	3680	28.23	3.22	38.64	49634	5102	39.14	4.46	10.3%
10		9 flocks	3/29/2006	7.83	22.89	40000	3620	31.68	4.12	29.68	51874	4695	41.08	5.34	9.1%
11		1 year	5/3/2006	8.54	50.35	15888	1137	19.29	1.52	101.41	32000	2290	38.85	3.06	7.2%
12	1-1-before	1 year	6/14/2006	8.11	18.15	37039	3272	30.18	3.44	22.17	45252	3998	36.87	4.20	8.8%
13	1-1-after	1 year	6/14/2006	7.87	17.43	34622	3347	30.56	3.37	21.11	41930	4054	37.01	4.08	9.7%
14	1-2-before	1 year	6/15/2006	7.81	17.08	35591	3337	30.25	3.38	20.60	42922	4024	36.48	4.08	9.4%
15	1-2-after	1 year	6/15/2006	7.71	16.16	35604	3337	30.43	3.32	19.27	42467	3980	36.30	3.96	9.4%
16	1-3-before	1 year	6/20/2006	7.80	20.53	32720	3407	29.22	3.3	25.83	41173	4287	36.77	4.15	10.4%
17	1-3-after	1 year	6/20/2006	7.73	19.73	33831	3312	29.61	3.12	24.58	42147	4126	36.89	3.89	9.8%

No	Sample code	Litter age	Analysis date	pH	Wet basis					Dry basis					TAN/T KN
					Moisture Content (w/w,%)	TKN (µg/g)	TAN (µg/g)	Total Carbon (%)	Total Nitrogen (%)	Moisture Content (w/w, %)	TKN (µg/g)	TAN (µg/g)	Total Carbon (%)	Total Nitrogen (%)	
18	1-4-before	1 year	6/21/2006	7.71	28.99	28191	3796	25.13	2.78	40.83	39700	5346	35.39	3.91	13.5%
19	1-4-after	1 year	6/21/2006	7.67	27.78	29222	3549	25.97	2.64	38.47	40462	4914	35.96	3.66	12.1%
20	1-5-before	1 year	6/22/2006	7.80	28.4	29574	3585	25.42	2.6	39.66	41304	5007	35.50	3.63	12.1%
21	1-5-after	1 year	6/22/2006	7.70	27.72	29932	3532	25.3	2.75	38.35	41411	4887	35.00	3.80	11.8%
22	1-6-before	1 year	6/26/2006	8.30	28.67	28542	3755	25.09	2.76	40.19	40014	5264	35.17	3.87	13.2%
23	1-6-after	1 year	6/26/2006	8.08	27.37	28676	3658	26.43	2.59	37.68	39482	5036	36.39	3.57	12.8%
24	1-7-before	1 year	6/27/2006	8.06	31.56	27964	3524	24.1	2.46	46.11	40859	5149	35.21	3.59	12.6%
25	1-7-after	1 year	6/27/2006	7.94	32.44	26191	3515	24.26	2.49	48.02	38767	5203	35.91	3.69	13.4%
26	1-8-before	1 year	6/28/2006	8.23	33.15	26255	3518	23.63	2.52	49.59	39274	5263	35.35	3.77	13.4%
27	1-8-after	1 year	6/28/2006	8.08	32.75	26498	3278	23.1	2.4	48.70	39402	4874	34.35	3.57	12.4%
28	1-9-before	1 year	6/16/2006	8.56	21.99	28085	815	29.48	2.72	28.19	36002	1045	37.79	3.49	2.9%
29	1-9-after	1 year	6/16/2006	8.47	21.21	28793	815	29.3	2.73	26.92	36544	1034	37.19	3.46	2.8%
30	4-1-before	< 1 year	2/5/2007	8.96	25.92	32546	2921	27.18	3.16	34.99	43934	3943	36.69	4.27	9.0%
31	4-1-after	< 1 year	2/5/2007	8.84	24.13	35322	2757	28.93	3.25	31.80	46556	3634	38.13	4.28	7.8%
32	4-2-before	< 1 year	2/6/2007	9.01	23.67	31471	1447	24.79	2.85	31.01	41230	1896	32.48	3.73	4.6%
33	4-2-after	< 1 year	2/7/2007	9.03	22.05	30675	1254	24.27	2.91	28.29	39352	1609	31.14	3.73	4.1%
34	4-3-before	< 1 year	2/13/2007	7.57	32.15	35563	2854	28.15	3.69	47.38	52414	4206	41.49	5.44	8.0%
35	4-3-after	< 1 year	2/13/2007	7.61	19.81	26495	3009	30.38	3.82	24.70	33040	3752	37.89	4.76	11.4%
36	4-4-before	< 1 year	2/14/2007	8.77	17.28	28173	2161	31.81	2.87	20.89	34058	2612	38.46	3.47	7.7%
37	4-4-after	< 1 year	2/14/2007	8.67	18.48	28473	2117	33.14	2.85	22.67	34928	2597	40.65	3.50	7.4%

No	Sample code	Litter age	Analysis date	pH	Wet basis					Dry basis					TAN/TKN
					Moisture Content (w/w,%)	TKN (µg/g)	TAN (µg/g)	Total Carbon (%)	Total Nitrogen (%)	Moisture Content (w/w, %)	TKN (µg/g)	TAN (µg/g)	Total Carbon (%)	Total Nitrogen (%)	
38	4-5-before	< 1 year	2/15/2007	8.11	19.9	31492	3752	30.31	3.17	24.84	39316	4684	37.84	3.96	11.9%
39	4-5-after	< 1 year	2/15/2007	8.16	15.73	31361	3890	30.99	3.26	18.67	37215	4616	36.77	3.87	12.4%
40	4-6-before	< 1 year	2/16/2007	7.73	22.95	27864	2441	29.23	1.97	29.79	36164	3168	37.94	2.56	8.8%
41	4-6-after	< 1 year	2/16/2007	7.16	20.86	28412	2877	27.31	2.99	26.36	35901	3635	34.51	3.78	10.1%
42	4-7-before	< 1 year	2/19/2007	7.42	27.48	30716	3788	24.77	3.03	37.89	42355	5223	34.16	4.18	12.3%
43	4-7-after	< 1 year	2/19/2007	8.15	26.48	28652	2939	25.04	2.78	36.02	38972	3998	34.06	3.78	10.3%
44	4-8-before	< 1 year	2/19/2007	8.25	26.02	27208	2040	27.7	2.83	35.17	36778	2758	37.44	3.83	7.5%
45	4-8-after	< 1 year	2/21/2007	8.01	23.52	29134	2524	26.89	2.89	30.75	38094	3300	35.16	3.78	8.7%
46	4-9-before	< 1 year	2/21/2007	8.71	27.28	28145	1866	27.73	2.75	37.51	38703	2566	38.13	3.78	6.6%
47	4-9-after	< 1 year	2/22/2007	8.91	23.88	28369	974	27.28	2.74	31.37	37269	1280	35.84	3.60	3.4%
48		< 1 year	2/21/2007	6.20	18.52	28089	3685	28.61	2.97	22.73	34473	4523	35.11	3.65	13.1%
49		< 1 year	2/21/2007	6.32	18.78	29105	4117	27.59	2.93	23.12	35835	5069	33.97	3.61	14.1%
50	House1-1	< 1 year	1/29/2007	7.73	22.95	27864	2441	29.23	1.97	29.79	36164	3168	37.94	2.56	8.8%
51	House1-2	< 1 year	3/30/2007	8.57	25.62	42231	3519	28.04	4.11	34.44	56777	4731	37.70	5.53	8.3%
52	House1-3	< 1 year	4/6/707	8.66	22.67	36473	1971	27.37	3.64	29.32	47165	2549	35.39	4.71	5.4%
53	House1-cake	< 1 year	3/30/2007	6.47	47.51	29938	5864	20.83	3.23	90.51	57036	11172	39.68	6.15	19.6%
54	House2-1	< 1 year	1/29/2007	7.42	27.48	30716	3788	24.77	3.03	37.89	42355	5223	34.16	4.18	12.3%
55	House2-2	< 1 year	3/30/2007	7.73	18.07	55137	3104	31.14	5.61	22.06	67298	3789	38.01	6.85	5.6%
56	House2-3	< 1 year	4/6/707	8.80	24.61	32943	2544	25.61	3.12	32.64	43697	3374	33.97	4.14	7.7%

No	Sample code	Litter age	Analysis date	pH	Wet basis					Dry basis					TAN/T KN
					Moisture Content (w/w,%)	TKN (µg/g)	TAN (µg/g)	Total Carbon (%)	Total Nitrogen (%)	Moisture Content (w/w, %)	TKN (µg/g)	TAN (µg/g)	Total Carbon (%)	Total Nitrogen (%)	
57	House3-1	< 1 year	1/29/2007	8.25	26.02	27208	2040	27.7	2.83	35.17	36778	2758	37.44	3.83	7.5%
58	House3-2	< 1 year	1/29/2007	8.71	27.28	28145	1866	27.73	2.75	37.51	38703	2566	38.13	3.78	6.6%
59	House3-3	< 1 year	3/30/2007	8.34	21.25	44065	2365	29.22	4.58	26.98	55956	3003	37.10	5.82	5.4%
60	House3-4	< 1 year	3/30/2007	8.30	20.38	43769	2116	27.83	4.25	25.60	54972	2658	34.95	5.34	4.8%
61	House4-1	< 1 year	1/29/2007	6.20	18.52	28089	3685	28.61	2.97	22.73	34473	4523	35.11	3.65	13.1%
62	House4-2	< 1 year	3/30/2007	8.34	20.06	43866	2768	29.78	4.55	25.09	54874	3463	37.25	5.69	6.3%
63	House4-3	< 1 year	4/6/707	8.32	19.35	43499	1811	30.47	4.31	23.99	53936	2246	37.78	5.34	4.2%
64	A-1	< 1 year	3/18/2008	8.31	22.32	41406	3809	25.95	4.05	28.73	53303	4903	33.41	5.21	9.2%
65	A-2	< 1 year	4/11/2008	8.36	24.68	46222	3952	25.91	4.55	32.77	61367	5247	34.40	6.04	8.6%
66	A-3	< 1 year	4/11/2008	8.63	25.03	46901	3514	26.19	4.2	33.39	62560	4687	34.93	5.60	7.5%
67	A-4	< 1 year	4/18/2008	8.61	22.81	45701	3515	26.71	4.23	29.55	59206	4554	34.60	5.48	7.7%
68	A-5	< 1 year	4/18/2008	8.51	20.73	46554	2964	26.49	4.41	26.15	58728	3739	33.42	5.56	6.4%
69	A-6	< 1 year	4/24/2008	8.53	22.01	50938	3059	27.51	4.16	28.22	65314	3922	35.27	5.33	6.0%
70	B-1	< 1 year	3/18/2008	8.01	34.74	31212	6789	22.01	3.01	53.23	47827	10403	33.73	4.61	21.8%
71	B-2	< 1 year	4/24/2008	8.91	37.19	33297	5738	20.65	2.41	59.21	53012	9135	32.88	3.84	17.2%
72	B-3	< 1 year	5/2/2008	8.72	35.36	32365	5369	22.46	2.62	54.70	50070	8306	34.75	4.05	16.6%
73	B-4	< 1 year	5/2/2008	8.60	35.34	29848	5494	22.78	2.61	54.66	46161	8497	35.23	4.04	18.4%
74	B-5	< 1 year	5/9/2008	8.81	36.54	27858	.	21.29	2.4	57.58	43899		33.55	3.78	
75	B-6	< 1 year	5/23/2008	8.87	38.24	29793	5894	20.91	2.31	61.92	48240	9543	33.86	3.74	19.8%

No	Sample code	Litter age	Analysis date	pH	Wet basis					Dry basis					TAN/TKN
					Moisture Content (w/w,%)	TKN ($\mu\text{g/g}$)	TAN ($\mu\text{g/g}$)	Total Carbon (%)	Total Nitrogen (%)	Moisture Content (w/w, %)	TKN ($\mu\text{g/g}$)	TAN ($\mu\text{g/g}$)	Total Carbon (%)	Total Nitrogen (%)	
76	C-1	< 1 year	3/18/2008	8.45	64.15	26858	9294	13.65	2.51	178.94	74918	25925	38.08	7.00	34.6%
77	C-2	< 1 year	5/23/2008	8.94	43.76	26262	7731	18.19	2.04	77.81	46696	13746	32.34	3.63	29.4%
78	C-3	< 1 year	6/6/2008	8.74	49.17	28019	9219	17.53	2.51	96.73	55123	18137	34.49	4.94	32.9%
79	C-4	< 1 year	6/6/2008	8.73	51.09	27181	9559	16.51	2.72	104.46	55574	19544	33.76	5.56	35.2%
80	C-5	< 1 year	6/20/2008	8.70	47.59	23702	4066	17.64	2.18	90.80	45224	7758	33.66	4.16	17.2%
81	C-6	< 1 year	6/20/2008	8.74	48.53	22631	3893	17.47	2.37	94.29	43969	7564	33.94	4.60	17.2%

Note: Litter samples were all taken from commercial broiler farms in North Carolina. The litter material used by the farms mainly consisted of wood shavings. Litter samples A, B, and E (No. 1, No. 2 and No. 5) were used in the study of comparison of techniques for determining ammonia emissions (chapter 4). Litter samples 1-1 to 1-9, 4-1 to 4-9 (No. 12 to No. 47) were used for the mass balance approach (chapter 4), and each of the samples were analyzed twice, before and after the test. Litter samples A, B, C, D, E (No. 1 to No. 5) were used in the study of effects of moisture (chapter 5). Litter samples 4-1 to 4-9 were also used in the dynamic flow through chamber study for developing sub-model of $C_{g,0}$ (chapter 6). Data from No. 64 to No. 81 were six repeat analyses for three litter samples (Data No.64 to No.69 were from litter A, and data No. 70 to No. 75 were from litter B that was used in the wind tunnel study in chapter 6 and chapter 7).

APPENDIX B. EFFECTS OF LITTER pH, MOISTURE CONTENT AND TOTAL CARBON CONTENT ON TAN/TKN RATIO

It was observed that the TAN content were 2.83% to 35.17% of the TKN content in the litter in Appendix A. The TAN/TKN ratios in litter showed wide variation. The litter TAN content is the direct source of ammonia released from litter and it is an important input in the emission model. On the other hand, litter TKN content, pH, moisture contents and total carbon content are variables that can be directly influenced by management and control strategies. A regression procedure was used to relate TAN/TKN ratio with litter pH, moisture contents and total carbon content (all in dry basis). Data for each different litter sample in Appendix A were used for the regression (for data No.12 to No.49, only the analysis data before the chamber test were used; for data No. 64 to No. 81, average values of six repeat analyses for each of the three litter samples were used). The results are shown in the following page.

It can be seen that litter pH and moisture content both significantly influence the TAN/TKN ratio (P-value < 0.001). The TAN/TKN ratio decreases with increasing pH and increases with increasing moisture content.

<i>Regression Statistics</i>	
Multiple R	0.725163
R Square	0.525861
Adjusted R Square	0.493534
Standard Error	0.0321
Observations	48

ANOVA

	<i>df</i>	<i>SS</i>	<i>MS</i>	<i>F</i>	<i>Significance F</i>
Regression	3	0.050284521	0.016762	16.26662	2.95E-07
Residual	44	0.045338619	0.00103		
Total	47	0.09562314			

	<i>Coefficients</i>	<i>Standard Error</i>	<i>t Stat</i>	<i>P-value</i>	<i>Lower 95%</i>	<i>Upper 95%</i>	<i>Lower 95.0%</i>	<i>Upper 95.0%</i>
Intercept	0.390063	0.082650741	4.719412	2.42E-05	0.223491	0.556635	0.223491	0.556635
pH	-0.02473	0.006982637	-3.54148	0.000955	-0.0388	-0.01066	-0.0388	-0.01066
MC (%)	0.001513	0.000250763	6.034072	3.01E-07	0.001008	0.002019	0.001008	0.002019
TC (%)	-0.00397	0.001850905	-2.14413	0.037586	-0.0077	-0.00024	-0.0077	-0.00024

APPENDIX C. EXPERIMENTAL DATA OF $C_{G,0}$ AND K_F IN THE DYNAMIC FLOW THROUGH CHAMBER STUDY

Litter sample No.	TAN ($\mu\text{g/g}$)	pH	Moisture content (w/w, %)	Observed $C_{G,0}$ (mg/m^3)	Dissolved $\text{NH}_3\text{-N}$		Dissolved $\text{NH}_4^+\text{-N}$		Adsorbed $\text{NH}_4^+\text{-N}$ ($\mu\text{g/g}$)	$\text{NH}_3\text{-N/TAN}$	Estimated K_f (L/kg)	The K_d ratio α
					(mg/L)	($\mu\text{g/g}$)	(mg/L)	($\mu\text{g/g}$)				
1	3787	8.90	33.4	163	278	93	767	256	3438	2.45%	4.48	0.069
2	1751	9.02	29.6	119	202	60	424	126	1566	3.43%	3.69	0.074
3	3961	7.59	35.1	27	46	16	2617	919	3026	0.41%	1.16	0.232
4	2605	8.72	21.8	143	244	53	1020	222	2330	2.04%	2.28	0.087
5	4650	8.14	21.7	86	147	32	2342	508	4110	0.69%	1.75	0.110
6	3405	7.45	28.1	13	23	6	1752	491	2907	0.19%	1.66	0.144
7	4607	7.79	36.9	81	138	51	4917	1817	2739	1.11%	0.56	0.399
8	3033	8.13	32.9	64	109	36	1769	582	2415	1.18%	1.37	0.194
9	4795	6.26	22.9	1	1.9	0.4	2285	524	4271	0.01%	1.87	0.109
10	1908	8.81	34.4	134	228	78	775	266	1563	4.11%	2.02	0.146

Note: All data expressed in dry basis. $T=22^\circ\text{C}$, Henry's constant $K_h=2073.48$, the dissociation constant in water $K_{d0} = 10^{-9.34}$.

APPENDIX D. EXPERIMENTAL DATA OF $C_{G,0}$ AND K_f FOR LITTER A IN THE WIND TUNNEL STUDY

T (°C)	Log K_{d0}	K_h	Observed $C_{g,0}$ (mg/m ³)	Dissolved NH ₃ -N		Dissolved NH ₄ ⁺ -N		Adsorbed NH ₄ ⁺ -N (µg/g)	NH ₃ -N /TAN	Estimated K_f (L/kg)	The K_d ratio α
				(mg/L)	(µg/g)	(mg/L)	(µg/g)				
21.7	-9.35	2100	164	284	84	2065	614	3802	1.88%	1.84	0.14
21.7	-9.35	2100	198	342	102	2489	740	3659	2.26%	1.47	0.17
21.7	-9.35	2100	220	381	113	2769	824	3564	2.52%	1.29	0.19
19.2	-9.43	2318	115	219	65	1912	569	3867	1.45%	2.02	0.13
23.3	-9.30	1968	140	227	68	1464	435	3998	1.50%	2.73	0.10
26.1	-9.21	1769	280	408	121	2163	643	3736	2.70%	1.73	0.15
26.1	-9.21	1769	294	428	127	2267	674	3699	2.83%	1.63	0.15
23.9	-9.28	1927	247	392	117	2428	722	3662	2.59%	1.51	0.16
21.1	-9.37	2146	148	262	78	1981	589	3834	1.73%	1.93	0.13
23.9	-9.28	1927	220	348	104	2159	642	3755	2.30%	1.74	0.15
25.0	-9.25	1846	250	380	113	2177	648	3740	2.51%	1.72	0.15
27.2	-9.18	1697	358	500	149	2450	729	3623	3.30%	1.48	0.17
26.7	-9.20	1733	381	543	162	2768	823	3516	3.59%	1.27	0.19
25.0	-9.25	1846	348	530	158	3033	902	3441	3.50%	1.13	0.21
21.1	-9.37	2146	191	337	100	2551	759	3642	2.23%	1.43	0.17
21.1	-9.37	2146	197	348	104	2634	784	3614	2.30%	1.37	0.18
21.1	-9.37	2146	221	390	116	2954	879	3506	2.58%	1.19	0.20

T (°C)	LogK _{d0}	K _h	Observed C _{g,0} (mg/m ³)	Dissolved NH ₃ -N		Dissolved NH ₄ ⁺ -N		Adsorbed NH ₄ ⁺ -N (µg/g)	NH ₃ -N /TAN	Estimated K _f (L/kg)	The K _d ratio α
				(mg/L)	(µg/g)	(mg/L)	(µg/g)				
16.1	-9.53	2621	106	229	68	2503	745	3688	1.51%	1.47	0.17
16.7	-9.51	2563	111	235	70	2467	734	3697	1.55%	1.50	0.17
21.1	-9.37	2146	139	246	73	1862	554	3874	1.63%	2.08	0.13
20.0	-9.40	2243	90	166	49	1365	406	4045	1.10%	2.96	0.09
20.0	-9.40	2243	100	184	55	1509	449	3997	1.22%	2.65	0.10
12.8	-9.64	3007	46	115	34	1623	483	3984	0.76%	2.46	0.11
20.0	-9.40	2243	115	213	63	1750	521	3917	1.41%	2.24	0.12
22.2	-9.33	2055	114	193	57	1345	400	4044	1.27%	3.01	0.09
22.2	-9.33	2055	166	282	84	1968	585	3832	1.86%	1.95	0.13
17.8	-9.48	2451	109	221	66	2133	634	3801	1.46%	1.78	0.14
21.1	-9.37	2146	127	224	67	1698	505	3929	1.48%	2.31	0.11
14.9	-9.57	2756	80	181	54	2169	645	3802	1.19%	1.75	0.15
8.2	-9.79	3644	27	81	24	1627	484	3993	0.53%	2.45	0.11

Note: All data expressed in dry basis. For litter A, TAN=4501 µg/g, pH=8.49, MC=29.8 w/w%.

APPENDIX E. EXPERIMENTAL DATA OF $C_{G,0}$ AND K_f FOR LITTER B IN THE WIND TUNNEL STUDY

T (°C)	Log K_{d0}	K_h	Observed $C_{g,0}$ (mg/m ³)	Dissolved NH ₃ -N		Dissolved NH ₄ ⁺ -N		Adsorbed NH ₄ ⁺ -N (µg/g)	NH ₃ -N /TAN	Estimated K_f (L/kg)	The K_d ratio α
				(mg/L)	(µg/g)	(mg/L)	(µg/g)				
21.1	-9.37	2146	243	430	243	2410	1366	7567	2.65%	3.14	0.15
26.1	-9.21	1769	500	729	413	2862	1622	7141	4.50%	2.50	0.19
26.7	-9.20	1733	563	803	455	3034	1719	7002	4.96%	2.31	0.20
25.6	-9.23	1807	528	786	445	3208	1818	6913	4.85%	2.15	0.21
25.0	-9.25	1846	448	681	386	2891	1638	7152	4.20%	2.47	0.19
22.8	-9.32	2011	357	591	335	2941	1666	7175	3.65%	2.44	0.19
22.8	-9.32	2011	405	671	380	3336	1891	6905	4.14%	2.07	0.21
23.3	-9.30	1968	479	777	440	3715	2105	6630	4.79%	1.78	0.24
22.8	-9.32	2011	282	467	265	2323	1316	7595	2.88%	3.27	0.15
22.8	-9.32	2011	361	597	339	2972	1684	7153	3.69%	2.41	0.19
26.1	-9.21	1769	497	724	410	2841	1610	7156	4.46%	2.52	0.18
23.9	-9.28	1927	459	728	412	3343	1895	6869	4.49%	2.05	0.22
20.0	-9.40	2243	457	844	478	5137	2911	5787	5.21%	1.13	0.33
20.6	-9.39	2194	516	933	529	5451	3089	5558	5.76%	1.02	0.36
23.9	-9.28	1927	628	996	564	4576	2593	6018	6.14%	1.32	0.30
24.4	-9.27	1886	517	803	455	3545	2009	6712	4.95%	1.89	0.23

T (°C)	LogK _{d0}	K _h	Observed C _{g,0} (mg/m ³)	Dissolved NH ₃ -N		Dissolved NH ₄ ⁺ -N		Adsorbed NH ₄ ⁺ -N (µg/g)	NH ₃ -N /TAN	Estimated K _f (L/kg)	The K _d ratio α
				(mg/L)	(µg/g)	(mg/L)	(µg/g)				
25.3	-9.24	1826	564	848	480	3529	2000	6696	5.23%	1.90	0.23
25.0	-9.25	1846	450	684	388	2904	1646	7143	4.22%	2.46	0.19
23.3	-9.30	1968	637	1033	586	4939	2799	5791	6.37%	1.17	0.33
20.0	-9.40	2243	146	269	152	1636	927	8097	1.66%	4.95	0.10
25.7	-9.23	1797	901	1334	756	5391	3055	5365	8.23%	1.00	0.36
24.8	-9.25	1860	589	902	511	3887	2203	6462	5.57%	1.66	0.25
23.6	-9.29	1948	562	901	511	4226	2395	6270	5.56%	1.48	0.28
24.6	-9.26	1875	681	1052	596	4595	2604	5976	6.49%	1.30	0.30
25.2	-9.24	1832	696	1050	595	4398	2492	6089	6.48%	1.38	0.29
24.8	-9.25	1860	665	1018	577	4386	2485	6113	6.28%	1.39	0.29
23.6	-9.29	1948	433	694	393	3256	1845	6937	4.28%	2.13	0.21
27.7	-9.17	1666	632	867	491	3046	1726	6959	5.35%	2.28	0.20
27.7	-9.17	1666	737	1012	573	3555	2015	6588	6.24%	1.85	0.23
28.3	-9.15	1629	588	788	447	2658	1506	7223	4.86%	2.72	0.17
25.1	-9.24	1839	494	748	424	3154	1788	6964	4.62%	2.21	0.20
25.5	-9.23	1811	559	834	473	3420	1938	6765	5.15%	1.98	0.22
29.1	-9.12	1581	782	1018	577	3248	1841	6759	6.28%	2.08	0.21

T (°C)	LogK _{d0}	K _h	Observed C _{g,0} (mg/m ³)	Dissolved NH ₃ -N		Dissolved NH ₄ ⁺ -N		Adsorbed NH ₄ ⁺ -N (µg/g)	NH ₃ -N /TAN	Estimated K _f (L/kg)	The K _d ratio α
				(mg/L)	(µg/g)	(mg/L)	(µg/g)				
30.0	-9.10	1529	696	876	497	2628	1489	7190	5.41%	2.74	0.17
24.6	-9.26	1875	220	340	193	1486	842	8141	2.10%	5.48	0.09
27.4	-9.17	1685	346	480	272	1721	975	7929	2.96%	4.61	0.11
26.2	-9.21	1763	674	978	554	3818	2164	6458	6.04%	1.69	0.25
24.6	-9.26	1875	500	772	438	3373	1912	6827	4.76%	2.02	0.22
24.1	-9.28	1911	511	803	455	3637	2061	6660	4.96%	1.83	0.24
27.6	-9.17	1673	600	826	468	2923	1656	7051	5.10%	2.41	0.19
28.8	-9.13	1599	516	679	385	2213	1254	7537	4.19%	3.41	0.14
23.2	-9.30	1978	213	347	197	1677	950	8029	2.14%	4.79	0.11
19.2	-9.43	2316	146	278	157	1794	1017	8002	1.71%	4.46	0.11
19.4	-9.42	2297	165	312	177	1984	1124	7875	1.93%	3.97	0.12
9.2	-9.76	3502	36	103	59	1433	812	8305	0.64%	5.79	0.09
11.8	-9.67	3133	63	161	91	1820	1032	8053	1.00%	4.42	0.11
8.4	-9.79	3613	42	125	71	1835	1040	8065	0.77%	4.39	0.11
10.6	-9.71	3289	63	171	97	2115	1198	7881	1.06%	3.73	0.13
8.7	-9.78	3573	37	108	61	1552	880	8235	0.67%	5.30	0.10
12.2	-9.66	3075	50	126	72	1378	781	8323	0.78%	6.04	0.09

T (°C)	LogK _{d0}	K _h	Observed C _{g,0} (mg/m ³)	Dissolved NH ₃ -N		Dissolved NH ₄ ⁺ -N		Adsorbed NH ₄ ⁺ -N (µg/g)	NH ₃ -N /TAN	Estimated K _f (L/kg)	The K _d ratio α
				(mg/L)	(µg/g)	(mg/L)	(µg/g)				
9.1	-9.77	3518	44	127	72	1776	1006	8098	0.78%	4.56	0.11
13.0	-9.63	2974	55	135	76	1382	783	8316	0.83%	6.02	0.09
11.0	-9.70	3245	48	127	72	1530	867	8237	0.78%	5.38	0.10
14.4	-9.58	2807	60	139	79	1280	726	8372	0.86%	6.54	0.08

Note: All data expressed in dry basis. For litter B, TAN=9176 µg/g, pH=8.62, MC=56.7 w/w%.

APPENDIX F. EXPERIMENTAL DATA FOR K_G REGRESSION MODEL DEVELOPMENT (LITTER A)
IN THE WIND TUNNEL STUDY

Q (m ³ /s)	U (m/s)	T (°C)	RH	C _{g, outlet} (mg/m ³)	J (mgN m ⁻² h ⁻¹)	C _{g, 0} (mg/m ³)	K _G (m/h)
0.00165	0.04	19.4		31.17	984	125.29	12.70
0.00276	0.06	19.4		25.09	1323	125.29	16.03
0.00283	0.07	18.3		22.43	1213	108.33	17.14
0.00321	0.07	23.3		20.82	1277	208.45	8.26
0.00321	0.07	21.1		18.82	1154	155.84	10.23
0.00314	0.07	13.3		11.76	706	56.30	19.23
0.00328	0.08	21.1		21.66	1357	155.84	12.28
0.00411	0.10	18.3		12.92	1015	108.33	12.91
0.00414	0.10	16.7		13.17	1043	87.10	17.13
0.00414	0.10	16.7		12.36	979	87.10	15.90
0.00411	0.10	22.8		15.93	1251	193.83	8.54
0.00421	0.10	13.9		7.04	567	60.55	12.86
0.00417	0.10	19.4		10.65	850	125.29	9.00
0.00487	0.11	24.4		9.91	923	241.09	4.85
0.00556	0.13	22.2		7.34	781	180.24	5.48
0.00611	0.14	16.1		2.95	344	80.99	5.36
0.00628	0.15	25.6		4.14	497	278.83	2.20
0.00684	0.16	13.9		3.11	406	60.55	8.59
0.00669	0.16	18.3		4.43	566	108.33	6.62
0.00677	0.16	16.7		2.57	333	87.10	4.78
0.00971	0.23	21.7		3.25	604	167.60	4.46
0.01078	0.25	18.3		1.38	285	108.33	3.24
0.01112	0.26	20.0		3.06	651	134.75	6.00
0.01124	0.26	20.6		4.3	925	144.91	7.99

Q (m ³ /s)	U (m/s)	T (°C)	RH	C _{g, outlet} (mg/m ³)	J (mgN m ⁻² h ⁻¹)	C _{g, 0} (mg/m ³)	K _G (m/h)
0.01107	0.26	18.3		2.28	483	108.33	5.53
0.01192	0.28	25.0		3.62	824	259.27	3.92
0.01653	0.38	17.2		2.93	925	93.67	12.38
0.01666	0.39	20.0		4.72	1503	134.75	14.04
0.0169	0.39	17.8		3.53	1140	100.74	14.25
0.01728	0.40	21.1		2.29	758	155.84	5.99
0.01762	0.41	18.6		1.88	632	112.35	6.95
0.01842	0.43	23.9		2.24	789	224.18	4.32
0.02111	0.49	18.9		2.16	874	116.51	9.28
0.02169	0.50	21.7		1.85	768	167.60	5.63
0.02201	0.51	23.3		2.03	855	208.45	5.03
0.02242	0.52	18.3		1.31	561	108.33	6.37
0.02353	0.55	17.2		2.01	905	93.67	11.98
0.02774	0.65	21.7		2.24	1191	167.60	8.75
0.02854	0.66	23.3		1.78	974	208.45	5.72
0.02913	0.68	21.1		1.82	1014	155.84	8.00
0.02951	0.69	15.3		1.05	591	72.62	10.02
0.03234	0.75	22.5		1.82	1124	186.91	7.38
0.03535	0.82	20.0		2.11	1427	134.75	13.06
0.03528	0.82	19.4		1.13	765	125.29	7.48
0.03524	0.82	20.6		2.32	1560	144.91	13.29
0.03672	0.85	18.9		1.92	1348	116.51	14.29
0.03714	0.86	13.9		0.97	686	60.55	13.97
0.03679	0.86	17.2		1	703	93.67	9.22
0.04208	0.98	23.9		1.61	1294	224.18	7.06
0.04404	1.02	19.4		1.72	1447	125.29	14.22
0.04374	1.02	14.1	49.2	0.62	520	62.33	10.23
0.0443	1.03	19.4		2.17	1835	125.29	18.09
0.04478	1.04	17.8		0.9	767	100.74	9.32

Q (m ³ /s)	U (m/s)	T (°C)	RH	C _{g, outlet} (mg/m ³)	J (mgN m ⁻² h ⁻¹)	C _{g, 0} (mg/m ³)	K _G (m/h)
0.04474	1.04	21.1		2.13	1823	155.84	14.40
0.04564	1.06	9.1	42.4	0.63	551	32.48	21.02
0.05165	1.20	25.0		1.37	1352	259.27	6.36
0.05307	1.23	13.9		0.75	757	60.55	15.37
0.05317	1.24	13.9		0.77	782	60.55	15.88
0.05372	1.25	21.1		1.62	1662	155.84	13.09
0.05411	1.26	18.9		1.82	1880	116.51	19.91
0.05417	1.26	10.8	38.6	0.65	676	40.36	20.69
0.05535	1.29	9.8	35.6	0.7	740	35.54	25.80
0.05632	1.31	14.4	48.9	0.87	938	64.74	17.84
0.0567	1.32	25.6		1.04	1126	278.83	4.92
0.05939	1.38	18.9		1.55	1761	116.51	18.60
0.05998	1.39	20.6		1.64	1885	144.91	15.98
0.06031	1.40	22.2		1.28	1477	180.24	10.02
0.06102	1.42	21.7		1.28	1490	167.60	10.88
0.06195	1.44	21.1		1.41	1677	155.84	13.18
0.06451	1.50	14.7	46.3	0.58	716	67.07	13.07
0.06493	1.51	11.4	38.1	0.71	884	43.91	24.85
0.06489	1.51	10.3	35.7	0.54	668	38.05	21.61
0.06593	1.53	25.6		1.28	1617	278.83	7.08
0.06761	1.57	20.0		1.24	1602	134.75	14.57
0.06731	1.57	19.7		1.31	1684	129.93	15.90
0.06826	1.59	20.0		1.11	1455	134.75	13.22
0.06881	1.60	23.3		1.23	1620	208.45	9.49
0.06872	1.60	22.8		1.11	1458	193.83	9.19
0.07086	1.65	21.1	57.6	2.09	2831	155.57	22.40
0.07116	1.65	20.6	60.1	1.83	2488	146.12	20.93
0.07276	1.69	18.1	62.5	1.12	1560	104.79	18.27
0.0781	1.82	27.2		0.75	1114	346.81	3.91

Q (m ³ /s)	U (m/s)	T (°C)	RH	C _{g, outlet} (mg/m ³)	J (mgN m ⁻² h ⁻¹)	C _{g, 0} (mg/m ³)	K _G (m/h)
0.07891	1.84	25.0		0.93	1411	259.27	6.63
0.07908	1.84	10.5	36.0	0.43	653	38.96	20.57
0.07895	1.84	10.6	36.8	0.5	756	39.26	23.68
0.08005	1.86	26.1		0.89	1358	299.87	5.52
0.08036	1.87	19.4		0.53	810	125.29	7.88
0.08026	1.87	14.8	45.4	0.43	662	68.31	11.85
0.08372	1.95	19.7		0.65	1043	129.93	9.79
0.08538	1.99	20.0		0.7	1136	134.75	10.29
0.08609	2.00	25.0		0.85	1392	259.27	6.54
0.08738	2.03	25.6		0.61	1012	278.83	4.42
0.08807	2.05	21.7	53.7	1.46	2467	168.42	17.94
0.08963	2.08	25.6		0.79	1352	278.83	5.90
0.08946	2.08	20.3	57.4	1.41	2409	139.54	21.17
0.09188	2.14	17.8		0.58	1022	100.74	12.39
0.09309	2.16	16.1		0.61	1092	80.99	16.50
0.09512	2.21	23.3		0.93	1689	208.45	9.88

Note: Emission surface area = 0.155m.

APPENDIX G. EXPERIMENTAL DATA FOR K_G REGRESSION MODEL VALIDATION (LITTER B)
IN THE WIND TUNNEL STUDY

Q (m ³ /s)	U (m/s)	T (°C)	RH	C _{g, outlet} (mg/m ³)	J (mgN m ⁻² h ⁻¹)	C _{g, 0} (mg/m ³)	K _G (m/h)
0.00359	0.08	12.3	51.5	4.78	328	67.99	6.31
0.00358	0.08	11.2	52.6	4.14	283	56.78	6.53
0.00400	0.09	29.6	58.4	36.94	2827	970.93	3.68
0.00421	0.10	28.9	57.4	43.05	3466	871.52	5.08
0.00416	0.10	24.8	61.7	28.88	2296	465.81	6.38
0.00421	0.10	25.1	62.7	30.67	2469	489.39	6.54
0.00476	0.11	26.3	64.7	34.35	3129	586.22	6.88
0.00455	0.11	27.6	63.4	28.99	2526	717.54	4.45
0.00459	0.11	20.8	60.3	12.47	1095	250.86	5.58
0.00504	0.12	25.7	65.5	17.62	1698	530.52	4.02
0.00511	0.12	12.8	54.6	2.01	196	73.34	3.34
0.00580	0.13	24.4	64.6	10.15	1126	437.32	3.20
0.00552	0.13	12.0	51.9	2.63	278	64.83	5.42
0.00583	0.14	25.0	64.2	14.76	1645	477.46	4.32
0.00587	0.14	24.5	63.0	15.02	1686	446.80	4.74
0.00611	0.14	27.1	64.0	17.64	2062	662.21	3.88
0.00635	0.15	26.1	61.2	6.47	786	566.65	1.70
0.00670	0.16	27.7	61.3	10.13	1298	721.98	2.21
0.00711	0.17	12.4	56.6	1.78	242	68.94	4.37
0.00780	0.18	26.7	65.0	9.91	1479	618.75	2.95
0.00780	0.18	25.5	65.3	7.90	1179	516.55	2.82
0.00794	0.18	28.8	60.6	9.21	1400	864.82	1.99
0.00780	0.18	26.4	62.8	8.90	1329	595.70	2.75
0.00769	0.18	21.4	60.8	5.14	757	276.60	3.39
0.00800	0.19	27.1	61.2	8.12	1242	662.62	2.31
0.00877	0.20	24.8	61.2	2.50	420	461.52	1.11
0.01065	0.25	26.6	64.5	3.70	753	612.10	1.50

Q (m ³ /s)	U (m/s)	T (°C)	RH	C _{g, outlet} (mg/m ³)	J (mgN m ⁻² h ⁻¹)	C _{g, 0} (mg/m ³)	K _G (m/h)
0.01057	0.25	25.3	63.6	3.19	644	503.17	1.56
0.01092	0.25	12.0	60.9	1.97	411	64.22	8.01
0.01173	0.27	25.9	64.8	2.71	608	548.58	1.35
0.01162	0.27	20.7	60.9	2.17	482	246.71	2.39
0.01202	0.28	29.3	62.8	8.53	1961	935.63	2.57
0.01237	0.29	27.1	63.9	2.92	692	666.31	1.27
0.01226	0.29	25.5	62.7	3.49	819	514.56	1.95
0.02148	0.50	26.4	61.8	2.87	1180	599.76	2.40
0.02197	0.51	25.2	62.8	7.14	3001	491.28	7.53
0.02206	0.51	24.2	62.6	1.67	703	421.56	2.03
0.02183	0.51	20.3	62.0	2.51	1049	232.16	5.55
0.02183	0.51	12.5	45.8	1.04	436	69.71	7.71
0.02256	0.52	25.5	61.8	2.16	931	515.67	2.20
0.02277	0.53	28.1	61.1	10.70	4660	774.73	7.41
0.02263	0.53	23.7	64.5	3.97	1717	394.80	5.34
0.03583	0.83	27.6	63.0	8.29	5680	714.33	9.77
0.03565	0.83	26.3	64.6	6.74	4594	586.22	9.63
0.03563	0.83	24.1	63.7	1.83	1248	418.12	3.64
0.03548	0.83	26.5	62.6	1.87	1272	606.83	2.55
0.03611	0.84	24.8	62.6	3.84	2655	467.83	6.95
0.03653	0.85	23.5	62.9	3.99	2785	381.44	8.96
0.03927	0.91	12.5	45.0	1.05	792	69.36	14.08
0.04035	0.94	11.9	48.4	1.29	993	63.25	19.46
0.04087	0.95	20.4	63.5	1.54	1208	236.75	6.23
0.04337	1.01	28.9	64.0	3.06	2535	877.19	3.52
0.04353	1.01	28.5	64.1	2.94	2446	826.47	3.61
0.04430	1.03	27.8	64.7	2.38	2013	738.09	3.32
0.04456	1.04	24.4	61.6	1.29	1102	436.58	3.07
0.04477	1.04	12.1	46.3	0.85	729	65.44	13.71
0.04581	1.07	26.3	61.7	2.44	2138	582.79	4.47

Q (m ³ /s)	U (m/s)	T (°C)	RH	C _{g, outlet} (mg/m ³)	J (mgN m ⁻² h ⁻¹)	C _{g, 0} (mg/m ³)	K _G (m/h)
0.04615	1.07	28.7	63.2	2.31	2036	846.60	2.93
0.04916	1.14	20.6	62.6	1.28	1204	243.38	6.04
0.05307	1.23	29.4	63.5	2.45	2485	940.70	3.22
0.05359	1.25	21.6	61.5	1.58	1614	283.47	6.95
0.05417	1.26	26.5	62.4	1.11	1146	605.52	2.30
0.05514	1.28	27.9	64.2	2.06	2169	750.37	3.52
0.05545	1.29	19.0	62.0	1.38	1460	190.23	9.39
0.05538	1.29	12.0	45.0	0.76	804	64.73	15.27
0.05587	1.30	27.8	63.3	2.26	2411	740.37	3.97
0.06482	1.51	11.6	45.4	0.61	759	60.39	15.41
0.06657	1.55	26.9	62.0	2.05	2605	641.49	4.95
0.06680	1.55	22.5	57.7	2.44	3116	324.39	11.75
0.06699	1.56	26.3	62.3	2.04	2609	588.12	5.41
0.06812	1.58	21.8	61.2	2.03	2645	294.02	11.00
0.06858	1.59	24.4	55.3	2.12	2775	435.51	7.78
0.07348	1.71	20.9	62.9	1.07	1497	254.17	7.18
0.07971	1.85	19.7	61.3	2.40	3666	213.07	21.13
0.07977	1.86	10.3	48.2	0.73	1117	49.80	27.64
0.08047	1.87	24.0	57.3	1.75	2692	411.85	7.97
0.08557	1.99	22.0	61.8	1.43	2348	299.89	9.55
0.08637	2.01	28.0	59.5	1.90	3139	756.65	5.05
0.08692	2.02	27.4	60.7	1.73	2870	692.30	5.05
0.08689	2.02	26.1	50.0	1.93	3209	567.53	6.89
0.08744	2.03	18.5	61.4	1.07	1788	175.37	12.46

Note: Emission surface area = 0.155m.

APPENDIX H. CALCULATION OF DIMENSIONLESS NUMBERS

Litter	U	T (°C)	K _G	D	ν	Sh (K _G L/D)	Re (UL/ ν)	Sc (ν /D)
A	0.04	19.4	12.70	2.36E-05	1.54E-05	30.4	507.3	0.653
A	0.06	19.4	16.03	2.36E-05	1.54E-05	38.4	847.3	0.653
A	0.07	18.3	17.14	2.34E-05	1.53E-05	41.3	874.8	0.652
A	0.07	13.3	19.23	2.27E-05	1.48E-05	47.8	1002.8	0.651
A	0.07	23.3	8.26	2.41E-05	1.58E-05	19.3	961.6	0.654
A	0.07	21.1	10.23	2.38E-05	1.55E-05	24.3	975.1	0.653
A	0.08	21.1	12.28	2.38E-05	1.55E-05	29.1	996.1	0.653
B	0.08	11.2	6.53	2.24E-05	1.46E-05	16.5	1159.9	0.651
B	0.08	12.3	6.31	2.26E-05	1.47E-05	15.8	1153.9	0.651
B	0.09	29.6	3.68	2.50E-05	1.64E-05	8.3	1154.5	0.655
A	0.10	18.3	12.91	2.34E-05	1.53E-05	31.1	1270.7	0.652
A	0.10	22.8	8.54	2.40E-05	1.57E-05	20.1	1235.4	0.653
A	0.10	16.7	17.13	2.32E-05	1.51E-05	41.7	1295.1	0.652
A	0.10	16.7	15.90	2.32E-05	1.51E-05	38.7	1295.1	0.652
B	0.10	24.8	6.38	2.43E-05	1.59E-05	14.8	1235.2	0.654
A	0.10	19.4	9.00	2.36E-05	1.54E-05	21.6	1283.0	0.653
A	0.10	13.9	12.86	2.28E-05	1.48E-05	31.9	1340.5	0.651
B	0.10	28.9	5.08	2.49E-05	1.63E-05	11.5	1219.6	0.655
B	0.10	25.1	6.54	2.44E-05	1.59E-05	15.1	1248.1	0.654
B	0.11	27.6	4.45	2.47E-05	1.62E-05	10.2	1330.0	0.655
B	0.11	20.8	5.58	2.38E-05	1.55E-05	13.3	1398.4	0.653
B	0.11	26.3	6.88	2.45E-05	1.61E-05	15.8	1401.9	0.654
A	0.11	24.4	4.85	2.43E-05	1.59E-05	11.3	1449.1	0.654
B	0.12	25.7	4.02	2.44E-05	1.60E-05	9.3	1489.3	0.654
B	0.12	12.8	3.34	2.26E-05	1.47E-05	8.3	1638.0	0.651
B	0.13	12.0	5.42	2.25E-05	1.47E-05	13.6	1780.3	0.651
A	0.13	22.2	5.48	2.40E-05	1.56E-05	12.9	1678.2	0.653
B	0.13	24.4	3.20	2.43E-05	1.59E-05	7.4	1727.6	0.654
B	0.14	25.0	4.32	2.43E-05	1.59E-05	10.0	1729.1	0.654

Litter	U	T (°C)	K _G	D	ν	Sh (K _G L/D)	Re (UL/ ν)	Sc (ν /D)
B	0.14	24.5	4.74	2.43E-05	1.59E-05	11.0	1746.6	0.654
A	0.14	16.1	5.36	2.31E-05	1.51E-05	13.1	1918.4	0.652
B	0.14	27.1	3.88	2.46E-05	1.61E-05	8.9	1790.0	0.654
A	0.15	25.6	2.20	2.44E-05	1.60E-05	5.1	1858.3	0.654
B	0.15	26.1	1.70	2.45E-05	1.60E-05	3.9	1872.6	0.654
A	0.16	18.3	6.62	2.34E-05	1.53E-05	16.0	2070.5	0.652
B	0.16	27.7	2.21	2.47E-05	1.62E-05	5.1	1955.4	0.655
A	0.16	16.7	4.78	2.32E-05	1.51E-05	11.6	2117.1	0.652
A	0.16	13.9	8.59	2.28E-05	1.48E-05	21.3	2177.3	0.651
B	0.17	12.4	4.37	2.26E-05	1.47E-05	10.9	2287.0	0.651
B	0.18	21.4	3.39	2.38E-05	1.56E-05	8.0	2334.5	0.653
B	0.18	26.7	2.95	2.46E-05	1.61E-05	6.8	2292.5	0.654
B	0.18	25.5	2.82	2.44E-05	1.60E-05	6.5	2309.3	0.654
B	0.18	26.4	2.75	2.45E-05	1.61E-05	6.3	2296.0	0.654
B	0.18	28.8	1.99	2.49E-05	1.63E-05	4.5	2302.1	0.655
B	0.19	27.1	2.31	2.46E-05	1.61E-05	5.3	2344.5	0.654
B	0.20	24.8	1.11	2.43E-05	1.59E-05	2.6	2607.5	0.654
A	0.23	21.7	4.46	2.39E-05	1.56E-05	10.5	2941.3	0.653
B	0.25	25.3	1.56	2.44E-05	1.60E-05	3.6	3130.9	0.654
B	0.25	26.6	1.50	2.46E-05	1.61E-05	3.5	3129.2	0.654
A	0.25	18.3	3.24	2.34E-05	1.53E-05	7.8	3335.9	0.652
B	0.25	12.0	8.01	2.25E-05	1.47E-05	20.1	3520.2	0.651
A	0.26	18.3	5.53	2.34E-05	1.53E-05	13.3	3426.8	0.652
A	0.26	20.0	6.00	2.36E-05	1.54E-05	14.3	3406.6	0.653
A	0.26	20.6	7.99	2.37E-05	1.55E-05	19.0	3428.9	0.653
B	0.27	20.7	2.39	2.37E-05	1.55E-05	5.7	3541.9	0.653
B	0.27	25.9	1.35	2.45E-05	1.60E-05	3.1	3461.9	0.654
A	0.28	25.0	3.92	2.43E-05	1.59E-05	9.1	3537.1	0.654
B	0.28	29.3	2.57	2.50E-05	1.64E-05	5.8	3473.5	0.655
B	0.29	25.5	1.95	2.44E-05	1.60E-05	4.5	3629.4	0.654

Litter	U	T (°C)	K _G	D	ν	Sh (K _G L/D)	Re (UL/ ν)	Sc (ν /D)
B	0.29	27.1	1.27	2.47E-05	1.61E-05	2.9	3622.2	0.654
A	0.38	17.2	12.38	2.32E-05	1.52E-05	30.1	5151.3	0.652
A	0.39	20.0	14.04	2.36E-05	1.54E-05	33.5	5100.6	0.653
A	0.39	17.8	14.25	2.33E-05	1.52E-05	34.5	5248.4	0.652
A	0.40	21.1	5.99	2.38E-05	1.55E-05	14.2	5254.1	0.653
A	0.41	18.6	6.95	2.34E-05	1.53E-05	16.7	5444.9	0.652
A	0.43	23.9	4.32	2.42E-05	1.58E-05	10.1	5504.1	0.654
A	0.49	18.9	9.28	2.35E-05	1.53E-05	22.3	6509.6	0.653
B	0.50	26.4	2.40	2.46E-05	1.61E-05	5.5	6316.8	0.654
A	0.50	21.7	5.63	2.39E-05	1.56E-05	13.3	6574.1	0.653
B	0.51	20.3	5.55	2.37E-05	1.55E-05	13.2	6673.5	0.653
B	0.51	12.5	7.71	2.26E-05	1.47E-05	19.3	7016.1	0.651
B	0.51	25.2	7.53	2.44E-05	1.59E-05	17.4	6513.9	0.654
A	0.51	23.3	5.03	2.41E-05	1.58E-05	11.8	6598.9	0.654
B	0.51	24.2	2.03	2.42E-05	1.58E-05	4.7	6580.2	0.654
A	0.52	18.3	6.37	2.34E-05	1.53E-05	15.4	6939.3	0.652
B	0.52	25.5	2.20	2.44E-05	1.60E-05	5.1	6675.1	0.654
B	0.53	23.7	5.34	2.42E-05	1.58E-05	12.5	6768.3	0.654
B	0.53	28.1	7.41	2.48E-05	1.62E-05	16.9	6627.2	0.655
A	0.55	17.2	11.98	2.32E-05	1.52E-05	29.1	7333.6	0.652
A	0.65	21.7	8.75	2.39E-05	1.56E-05	20.7	8407.5	0.653
A	0.66	23.3	5.72	2.41E-05	1.58E-05	13.4	8558.3	0.654
A	0.68	21.1	8.00	2.38E-05	1.55E-05	19.0	8857.6	0.653
A	0.69	15.3	10.02	2.30E-05	1.50E-05	24.6	9313.5	0.652
A	0.75	22.5	7.38	2.40E-05	1.57E-05	17.4	9749.6	0.653
A	0.82	20.6	13.29	2.37E-05	1.55E-05	31.6	10753.5	0.653
A	0.82	19.4	7.48	2.36E-05	1.54E-05	17.9	10842.9	0.653
A	0.82	20.0	13.06	2.36E-05	1.54E-05	31.2	10825.9	0.653
B	0.83	26.5	2.55	2.46E-05	1.61E-05	5.9	10430.0	0.654
B	0.83	24.1	3.64	2.42E-05	1.58E-05	8.5	10631.8	0.654

Litter	U	T (°C)	K _G	D	ν	Sh (K _G L/D)	Re (UL/ ν)	Sc (ν /D)
B	0.83	26.3	9.63	2.45E-05	1.61E-05	22.1	10495.3	0.654
B	0.83	27.6	9.77	2.47E-05	1.62E-05	22.3	10465.4	0.655
B	0.84	24.8	6.95	2.43E-05	1.59E-05	16.1	10727.4	0.654
B	0.85	23.5	8.96	2.41E-05	1.58E-05	21.0	10940.7	0.654
A	0.85	18.9	14.29	2.35E-05	1.53E-05	34.3	11326.4	0.653
A	0.86	17.2	9.22	2.32E-05	1.52E-05	22.4	11469.1	0.652
A	0.86	13.9	13.97	2.28E-05	1.48E-05	34.6	11828.1	0.651
B	0.91	12.5	14.08	2.26E-05	1.47E-05	35.2	12624.0	0.651
B	0.94	11.9	19.46	2.25E-05	1.46E-05	48.8	13021.8	0.651
B	0.95	20.4	6.23	2.37E-05	1.55E-05	14.8	12483.7	0.653
A	0.98	23.9	7.06	2.42E-05	1.58E-05	16.5	12575.9	0.654
B	1.01	28.9	3.52	2.49E-05	1.63E-05	8.0	12563.0	0.655
B	1.01	28.5	3.61	2.49E-05	1.63E-05	8.2	12640.5	0.655
A	1.02	14.1	10.23	2.28E-05	1.49E-05	25.3	13911.1	0.651
A	1.02	19.4	14.22	2.36E-05	1.54E-05	34.1	13536.3	0.653
A	1.03	19.4	18.09	2.36E-05	1.54E-05	43.3	13613.3	0.653
B	1.03	27.8	3.32	2.47E-05	1.62E-05	7.6	12919.7	0.655
B	1.04	24.4	3.07	2.43E-05	1.59E-05	7.2	13275.5	0.654
A	1.04	21.1	14.40	2.38E-05	1.55E-05	34.2	13607.0	0.653
B	1.04	12.1	13.71	2.25E-05	1.47E-05	34.3	14426.2	0.651
A	1.04	17.8	9.32	2.33E-05	1.52E-05	22.6	13909.0	0.652
A	1.06	9.1	21.02	2.21E-05	1.44E-05	53.6	14995.5	0.650
B	1.07	26.3	4.47	2.45E-05	1.60E-05	10.3	13488.1	0.654
B	1.07	28.7	2.93	2.49E-05	1.63E-05	6.6	13388.1	0.655
B	1.14	20.6	6.04	2.37E-05	1.55E-05	14.4	14998.2	0.653
A	1.20	25.0	6.36	2.43E-05	1.59E-05	14.8	15328.4	0.654
A	1.23	13.9	15.37	2.28E-05	1.48E-05	38.1	16901.2	0.651
B	1.23	29.4	3.22	2.50E-05	1.64E-05	7.3	15329.2	0.655
A	1.24	13.9	15.88	2.28E-05	1.48E-05	39.3	16934.2	0.651
B	1.25	21.6	6.95	2.39E-05	1.56E-05	16.4	16246.6	0.653

Litter	U	T (°C)	K _G	D	ν	Sh (K _G L/D)	Re (UL/ ν)	Sc (ν /D)
A	1.25	21.1	13.09	2.38E-05	1.55E-05	31.0	16337.9	0.653
A	1.26	18.9	19.91	2.35E-05	1.53E-05	47.9	16687.1	0.653
A	1.26	10.8	20.69	2.24E-05	1.45E-05	52.2	17605.2	0.651
B	1.26	26.5	2.30	2.46E-05	1.61E-05	5.3	15927.1	0.654
B	1.28	27.9	3.52	2.48E-05	1.62E-05	8.0	16072.8	0.655
A	1.29	9.8	25.80	2.22E-05	1.44E-05	65.5	18102.1	0.650
B	1.29	12.0	15.27	2.25E-05	1.47E-05	38.3	17854.4	0.651
B	1.29	19.0	9.39	2.35E-05	1.53E-05	22.6	17090.2	0.653
B	1.30	27.8	3.97	2.48E-05	1.62E-05	9.0	16293.2	0.655
A	1.31	14.4	17.84	2.29E-05	1.49E-05	44.1	17876.9	0.651
A	1.32	25.6	4.92	2.44E-05	1.60E-05	11.4	16768.2	0.654
A	1.38	18.9	18.60	2.35E-05	1.53E-05	44.7	18318.4	0.653
A	1.39	20.6	15.98	2.37E-05	1.55E-05	38.0	18305.0	0.653
A	1.40	22.2	10.02	2.40E-05	1.56E-05	23.6	18212.7	0.653
A	1.42	21.7	10.88	2.39E-05	1.56E-05	25.7	18491.3	0.653
A	1.44	21.1	13.18	2.38E-05	1.55E-05	31.3	18840.1	0.653
A	1.50	14.7	13.07	2.29E-05	1.49E-05	32.2	20442.1	0.651
B	1.51	11.6	15.41	2.25E-05	1.46E-05	38.7	20958.4	0.651
A	1.51	10.3	21.61	2.23E-05	1.45E-05	54.7	21150.3	0.650
A	1.51	11.4	24.85	2.24E-05	1.46E-05	62.5	21010.6	0.651
A	1.53	25.6	7.08	2.44E-05	1.60E-05	16.3	19498.1	0.654
B	1.55	26.9	4.95	2.46E-05	1.61E-05	11.3	19525.6	0.654
B	1.55	22.5	11.75	2.40E-05	1.57E-05	27.7	20142.0	0.653
B	1.56	26.3	5.41	2.45E-05	1.61E-05	12.4	19718.5	0.654
A	1.57	19.7	15.90	2.36E-05	1.54E-05	38.0	20650.5	0.653
A	1.57	20.0	14.57	2.36E-05	1.54E-05	34.8	20704.2	0.653
B	1.58	21.8	11.00	2.39E-05	1.56E-05	26.0	20620.6	0.653
A	1.59	20.0	13.22	2.36E-05	1.54E-05	31.6	20905.3	0.653
B	1.59	24.4	7.78	2.43E-05	1.59E-05	18.1	20432.9	0.654
A	1.60	22.8	9.19	2.40E-05	1.57E-05	21.6	20679.8	0.653

Litter	U	T (°C)	K _G	D	ν	Sh (K _G L/D)	Re (UL/ ν)	Sc (ν /D)
A	1.60	23.3	9.49	2.41E-05	1.58E-05	22.2	20633.8	0.654
A	1.65	21.1	22.40	2.38E-05	1.55E-05	53.1	21551.7	0.653
A	1.65	20.6	20.93	2.37E-05	1.55E-05	49.8	21708.1	0.653
A	1.69	18.1	18.27	2.34E-05	1.52E-05	44.1	22555.7	0.652
B	1.71	20.9	7.18	2.38E-05	1.55E-05	17.1	22378.4	0.653
A	1.82	27.2	3.91	2.47E-05	1.61E-05	8.9	22859.5	0.655
A	1.84	25.0	6.63	2.43E-05	1.59E-05	15.4	23418.3	0.654
A	1.84	10.6	23.68	2.23E-05	1.45E-05	59.9	25690.3	0.650
A	1.84	10.5	20.57	2.23E-05	1.45E-05	52.0	25745.5	0.650
B	1.85	19.7	21.13	2.36E-05	1.54E-05	50.5	24450.0	0.653
B	1.86	10.3	27.64	2.23E-05	1.45E-05	70.0	26004.6	0.650
A	1.86	26.1	5.52	2.45E-05	1.60E-05	12.7	23593.2	0.654
A	1.87	14.8	11.85	2.29E-05	1.49E-05	29.2	25409.1	0.652
A	1.87	19.4	7.88	2.36E-05	1.54E-05	18.9	24697.9	0.653
B	1.87	24.0	7.97	2.42E-05	1.58E-05	18.6	24027.9	0.654
A	1.95	19.7	9.79	2.36E-05	1.54E-05	23.4	25683.2	0.653
A	1.99	20.0	10.29	2.36E-05	1.54E-05	24.6	26146.2	0.653
B	1.99	22.0	9.55	2.39E-05	1.56E-05	22.5	25882.5	0.653
A	2.00	25.0	6.54	2.43E-05	1.59E-05	15.2	25549.9	0.654
B	2.01	28.0	5.05	2.48E-05	1.62E-05	11.5	25166.4	0.655
B	2.02	26.1	6.89	2.45E-05	1.60E-05	15.9	25611.5	0.654
B	2.02	27.4	5.05	2.47E-05	1.62E-05	11.5	25417.9	0.655
A	2.03	25.6	4.42	2.44E-05	1.60E-05	10.2	25842.4	0.654
B	2.03	18.5	12.46	2.34E-05	1.53E-05	30.0	27039.0	0.652
A	2.05	21.7	17.94	2.39E-05	1.56E-05	42.4	26683.0	0.653
A	2.08	20.3	21.17	2.37E-05	1.55E-05	50.5	27349.2	0.653
A	2.08	25.6	5.90	2.44E-05	1.60E-05	13.6	26507.0	0.654
A	2.14	17.8	12.39	2.33E-05	1.52E-05	30.0	28537.5	0.652
A	2.16	16.1	16.50	2.31E-05	1.51E-05	40.3	29223.8	0.652
A	2.21	23.3	9.88	2.41E-05	1.58E-05	23.1	28523.4	0.654

Note: the characteristic length L = 0.2032 m.